DETERMINING THE SUBCELLULAR LOCALIZATION OF ADENOSINE KINASE AND SAH HYDROLASE AND THEIR ROLES IN ADENOSINE METABOLISM

by

Sarah M Schoor

A thesis

presented to the University of Waterloo

in fulfillment of the

thesis requirement for the degree of

Master of Science

in

Biology

Waterloo, Ontario, Canada, 2007

I hereby declare that I am the sole author of this thesis. This is a true copy of the thesis, including any required final revisions, as accepted by my examiners.

I understand that my thesis may be made electronically available to the public.

Signature

ACKNOWLEDGEMENTS

I would foremost like to thank my supervisor Dr. Barb Moffatt for her infinite patience and guidance, and for never giving up on the project or on me. However, there are lots of other people that have aided me along the way, and I would like to thank them. All the members of the Moffatt lab have not only provided help at some point in my research but made it that much more enjoyable, however there are those who need special thanks and they are Luiz Pereira, Jane Wei, Filomena Ng, Sang Lee, Jing Zhang and Yong Lee. In addition, I would like to express my appreciation to Dr. Matt Smith, Dr. Frederique, Dale Weber and Lynn Hoyles for trying to teach me a portion of their knowledge and skills. Lastly I would like to thank my friends and family for sticking with me and offering me endless distractions.

ABSTRACT

Housekeeping enzymes are vital to the metabolism of all plant cells. Two such enzymes adenosine kinase (ADK) and *S*-adenosylhomocysteine (SAH) hydrolase share a similar function: both sustain *S*-adenosylmethionine-dependent methylation reactions by removing inhibitory by-products. SAH hydrolase breaks down SAH which is a competitive inhibitor of all methyltransferase activities. ADK phosphorylates the Ado produced by SAH hydrolase and in doing so drives this reversible reaction in the hydrolysis direction. By catalyzing the phosphorylation of Ado into adenosine monophosphate, ADK not only prevents SAH from re-forming but also initiates the recycling of Ado into adenylate nucleotides and cofactors.

This thesis documents two distinct research topics related to methyl recycling in plants. The first goal was to identify ADK-deficient mutants to establish the contribution of this enzyme activity to adenosine salvage. The second goal was to determine the subcellular localization of ADK and SAH hydrolase in *Arabidopsis thaliana* (Columbia). T-DNA insertion lines for highly similar ADK isoforms (ADK1 and ADK2) and silencing lines of overall ADK activity (sADK) were compared to WT Arabidopsis to identify phenotypic abnormalities associated with ADK deficiency. In addition to following their growth, microscopic analysis was performed on the sADK lines. While removal of either ADK1 or ADK2 had no phenotypic effect, lowering ADK levels to 6-20% that of WT lead to several changes including small, wavy rosette leaves, delayed leaf senescence, decreased internode length, reduced branching, clustered inflorescences and lack of petal abscission and silique dehiscence. Further analysis linked the abnormal phenotype to increased levels of hypomethylation throughout the plant (K Engel

unpublished data), as was expected; however higher levels of active cytokinin were also observed. Thus ADK appears to be integral in regulating cytokinin levels as well as recycling methylation intermediates.

To investigate the relationship between the subcellular localization of SAH production and its metabolism, immunogold labelling was performed on leaf and meristematic tissues of Arabidopsis using antibodies specific for either ADK or SAH hydrolase. As well, β-glucuronidase and green fluorescent protein translational fusions of each enzyme were examined (S. Lee unpublished data). Results of both the immunogold labelling and fusion lines revealed that all ADK and SAH hydrolase isoforms localize to the cytosol, chloroplast and nucleus. Further analysis of purified chloroplasts has given varying results regarding the targeting of these enzymes to the organelle, and further research will be required before ADK and SAH hydrolase can be conclusively localized to the chloroplast.

TABLE OF CONTENTS

LIST OF FIGURES

LIST OF TABLES

ABBREVIATIONS

ADA	Ado deaminase
Ade	Adenine
Ado	Adenosine
ADK	Adenosine kinase
AMP	Adenosine monophosphate
AN	Adenosine nucleosidase
ATP	Adenosine triphosphate
APT	Adenine phosphoribosyltransferase
BSA	Bovine serum albumin
CK	Cytokinin
EDTA	Ethylene diamine tetraacetic acid
EST	Expressed sequence tag
GFP	Green fluorescent protein
GUS	β-glucuronidase
Hcy	Homocysteine
HEPES	N-[2-Hydroxyethyl]piperazine-N'-[2-ethanesulfonic acid]
LR	London Resin
MT	Methyltransferase
PBS	Phosphate buffered saline
PCR	Polymerase chain reaction
PVP	Polyvinylpyrrolidone

RT-PCR	reverse transcription-polymerase chain reaction
SAH	*S*-adenosylhomocysteine
SAHH	*S*-adenosylhomocysteine hydrolase
SAM	S-adenosylmethionine
SEM	Scanning electron microscope
SD	Standard deviation
SMM	*S*-methyl-methionine
SDS	Sodium dodecyl sulphate
TEM	Transmission electron microscope
WT	Wild-type

INTRODUCTION

Overview

The recycling of adenosine (Ado) into adenosine monophosphate (AMP) plays an important role in plant development and metabolism by not only providing the necessary precursors for primary and secondary metabolites including adenylate nucleotides, but by also maintaining methyl recycling throughout the cell. Although plant genomes encode more than one enzyme capable of Ado metabolism, adenosine kinase (ADK, EC 2.7.1.20) is believed to catalyze the predominant route for Ado salvage by phosphorylating Ado to AMP.

Of the Ado being recycled, a large quantity is committed to synthesizing *S*-adenosylmethionine (SAM). SAM is the predominant methyl donor in transmethylation reactions. The transfer of a methyl group from SAM during transmethylation generates the by-product *S*-adenosyl-L-homocysteine (SAH). The subsequent breakdown of SAH by *S*-adenosyl-L-homocysteine hydrolase (SAHH, SAH hydrolase; EC 3.3.1.1) releases Ado back into the nucleotide pool, as well as providing homocysteine (Hcy) to be used in the regeneration of SAM. Thus by breaking down SAH, SAH hydrolase is able to ensure that Ado and SAM are recycled.

The research described in this thesis explores several aspects of ADK and SAH hydrolase activities in plants, using *Arabidopsis thaliana* as a model system. To determine the importance of ADK in plant metabolism, mutant lines deficient in ADK were examined for their abundance of ADK transcripts and enzyme activity, methyl-metabolite synthesis, methylation and organ development. Additionally, transgenic plants

expressing the β-D-glucuronidase (GUS) reporter under the control of either ADK or SAH hydrolase promoters were also generated to study the expression of the genes throughout the plant at the transcriptional level. Finally, to further our understanding of how methylation occurs in multiple compartments within the plant cell, the subcellular localization of ADK and SAH hydrolase isoforms was studied.

Arabidopsis thaliana

Arabidopsis thaliana is in many ways a classic example of the model organism, having more value in the laboratory than in the field. A member of the Brassicaceae family, *A. thaliana* is a small, self-fertilizing plant (see Figure 1) native to the Northern Hemisphere. Numerous ecotypes of *A. thaliana* have been isolated with Columbia (Col) and Landsberg (Ler) being two of the most commonly used. Due to its lack of agricultural value, *A. thaliana* has been traditionally considered nothing more than a weed. However, in the past 40 years *A. thaliana* has risen to become one of the most studied and characterized organisms in the field of genetics.

There are several factors that make *A. thaliana* ideal for research, including that it is easily maintained in a laboratory setting, only reaching a maximum height of 30 cm and requiring a moderate temperature and light regimes (19°C and 120 μE, respectively). Additionally, *A. thaliana* has a short generation time and high seed production. For example, *A. thaliana* (*Col*) has a lifespan of 6-8 weeks and begins producing seed after 4-5 weeks, ultimately releasing 1000-5000 seeds per plant (Bowman, 1994). Along with these physiological advantages, the genome has several features that make it amendable to molecular studies. One such advantage is its small (125 Mbp), diploid genome (Dennis and Surridge, 2000), making it much easier to manipulate than other higher plants such as

the 466 Mbp rice (*Oryza sativa L.* ssp. *Indica*) genome (Yu et al., 2002). The *A. thaliana* genome is further simplified by containing a relatively low abundance of transposable elements and repetitive DNA, small introns and few gene families (The *Arabidopsis* Genome Initiative, 2000). Finally, *A. thaliana* is easily transformed using *Agrobacterium tumefacians* (Clough and Bent, 1998).

An additional benefit to using *A. thaliana* is the large knowledge base that already exists and the extensive scientific community actively sharing information and research. The fully sequenced genome of *A. thaliana*, stocks of mutant lines and results of high throughput experiments are all publicly available. This project has relied on several of these features to examine the involvement of SAH hydrolase and ADK in methyl recycling.

Activated Methyl Cycle

SAM is the predominant methyl donor in eukaryote transmethylation reactions, with the actual transfer of the methyl group catalyzed by methyltransferases (MTs, EC 2.1.1) specific for particular substrates (Poulton 1981). MT activities are essential for the synthesis/ functionality of hundreds of compounds in plant cells including DNA and mRNAs, pectin, lignin and phosphatidylcholine. Upon methylation of these acceptors a molecule of *S*-adenosyl-L-homocysteine (SAH) is produced (see Figure 2). Thus, given the breadth of SAM-dependent methylation activities, cells are continuously generating SAH. In eukaryotes and some prokaryotes, SAH is cleaved into L-homocysteine (Hcy) and Ado by SAH hydrolase (de la Haba and Cantoni, 1959). The SAH hydrolase-catalyzed reaction serves two important functions: it provides the precursor for the regeneration of Met and ultimately SAM, thereby maintaining the availability of these

compounds for cellular metabolism, and it also reduces the accumulation of SAH which would otherwise competitively inhibit MT activities (Poulton, 1981).

However, since the reaction catalyzed by SAH hydrolase is reversible and its equilibrium lies in the direction of SAH formation (de la Haba and Cantoni 1959), it must be drawn in the direction of SAH hydrolysis through the constant removal of both products, Ado and Hcy. Otherwise SAH would not be broken down and MT activities would be inhibited. Hcy is metabolized to Met, either by Met synthase (EC 2.1.1.13) or Hcy *S*-methyltransferase (EC 2.1.1.10), and the resulting Met is subsequently converted to SAM, via SAM synthetase (EC 2.5.1.6) or back to *S*-methylmethionine (SMM) by Met *S*-methyltransferase (MMT, EC 2.1.1.12) (Hanson et al., 1994). Although it is not yet known in *A. thaliana*, the amount of Met tied up in the SMM cycle has been studied in maize, where MMT knockout mutants exhibit SAM levels 15% higher than that of the WT control (Kocsis et al., 2003). The purpose of diverting Met through the SMM cycle has been suggested as a mechanism to regulate SAM levels, with the formation of SMM serving as a reservoir of SAM precursors during periods of increased methylation.

In plant cells, the majority of the Ado resulting from SAM-dependent MT activities is salvaged by ADK (Moffatt et al., 2000). This was most clearly demonstrated during periods of increased methylation activity in spinach, where during the synthesis of the methylated osmolite glycine betaine, in response to salinity stress, ADK and SAH hydrolase expression and activities increase 2-3 fold (Weretilnyk et al., 2001).

Figure 1. Five-week-old *Arabidopsis thaliana.*

A fully developed Arabidopsis plant is shown. The rosette leaves form at the base of the plant from which the shoots develop, while cauline leaves arise from the shoots and secondary branches. Located on top of the developing shoots, floral meristems produce buds which then develop into flowers, and upon self fertilization, become siliques (fruit). As long as the plant is viable, siliques are formed thus various stages of silique development can be observed along the same shoot.


Inflorescence
Silique
Cauline leaf
Rosette leaf
5 cm

These increases match well with the changes in the MT activity required to synthesize glycine betaine indicating that ADK expression is responsive to the increased flux through the activated methyl cycle (Weretilnyk et al. 2001). In addition to responding to stress, ADK and SAH hydrolase expression fluctuates accordingly to lignin synthesis (methylation being a key component in lignin monomers) throughout Arabidopsis (Pereira et al., 2006).

Methyl Sinks

SAM, along with donating methyl groups to MT, is a precursor for the synthesis of various compounds including ethylene, polyamines, biotin and nicotinamides, all of which are necessary for plant development. Both biotin and nicotinamide serve as vitamins essential to all eukaryotes, with biotin transports dissolved bicarbonates needed for macromolecule metabolism (McMahon, 2002) and nicotinamides actings as precursors to ß-nicotinamide adenine dinucleotide (NAD^+) coenzymes responsible for generating ATP in the mitochondria (Ishaque and Al-Rubeai, 2002). Due to their reliance on SAM as a common precursor, the plant growth regulators ethylene and polyamines are of particular interest to this study.

Ethylene is formed through the conversion of SAM to 1-aminocyclopropane-1-carboxylic acid (ACC) by way of ACC synthase; ACC oxidase then reacts with ACC to produce ethylene (Jakubowicz, 2002). As a growth regulator, ethylene affects numerous stages of plant development by promoting the induction of fruit ripening (Nakatsuka et al., 1998), flower senescence (Kamachi et al., 1997), petal (Clark et al., 1997) and leaf abscission, the inhibition of seedling elongation (Ishiki et al., 2000), and the stimulation

of root initiation (Llop-Tous et al., 2000). Additionally, ethylene mediates cell signalling associated with responses to a variety of stresses including drought, cold, anoxia and pathogens (Avni et al., 1994; Lelievre et al., 1997; Kato et al., 2000; Cao et al., 2006).

Like ethylene, polyamines have been associated with root growth, somatic embryogenesis, floral initiation, and the development of flowers and fruits, as well as cell signalling in response to plant stress (Walters, 2003). Although there is more than one kind of polyamine present in higher plants, the most common are putrescine, spermidine and spermine, all of which arise from decarboxylated SAM (Pandey et al., 2000). While ethylene and polyamines share a common precursor, it is not quite clear whether or not SAM is prioritized to ethylene or polyamine synthesis. In many cases during development, such as during fruit ripening and leaf/flower senescence, ethylene and polyamine biosynthesis are in fact antagonistic and inhibit the production of the other (Pandey et al., 2000).

Despite these multiple sinks, it is commonly believed that SAM is never limiting for the transmethylation cycle. For example, in the case of *Lemna* it is estimated that >90% of SAM is tied up in the activated methyl cycle (Mudd and Datko, 1986). However in mutants unable to produce SAH hydrolase or ADK at high enough levels to ensure proper recycling of SAH, there is a potential for reallocation of SAM flux to different sinks. Such mutants can also be used to study the impact of ADK deficiency on functions requiring Ado salvage, including the maintenance of nucleotide pools, cytokinin (CK) interconversion and gene silencing in response to pathogens.

Figure 2. SAM methylation cycle.

Upon methylation of the acceptor, a molecule of *S*-adenosyl-L-homocysteine (SAH) is produced and cleaved into L-homocysteine (Hcy) and Ado by SAH hydrolase (SAHH). However, since the reaction catalyzed by SAH hydrolase is reversible and its equilibrium lies in the direction of SAH formation, it must be drawn in the direction of SAH hydrolysis through the constant removal of both products, Ado and Hcy. Hcy is metabolized to Met, either by Met synthase or Hcy *S*-methyltransferase (HMT) and the resulting Met is subsequently converted to SAM, via SAM synthetase (EC 2.5.1.6) or back to *S*-methylmethionine (SMM) by Met *S*-methyltransferase (Met S-MT). Other minor routes for Ado salvage are discussed in Chapter 1.

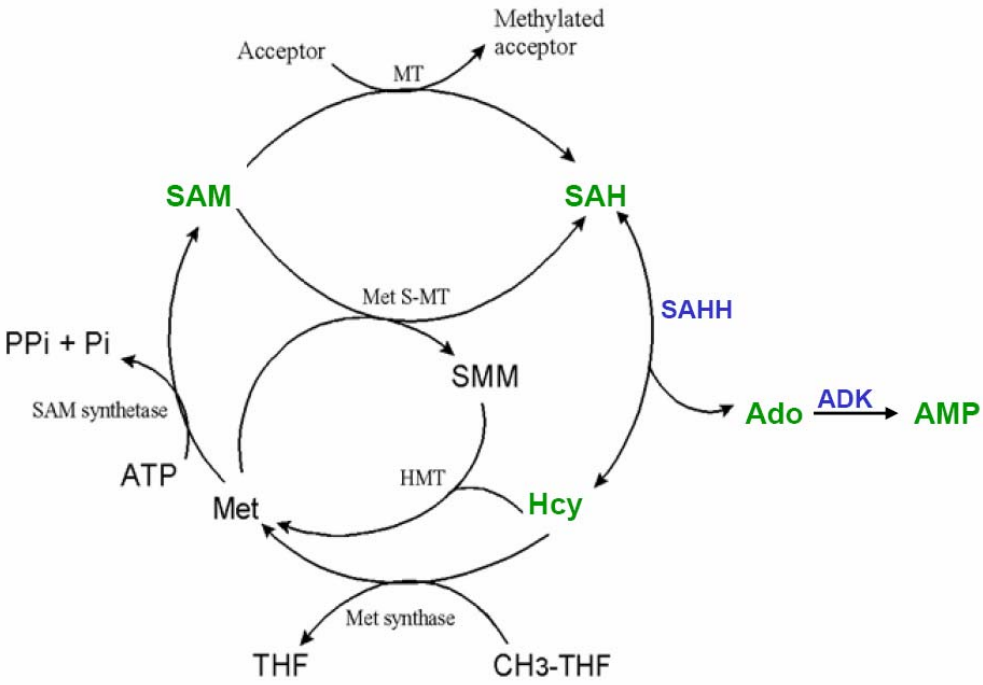
Acceptor
Methylated acceptor
MT
SAM
SAH
Met S-MT
SAHH
PPi + Pi
SMM
SAM synthetase
Ado
ADK
AMP
ATP
HMT
Met
Hcy
Met synthase
THF
CH3-THF

Maintenance of Nucleotide Pools

Plants as well as animals are capable of regenerating their nucleotide pools through salvage pathways. Nucleotide bases and nucleosides resulting from the breakdown of nucleic acids (Guranowski and Wasternack, 1982), and the hydrolysis of SAH within the SAM cycle and from by-products formed by the conversion of methionine (Met) to ethylene, are all potential sources for the salvage of Ado and adenine (Stasolla et al., 2003). The advantages associated with the salvaging of nucleotides as opposed to the *de novo* pathway are the recycling of limited nitrogen sources and energy conservation. In addition to conserving nucleotide pools, the conversion of Ado to AMP plays a vital role in cell signalling by way of CK interconversion and biosynthesis.

Cytokinin Interconversion and Biosynthesis

CKs are a class of plant-specific growth regulators that play a central role in controlling the cell cycle and influencing numerous developmental programs including cell signalling for apoptosis (Carimi et al., 2003), pollen development in response to gibberellin (Huang et al., 2003), meristem activity and morphology (Huang et al., 2003), chloroplast biogenesis (Hoth et al., 2003) and cell division (Hoth et al., 2003). The most predominant class of CKs is comprised of N^6-substituted adenines, which are generally thought to be synthesized via the addition of an isopentenyl group to ATP creating isopentenyladenosine monophosphate (iPMP) (Kakimoto, 2003). Modification of the side chain leads to the formation of zeatin monophospate (ZMP) and other derivatives. An alternate iPMP-independent pathway has been proposed to exist in *A. thaliana* in which ZMP is formed directly by the addition of an alternate side chain to AMP (Mlejnek and

Prchazka, 2002). Thus by converting Ado to AMP, ADK helps maintain CK precursor levels.

It is thought that the free bases and riboside forms of CKs are the biologically active compounds and their interconversion to the nucleotide and conjugation with sugars, amino acids or phosphorylation creates storage, transport or inactivated forms of the molecule (Astot et al., 2000). Based on the results of *in vitro* assays it has been proposed that ADK contributes to the interconversion of CK ribosides and nucleotides (Chen and Eckert, 1977; Moffatt et al., 2000), although it is not clear if this occurs in *in vivo* since the affinity of *A. thaliana* ADK for a CK riboside, as estimated by its apparent K_m, is 10-fold lower than for Ado and ADK's catalytic efficiency (V_{max}/K_m) is 250-fold lower on CK ribosides versus Ado (Moffatt et al. 2000). A more recent study found that the 4 isoforms of ADK in BY-2 tobacco cells had strong affinities for not only Ado but isopentenyladenosine, zeatin riboside and dihydrozeatin riboside (Kwade et al., 2005). ADK's *in vivo* role in CK metabolism has only been documented in a few cases to date. Chloronemal tissues of the moss *Physcomitrella patens* incorporate exogenously fed isopentenyladenosine into its nucleotide pools, via a route that must depend on ADK activity (von Schwartzenberg et al., 1998). The importance of ADK in such a role has also been shown in tobacco where isopentenyladenosine-induced apoptosis in BY-2 cultured cells was dependent on the intracellular phosphorylation of iPA to iPMP by ADK (Mlejnek and Prchazka, 2002). Analysis of CK metabolism and CK composition in the ADK-deficient lines of *A. thaliana* may provide further insight into the contribution of ADK to CK homeostasis.

Plant Pathogen Responses and Gene Silencing

As well as maintaining methylation needs associated with abiotic stress responses, ADK activity is also involved in pathogen resistance. Studies conducted by (Wang et al., 2005) indicated that in *Nicotiana tabacum,* ADK activity increases in response to geminivirus infection that depletes cellular ATP, most likely to provide alternate routes for the synthesis of adenylate nucleotides. The rise in ADK activity is mediated by the action of the metabolic regulator SNF kinase which is induced by increased AMP: ATP ratios. Interestingly, infection of *N. tabacum* by *Begomovirus* and *Curtovirus* geminiviruses leads to the expression of viral proteins (AL2 and L2) that inactivate both SNF kinase and ADK in order to disable this plant defence system.

It has become evident in the last few years that RNA silencing is a key mechanism used by plants to limit viral infections. In the case of RNA silencing, small RNAs resulting from the cleavage of double-stranded RNA inhibit epigenetic gene expression in both the cytoplasm and the nucleus (Matzke et al., 2001). The gene silencing itself can occur by the post-transcriptional degradation of complementary mRNAs, and in the case of plants, transcriptional gene silencing of homologous DNA sequences. Viral sequences can then serve as both a trigger and a target of RNA silencing as viral double-stranded RNA is detected by the RNAi surveillance mechanism and cleaved into single-stranded RNA (Waterhouse et al., 2001). To adapt to this defence mechanism, many plant viruses develop proteins such as AL2 and L2 that interfere with silencing pathway components and as a result counter the silencing activity of the host (Brigneti et al., 1998; Voinnet et al., 1999). Plants may also suppress viral replication through the methylation of viral DNA (Brough et al., 1992), in which case the virus may avoid the defence mechanism by

inhibiting ADK and thereby SAM-dependent DNA methylation. Thus a loss of ADK may leave the plant more vulnerable to viral infection.

ADK

ADK has been characterized from a wide range of eukaryotes, including yeast (Caputto 1951, Kornberg and Pricer 1951), humans (Spychala et al., 1996), wheat (Chen and Eckert, 1977), lupin (Guranowski, 1979), peach (Faye and Le Floch, 1997) *Physcomitrella patens* (Von Schwartzenberg et al., 1998) and *A. thaliana* (Moffatt et al.,2000). The enzyme functions as a monomer, and depending on the organism, has a molecular weight of 34 to 56 KDa (34 KDa in Arabidopsis), a pH optimum between 4.8 and 8.0 and a temperature optimum ranging from 30 to 41°C (Schomburg et al., 2004). Kinetic studies conducted using purified enzyme established ADK's utilization of Ado versus other ribose sugars and the requirement for ATP and divalent cations such as Mg^{2+} to catalyze the phosphorylation of Ado to AMP (Moffatt et al., 2002). Further examination of the crystal structure of human ADK found it to closely resemble ribokinase, in addition to containing the substrate binding sites for ATP and divalent cations (Mathews et al., 1998).

Until recently, it was believed that ADK was only expressed in eukaryotes; however, the recent identification and characterization of an ADK in *Mycobacterium tuberculosis* indicates it is present in some prokaryote species as well. The *M. tuberculosis* ADK had been categorized previously as a sugar kinase with unknown function due to its stronger sequence homology with ribokinase and fructokinase than other ADKs. Whether or not other prokaryotes are also expressing ADK activities requires further study.

ADK Gene Expression

To begin to formulate a model for the role of ADK activity, the expression of ADK genes in the major organs of different plants must be known, as the demand for ADK varies between specific tissues in order to sustain their adenylate nucleotide and SAM pools and possibly, CK interconversion. In addition, if multiple ADK coding sequences are present in a genome, they may be expressed in response to different signals. In the case of *A. thaliana*, there are two genes encoding ADK designated as *ADK1* (At3g09820) and *ADK2* (At5g03300); these genes share 92% amino acid and 89% nucleotide identity (Moffatt et al., 2000).

Studies on the response of *ADK* transcripts to stress are consistent with the hypothesis that transcription of *ADK* increases in association with SAM-dependent methylation activities (Koshiishi et al., 2001; Kocsis et al., 2003). Examination of *ADK* transcript abundance in major organs of *A. thaliana* by northern analysis showed that both genes are expressed constitutively, with higher steady-state mRNA levels in stem and root (Moffatt et al., 2000). In all cases, *ADK* transcript abundance increased in association with changes in SAH hydrolase transcript levels (Todorova 2002) and methylation indicators.

More than one high-throughput method has been used to assess changes in transcript abundance in different organs of *A. thaliana*; several of them detected changes in *ADK* expression. Massively Parallel Signature Sequencing (MPSS) is a relatively new technique which has been applied to evaluate Arabidopsis expression (Brenner et al., 2000). MPSS produces short sequence signatures originating from a defined position within an mRNA, and the relative abundance of these signatures in a given library

represents a quantitative estimate of expression of that gene. In all the tissues tested, with the exception of siliques, *ADK1* transcripts were twice as high as those of *ADK2*. In expanding green siliques (stage 16-17) *ADK1* transcript levels were four-fold higher than those of *ADK2* (see Figure 3).

The analysis of microarray data compiled by Genevestigator database (Zimmermann et al., 2004) also indicates higher *ADK1* transcript abundance in stems and roots as compared to flowers and leaves. Although the microarray data does not show a significant difference in *ADK1* and *ADK2* transcript abundance, possibly due to lack of specificity in detection of the mRNAs, a trend of higher levels of *ADK1* is still observed. In order to further assess the possible role of these isoforms, mutants lacking either ADK1 or ADK2 through T-DNA insertions (tagged lines) were identified and examined in this thesis research.

ADK Mutants

GT6-2 is an *A. thaliana* (Landsberg) mutant containing a T-DNA insertion in *ADK1-1* that exhibits cytokinin overproduction and an over-proliferating shoot apical meristem (A. Para and A. Sundås-Larsson, Uppsala University, unpublished results). Overall, however, the insertion does not appear to affect the vitality of the plant since the mutant retains 45% of the ADK activity found in WT plants. On the other hand, *A. thaliana* lines deficient in ADK activity due to trans-gene silencing (sADK lines) have very little residual ADK activity (Moffatt et al., 2000). Use of these sADK lines has provided direct evidence that this enzyme is essential for maintaining SAM-dependent transmethylation activities in Arabidopsis, for most affected lines have up to 40-fold higher levels of SAH than that of the wild-type parent, presumably due to the reversal of SAH hydrolase

activity resulting from excess Ado. In addition to increased SAH levels, the mutants display wrinkled leaves, clustered inflorescences and weak apical stem development (Moffatt et al., 2000). The increased SAH levels are correlated with the severity of their phenotype and with the inhibition of the MTs acting on pectin (Pereira et al. 2006). The observation that tobacco plants deficient in SAH hydrolase activity have morphological changes similar to those observed in the ADK-deficient lines and their genomic DNA is also hypomethylated (Masuta et al., 1995b) supports the conclusion that the changes in the ADK-deficient lines are associated with ADK's role in the activated methyl cycle.

SAH Hydrolase

As SAH hydrolase is the only eukaryotic enzyme capable of metabolizing SAH generated by intercellular SAM methylation, much study has been dedicated to understanding its composition and activity, although the vast majority of this work has been focused on the enzyme from animals rather than plants. While SAH hydrolase was once believed to be exclusive to eukaryotes, it has also found in many prokaryotes (Shimizu et al., 1984). However, prokaryotes containing SAH hydrolase are still in the minority; the majority rely on SAH nucleosidase (EC 3.2.2.9); 5′-methylthioadenosine nucleosidase (EC 3.2.2.16) and/or *S*-ribosyl-homocysteine hydrolase (EC 3.3.1.3) (Duerre and Schlenk 1962; Walker and Duerre 1975).

Mammalian SAH hydrolases are composed of homotetramer 48 kDa subunits (Bethin et al., 1995), while plants generally have a homotetramer of 53 kDa subunits; the exception being yellow lupin, which is reported to be a homodimer (Guranowski and Pawelkiewicz, 1977). The difference between the plant and mammalian SAH hydrolase subunit molecular weights results from an internal stretch of 41 amino acids (positions

164-205) and a longer NH_2-terminal region in the plant enzyme, for a total of 485, whereas the mammalian protein consists of 432 residues. Overall, SAH hydrolase has a pH optimum ranging between 6.4 and 8.5, and temperature optimum between 30 to 55°C (Schomburg et al., 2004). A comparison of the apparent K_ms for Ado, SAH and Hcy reveals SAH hydrolase to have a higher affinity for Ado (Schomburg et al., 2004).

Sequence alignments at either the nucleic or amino acid level show SAH hydrolase to be highly conserved across species (Schomburg et al., 2004), even between humans and prokaryotes. The most conserved sequences of SAH hydrolase can be found around the catalytic sites, which consist of three domains: the SAH-binding domain, the nicotinamide adenine dinucleotide (NAD)-binding domain and the Ado binding domain (Gomi et al., 1989). Thus study of SAH hydrolase activity and function in plants is relevant to other eukaryotes.

SAH hydrolase Expression

As with ADK, *A. thaliana* has two highly similar SAH hydrolase isoforms: SAHH1 (encoded by At4g13940) and SAHH2 (encoded byAt3g23810) which have a 92% nucleic acid and 95% amino acid identity. These genes are also constitutively expressed throughout the plant at different levels. Northern blots and semi-quantitative PCR, show that *A. thaliana* SAH hydrolase transcripts are present in all organs with stems and siliques stages 16, 17a having the highest abundance; buds, flowers and 17b siliques at moderate levels and leaves and dry seeds the lowest (Todorova 2002). In all cases, *SAHH*1 mRNA transcripts are higher than *SAHH*2. In fact *SAHH*2 is near the limit of detection in roots and leaves (Todorova, 2002), in mature plants.

Figure 3. Expression of ADK and SAH hydrolase genes in mature Arabidopsis.

Transcript levels were examined using microarray data obtained from Genevestigator (A; Zimmermann et al. 2004) and MPSS (B; Brenner et al. 2000) databases in September 2006. In the microarray data obtained (A), standard deviations were obtained using triplicates of normalized signal data while MPSS data only had one data set of measured transcript (B) so a standard deviation could not be obtained. Both methods of measurement show *ADK1* to be present at higher levels in all organs, the only exception being in the root tip where isoforms are almost equal. However there is a discrepancy between the two types of measurements in that the MPSS data shows significantly lower levels of *ADK2* transcripts relative to that of *ADK*. This inconsistency also emerges for the SAH hydrolase isoforms. Aside from the stem, microarray data shows *SAHH1* to be present at higher levels than *SAHH2*. Despite showing the same pattern of expression, MPSS data shows a larger disparity in expression levels between the two isoforms.

A

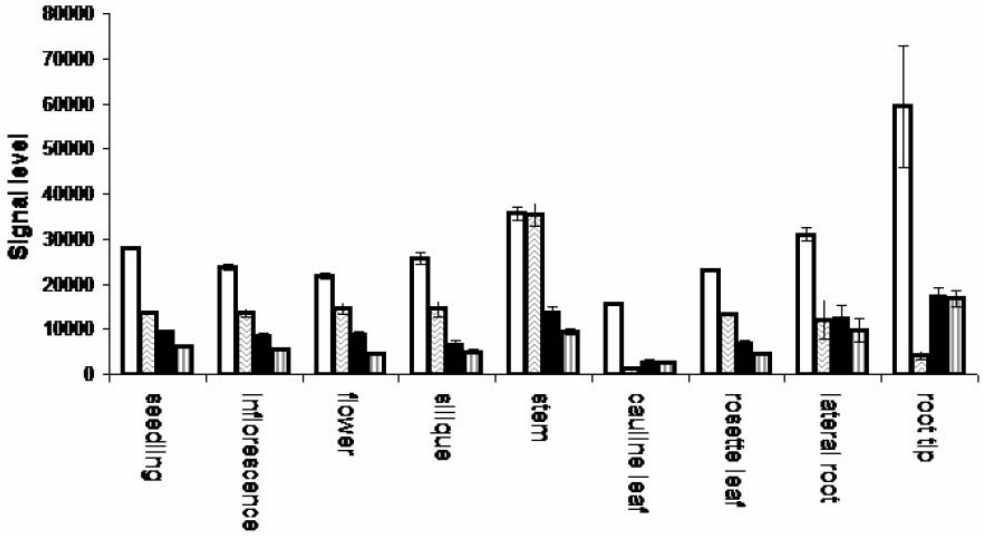
Signal level
80000
70000
60000
50000
40000
30000
20000
10000
0
seedling
inflorescence
flower
silique
stem
cauline leaf
rosette leaf
lateral root
root tip

B

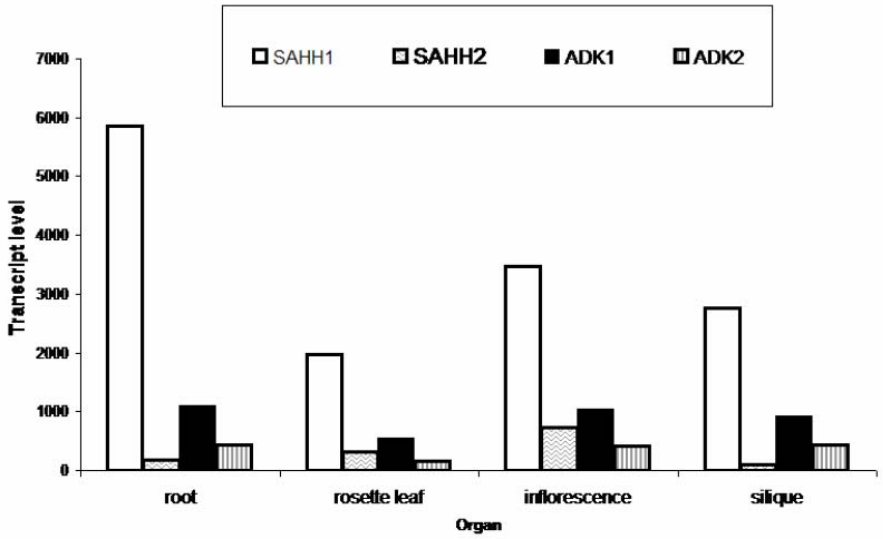
SAHH1
SAHH2
ADK1
ADK2
Transcript level
7000
6000
5000
4000
3000
2000
1000
0
root
rosette leaf
inflorescence
silique
Organ

Examination of high throughput transcript profiling data also reveals *SAHH*1 to be the more highly expressed of the two genes. MPSS data (Brenner et al. 2000) suggest *SAHH*1 mRNA levels are 10-fold higher than *SAHH*2 transcript levels (see Figure 3B). *SAHH1* displayed the following pattern of tissue expression (from highest to lowest): root > inflorescence > siliques > leaf. In many organs and stages of development, *SAHH*2 mRNA was barely detected, with the greatest abundance being found in the stem, whereas the lowest levels were found in roots (Figure 3B). Although microarray data compiled in Genevestigator also revealed *SAHH*1 to be present at higher levels than *SAHH*2, the difference in expression only ranged between 1.5 to 4-fold (Figure 3A). Both isoforms had higher levels of expression in stem, stamen, hypocotyls and zone of elongation in *A. thaliana*.

The relationship between SAH hydrolase activity and the synthesis of methylated compounds has been investigated in several plants. SAH hydrolase activity has been characterized in spinach (Poulton and Butt, 1976), tobacco (Sebestova L et al., 1983), alfalfa (Edwards and Dixon, 1991), parsley (Kawalleck et al., 1992) and *Catharanthus roseus* (Schroder et al., 1994; Eckermann et al., 2000) and in each case SAH hydrolase activity fluctuated with metabolic and developmental processes such as the synthesis of methylated secondary products such as lignin.

SAH Hydrolase Mutants

Mutants deficient in SAH hydrolase activity have been isolated from several organisms including Rhodobacter (Sganga et al., 1992), mice (Miller et al., 1994), and tobacco (Tanaka et al., 1997). Not surprisingly, deletion of the only SAH hydrolase gene in the mice genome results in embryo lethality (Miller et al., 1994). An insertional mutant in the

SAH hydrolase gene of Rhodobacter lacks detectable SAH hydrolase activity, and as a result, the intracellular SAM: SAH ratio decreases 16-fold as compared to that of wild-type cells. The only phenotypic change in these mutants noted by the authors was a significant reduction in bacteriochlorophyll biosynthesis (Sganga et al., 1992); this is significant as the synthesis of this compound requires methylation. The authors propose SAH hydrolase deficiency is tolerated by the bacteria due to the presence of SAH nucleosidase or *S*-ribosyl-homocysteine hydrolase (Walker and Duerre 1975).

SAH hydrolase-deficient tobacco lines, created through antisense gene silencing, (Tanaka et al., 1997) have higher SAH levels, in some cases 10-fold higher than the wild-type (WT) parent (Masuta et al., 1995). These lines are also associated with floral organ abnormalities, stunting of growth, loss of apical dominance, delayed senescence, hypomethylation of repetitive DNA, resistance to plant viruses requiring a methylated cap for their replication and cytokinin levels three-times that of the wild-type parent (Masuta et al., 1995a; Tanaka et al., 1997).

Interestingly, insertion mutants of SAHH1 (SALK 23915) and SAHH2 (SALK 134541) in *A. thaliana* have distinct phenotypes; while eliminating the expression of SAHH2 does not appear to have any affect on development, removing SAHH1 results in embryo lethality (Seed Genes Project; www.seedgenes.org; emb1395). Taken together with the expression data, these phenotypes suggest that SAHH1 is the predominant form of the enzyme in plants, with SAHH2 playing only a limited role.

Subcellular Localization of SAHH and ADK

SAM-dependent transmethylation occurs throughout the entire cell, mediating vital processes such as cell signalling in the cytosol to chromatin modification in the nucleus

and methylation of chlorophyll precursors in organelles. Each of these reactions produces SAH which must be metabolized to prevent inhibition of MTs. Since SAH hydrolase is thought to reside only in the cytosol it remains to be determined how SAH is removed in other compartments. One possibility is that SAH is transferred out of the compartment and into the cytosol (Ravanel et al., 2004; Palmieri et al., 2006). Conversely, SAH hydrolase and ADK may reside within each subcellular compartment. In order to address the validity of either hypothesis, the current understanding of protein transport must first be understood.

Proteins are translated in the cytoplasm on either free or 'bound' ribosomes (cytosolic or ER-associated respectively). Upon being synthesized, proteins are directed to their appropriate cellular compartments. One method utilized by the cell to mediate protein trafficking is the use of target signals within the peptide sequence (Emanuelsson et al., 2000). Proteins destined for the mitochondria or chloroplast, contain signal peptides located within their N-termini (Peeters and Small, 2001). While most nuclear localization signals (NLS) are distributed throughout the coding sequence, although other nuclear bound proteins having no apparent targeting motif (Nair et al., 2003). In addition to specific transport systems, nuclei also contain nuclear pores which are believed to transport proteins up to 50-70 kDa (Merkle et al., 1996; Liu et al., 2003), thus allowing simple diffusion to occur. Assuming this to be the case, it may not be possible for a 4 x 53 kDa SAH hydrolase to enter via the NP, unlike the 32 kDa ADK.

Computer algorithms have been created based on documented motifs present in proteins found in each cellular compartment. The most commonly used programs to predict subcellular location are Mitoprot (Claros and Vincens, 1996), ChloroP

(Emanuelsson et al., 1999), PSORT (Nakai and Horton, 1999) and TargetP (Emanuelsson et al., 2000). However the main limitation associated with these prediction methods is the lack of known targeting signals. So while a program like TargetP may have 85% reported accuracy for proteins with known signal motifs, proteins with unconventional targeting signals are not recognized (Heazlewood et al., 2005). Therefore, the prediction that ADK and SAH hydrolase are exclusively localized to the cytosol based on these programs is not conclusive (see Table 1). Part of the research described in this thesis sought to establish whether SAH hydrolase and ADK are purely cytosolic proteins or whether they are in fact targeted to other subcellular compartments as well.

Objectives

The research described in this thesis had three principal objectives:

1. *A. thaliana* lines deficient in ADK activity have a distinct vegetative morphology (Moffatt et al. 2000) but this has yet to be examined in detail; particularly in comparison to that of mutants lacking only ADK1 or ADK2. Thus the first goal of this research was to perform a series of growth assessments and microscopic analyses on the lines to evaluate the contribution of overall ADK activity, as well as each isoform individually, to plant development.
2. In order to gain further insight into ADK and SAH hydrolase expression, transgenic lines expressing a reporter gene under the control of ADK and SAH hydrolase promoters were generated. Lines were selected based on expression patterns obtained from northern blots and microarray data. Future use of these

lines will not only display the role of each isoform in plant growth but also reveal the molecular mechanism underlying these functions.

3. The final goal was to test the hypothesis that ADK and SAH hydrolase reside in multiple subcellular compartments. This was done using immunogold labelling and GUS fusion lines generated by fusing ADK or SAHH cDNA to GUS under the control of a constitutive promoter.

Table 1. Predictions for subcellular localization of ADK and SAH hydrolase isoforms.

Based on recurring signal sequences identified in targeted proteins, programs have been created to predict the subcellular localization of proteins. Aside from SignalP, the programs shown are capable of generating a number values corresponding to the probability of the protein localizing to a particular compartment. WoLF requires a reading of 6; TargetP 1.1 and ChloroP 1.1 need a score of 1.0 and SubLoc 1.0 assigns a compartment with a value of accuracy, the highest being 1.0). All five programs have the cytosol set as their default localization if no known signal is detected in the protein. Thus, based upon these computer algorithms, ADK and SAH hydrolase isoforms are predicted to be localized in the cytosol. However, these findings do not exclude the possibility that ADK and SAH hydrolase may contain novel or cryptic signal sequences that direct them to compartments in addition to the cytosol Data were collected January 2006.

Program	Localization	ADK1	ADK2	SAHH1	SAHH2	Publication	URL
SignalP 3.0	Mt	-	-	-	-	Bendsten et al. 2004	http://www.cbs.dtu.dk/services/SignalP
	Chl	-	-	-	-		
	Nuc	-	-	-	-		
	Cyt	+	+	+	+		
WoLF	Mt	1	0	2	1		http://wolfpsort.seq.cbrc.jp/
	Chl	0	0	1	1		
	Nuc	0	2	2	1		
	Cyt	10	12	9	11		
TargetP 1.1	Mt	0.038	0.058	0.041	0.042	Emanuelsson et al. 2000	http://www.cbs.dtu.dk/services/TargetP/
	Chl	0.184	0.077	0.153	0.141		
ChloroP 1.1	Chl	0.431	0.429	0.432	0.432	Emanuelsson et al. 1999	http://www.cbs.dtu.dk/services/ChloroP/
SubLoc 1.0	Cyt	0.74	0.74	0.84	0.84		http://www.bioinfo.tsinghua.edu.cn/SubLoc/

CHAPTER 1: ANALYSIS OF THE PHENOTYPE OF ADK-DEFICIENT PLANTS

Introduction

Adenosine (Ado) is generated by numerous processes including the breakdown of nucleic acids (Guranowski and Wasternack 1982), the hydrolysis of *S*-adenosyl-L-homocysteine (SAH) generated from transmethylation and as a result of by-products formed by the conversion of methionine (Met) to ethylene (Stasolla et al., 2003). The Ado is recycled into various compounds including those for energy reserves (ATP, GTP), nucleic acids, nucleotide cofactors and cytokinins (CK). In addition to ensuring the synthesis of energy and metabolites, enzymes capable of recycling Ado also serve to maintain methylation throughout the cell by lowering SAH levels. SAH is a by-product of *S*-adenosylmethionine (SAM)-dependent transmethylation that is inhibitory to methyltransferase activities (de la Haba and Cantoni, 1959). The SAH can be broken down into homocysteine and Ado, in a reversible reaction that is driven in the hydrolysis direction by the removal of Ado. By reducing Ado accumulation that would otherwise inhibit methylation, Ado salvage is vital to a large number of cellular processes including gene regulation/expression, cell signalling and synthesis/ functionality of hundreds of compounds in plant cells including DNA and mRNAs, pectin, lignin and phosphatidylcholine (Vanyushin, 2006).

In addition to decreasing Ado levels, Ado recycling activities may contribute to CK interconversion (Moffatt et al., 2002). CKs are a class of plant-specific growth regulators that play a central role in controlling the cell cycle and influencing numerous

developmental programs. It is thought that the free bases and riboside forms of CKs are the biologically active compounds and their interconversion to the nucleotide along with conjugation to sugars, amino acids or phosphorylation creates storage, transport or inactivated forms of the molecule (Mlejnek and Prochazka, 2002). Thus Ado metabolizing enzymes contribute to several important metabolic pathways in plants.

One route for Ado salvage is catalyzed by the sequential activities of two enzymes: Ado nucleosidase (EC 3.2.2.9; AN) and adenine phosphoribosyltransferase (EC 2.4.2.7; APT) (see Figure 4). AN converts Ado into adenine, while the APT phosphoribosylates adenine into adenosine monophosphate (AMP). Although these enzymes are known to be expressed in plants (Moffatt et al., 1994), with APT even being vital to pollen development (Moffatt and Somerville, 1988), their overall roles in Ado metabolism are considered negligible except for a few cases including caffeine synthesis in tea (*Camellia sinensis* L., (Ashihara and Crozier, 1999; Ashihara and Crozier, 2001) and osmolyte synthesis in *Avicennia marina* (Suzuki et al., 2003).

Another enzyme capable of recycling Ado is adenosine deaminase (EC 3.5.4.4; ADA), which catalyzes the irreversible deamination of adenosine to inosine. ADA activity has been documented in bacteria, vertebrates and invertebrates (Cristalli et al., 2001) where it is considered to be a significant contributor to Ado salvage. Despite the importance of ADA in eukaryotes, it has long been the belief that it is not present in plants (Brady and Hegarty, 1966; Dancer et al., 1997). However with the latest annotation of the Arabidopsis genome now includes the designation of a putative Ado/AMP deaminase enzyme (At4g04880; TAIR database 2005). Comparison of ADA amino acid sequences from animals show a significant homology to At4g04880,

suggesting it is indeed an ADA (Maier et al., 2005). However, analysis at the sequence level does not give information on whether or not the enzyme is functional and what kind of role, if any, the enzyme plays.

The third enzyme and likely the predominant contributor to Ado salvage based on its estimated kinetic activity and high constitutive expression throughout the plant is Ado kinase (ADK, adenosine 5′-phosphotransferase; EC 2.7.1.20) (Moffatt et al., 2000). This enzyme catalyzes the phosphorylation of Ado to AMP.

Mutants can be invaluable tools in determining a protein's role in metabolism and development. Previous studies revealed the presence of 3 APT genes in the Arabidopsis genome, with only *apt1-3* showing a phenotype, of male sterility (Moffatt and Somerville, 1988). ADA mutants have no obvious phenotype (K. Engel and B. Moffatt, unpublished data) and there is no identified AN gene in Arabidopsis as of yet. Thus this study focused on identifying and analyzing Arabidopsis lines deficient in ADK and ADA. ADK-deficient lines were chosen because it is considered the key enzyme for Ado metabolism; ADA-deficient lines were investigated to determine whether or not the corresponding gene product contributes to Ado salvage.

ADK silencing (sADK) lines induced by over-expression of the ADK1 cDNA using a 35S promoter have already been generated (Moffatt et al., 2002). While these lines retain between 4-50% residual ADK activity, their phenotype includes wrinkled leaves, decreased internode length and clustered inflorescences. How a loss of ADK activity leads to this phenotype has not been established and is one focus of this project.

Figure 4. Enzymes involved in Ado salvage.

Three possible routes for Ado salvage are shown; these are catalyzed by Ado nucleosidase (AN), adenine phosphoribosyltransferase (APT) and Ado deaminase (ADA), and adenosine kinase (ADK). AN converts Ado into adenine (A), while the APT phosphoribosylates adenine into AMP (B). ADA catalyzes the formation of inosine from Ado (C). Lastly ADK phosphorylates Ado into AMP (D) Images of the molecular structures were obtained from MetaCyc (Caspi et al., 2006).

A

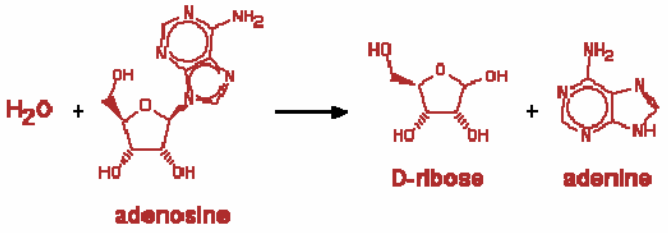
H2O +
adenosine
D-ribose
adenine

B

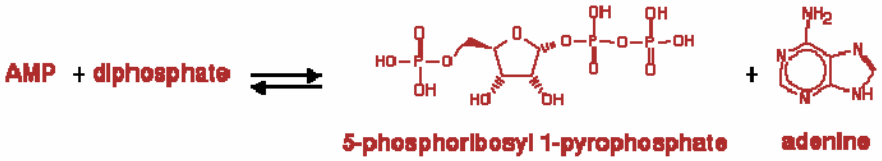
AMP + diphosphate
5-phosphoribosyl 1-pyrophosphate
adenine

C

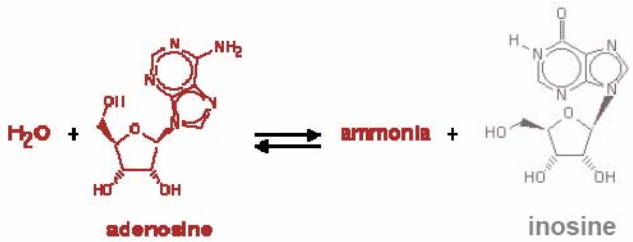
H2O +
ammonia +
adenosine
inosine

D

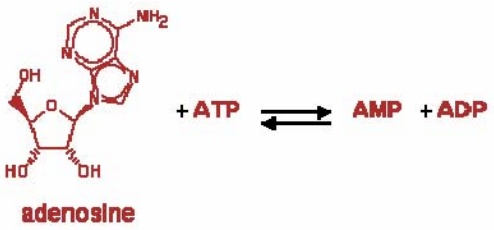
+ ATP
AMP + ADP
adenosine

In addition to examining the sADK lines, plants containing a T-DNA insertion in either *ADK1* (At3g09820) or *ADK2* (At5g03300) were also characterized (see Figure 5). Studying these lines allows one to separate the contributions of the two individual genes. A putative ADA-deficient line was also identified from the T-DNA tagged collection (S. Fry, unpublished data) and used in these experiments.

To establish their impact on Arabidopsis, the mutants' growth was phenotypically analyzed over a period of 8 weeks. During this time, samples were also taken to assess morphology at the microscopic level, Ado and CK levels using GC-MS and degree of genomic methylation. Careful examination of the T-DNA tagged mutants revealed no phenotypic differences in comparison to the WT. RT-PCR performed on the T-DNA insertion lines confirmed that the transcripts are indeed no longer present thus lack of phenotype was not due to the enzyme still being expressed leading to the conclusion that ADK1 and ADK2 do not appear to perform specialized functions, and are instead interchangeable. However, simultaneous loss of both enzymes in the sADK lines results in numerous morphologic and metabolic defects which are concluded to be due to a combination of hypomethylation and increased CK abundance. Although no phenotype was observed in the ADA-deficient line, crossing the mutant with a sADK line resulted in lower levels of ADK activity and a more severe sADK phenotype suggesting ADA does play a role in plant metabolism. Several of the areas of investigation outlined in this thesis were directed by others including studies of DNA methylation (G. Perry and K. Engel) and Ado and CK profiling (R. J. W. Emery, Trent University).

Figure 5. Methods used to generate ADK deficient lines.

Comparison of T-DNA insertion, or tagged lines (A) to silencing lines (B). T-DNA insertion mutants (A) are created by inserting vector DNA into the gene of interest, interrupting or altering gene expression. Screening for a mutant is then performed using right (RP) and left primers (LP) flanking the insert, if the T-DNA is present in both copies of the gene then no amplification should occur. To further confirm the homozyous status of the mutant, PCR is performed with one of the flanking primers and a primer corresponding to the left border of the T-DNA sequence (LB); no amplification occurs in WT gene. While silencing lines (B) are generated by transforming the plant with a vector for the purpose of over-expressing a target cDNA in the sense or antisense orientation; the native gene is not altered. The over-production of the transgene signals the plant's natural defence mechanisms, resulting in the degradation of the target transcript and all similar sequences; the synthesis of the corresponding protein product is thus reduced.

A

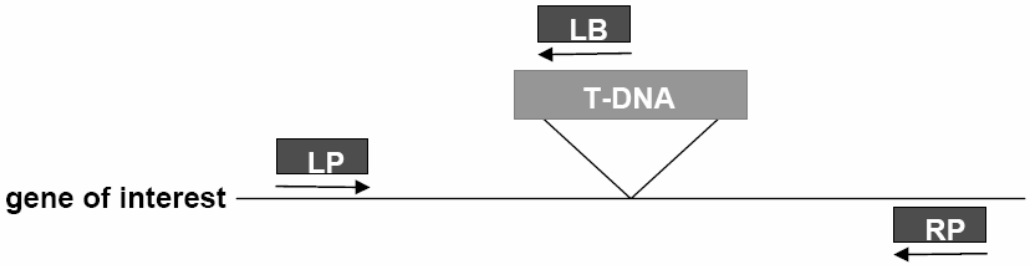
LB
T-DNA
LP
gene of interest
RP

B

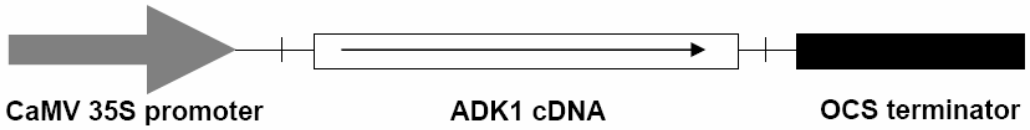
CaMV 35S promoter
ADK1 cDNA
OCS terminator

Experimental Methods

Plant Growth

For growth on soil, 5.5 x 7.8 cm pots were filled with a 50:50 mixture of Sunshine LC1 Mix and Sunshine LG3 Germination Mix (JVK). Through suspension in 0.1% agar solution, seeds were applied to the soil using a Pasteur pipette. Upon adding the seeds, the pots were covered with plastic and incubated in the dark at 4ºC for 24 to 72 hrs. After the mandatory incubation period, the pots were moved to a growth chamber set at 22ºC and 16 hr light (150 ± 20 µmol m^{-2} s^{-1} photosynthetically active radiation [PAR]). The plants were watered daily and fertilized with 20:20:20 fertilizer (Plant-Prod) until reaching maturity (6 weeks), at which point they were allowed to dry out and seeds were collected.

For growth on media, seeds were first sterilized using chlorine gas. To do this, an open microfuge tube containing approximately 0.1 mL of seed was placed in a bell jar containing 100 mL of 3-6% (v/v) sodium hypochlorite (Javex). Upon adding 4 mL of concentrated hydrochloric acid to the sodium hypochlorite, the lid of the bell jar was closed, sealing the seeds in with the generated chlorine gas for 1-2 hrs. After the requisite exposure time, 100-250 sterile seeds were then sprinkled onto a Petri plate containing 25 mL of half strength Murashige and Skoog basal salts media (Murashige and Skoog 1962) supplemented with B5 vitamins (Sigma 85K2400; 2.5 mM MES, 30 g/L sucrose, 8g/L agar, pH 5.7-5.8). The plates were then wrapped and incubated for 24-72 hrs in the dark at 4ºC before being placed in 24 hr light (150 ± 20 µmol m^{-2} s^{-1} PAR) at 20ºC using a TC7 tissue culture chamber (Conviron).

DNA Extraction

Leaf tissue the size of a dime, was homogenized in 1.5 mL microfuge tube containing 0.4 mL of extraction buffer (200 mM Tris-Cl [pH 7.5], 250 mM sodium chloride [NaCl], 25 mM ethylenediaminetetraacetic acid [EDTA, pH 8], 0.5% sodium dodecyl sulphate [SDS]). After 2-5 min homogenization, the sample was centrifuged at 13,200 rpm for 5 min at 4ºC. The resulting supernatant was moved to a new tube and 0.2 mL of chilled isoproponal was added. After mixing for 15 sec and incubating on ice for 2 min, the sample was once again centrifuged at 13,200 rpm for 5 min at 4ºC. After discarding the supernatant, the DNA pellet was washed in 0.4 mL of 70% ethanol (EtOH) and centrifuged at 13,200 rpm (4ºC). After removing as much extraneous ethanol as possible, the pellet was air dried for 15 min. The pellet was then re-suspended in 0.1 mL 1x TE buffer (10 mM Tris-Cl [pH 7.5], 1mM EDTA [pH 8]) and stored at -80ºC.

Screening T-DNA Insertion Lines

Heterozygous, T1 seed stocks of T-DNA insertion (tagged) lines were obtained from the Arabidopsis Resource Biological Centre (ARBC), Ohio State University. To identify homozygous tagged lines in the T2 generation, DNA was extracted and screened using polymerase chain reaction (PCR) with primers specific to sequences flanking the insertion site (see Table 2) or in the left border (LB) of the T-DNA insertion sequence itself:

GARLIC LB3 5′ TAGCATCTGAATTTCATAACCAATCTCGATACAC 3′

SALK LBb1 5′ GCGTGGACCGCTTGCTGCAACT 3′

Amplification using the LB primers were performed with both flanking primers (LB + RP and LB + LP), as the orientation of the insert was unknown. If the mutant was

homozygous for the insert, then the genome was disrupted and no amplification using flanking primers occurred; while use of the appropriate flanking and LB primer resulted in a PCR product. To ensure the DNA was of good quality, primers specific to the constitutive Actin 2/7 were also used (Act F: 5' GGCCGATGGTGAGGATATTCA 3', ActR: 5' AGCTCGTTGTAGAAAGTGTGAT 3'). Standard PCR conditions were then used to screen the DNA, with the only variation being the Tm (listed in Table 2 for the flanking primers, used 59 °C for LB amplifications and 54 °C for actin):

94 °C (5 min) – 1 cycle
94 °C (45 sec), Tm (45 sec), 72 °C (1 min) – 35 cycles
72 °C (10 min) – 1 cycle

The resulting PCR products were analysed on a 1% (w/v) agarose gel and visualized using ethidium bromide. Individual plants exhibiting only insert amplification were selected for and subsequent generations were tested to confirm homozygous insertions.

Table 2. Primers used in tagged line analysis.

Tagged line	Gene	Flanking Primer	Sequence (-)	Tm (°C)	Product Size (bp)
GARLIC 597_D09	ADK1	D09 upper	GATTAGGATGTGCTTACGGC	54	835
		D09 lower	GATGCTTCAAGTTCCTGGGG		
GARLIC 157_F06	ADK1	F06 upper	CTCAGGGTAAGTGCAACCAG	54	734
		F06 lower	TTGGCAATGAGACCGAGGC		
SALK_103258	ADK1	103258 LP	CAGGACTTTTCAATGCCACCG	56	905
		103258 RP	TGAATTCAAATGCACGCTAGGA		
GARLIC 625_D04	ADK2	ADK2L	CAAGACGCTTCACTCAGCAG	58	2519
		ADK2R	CAAAACTGAGGGTAACCCAA		
SALK_028066	ADK2	28066 LP	GCTTCAAATTCCTGGGGCAAC	53	930
		28066 RP	TACCTCCCAGCCATGAACCCT		
SALK_000565	ADK2	565 LP	TGCAGGAGAAGTTCTTGCCGT	53	905
		565 RP	GTGGTAAAAAGTACACTCAAGCAA		

RNA Extraction

Prior to RNA extraction, all materials were either baked at 275ºC O/N or washed in 0.5N sodium hydroxide (NaOH) and diethylpyrocarbonite (DEPC)-treated water to eliminate contaminating RNAses. For each sample, a leaf the size of a dime or 3 inflorescences were placed in a 2 mL microfuge tube and flash frozen in liquid nitrogen. The sample was then quickly homogenized in 1.2 mL Tripure Isolating Reagent (Roche) and kept at room temperature (RT) for 5 min before mixing with 0.4 mL of chloroform. After sitting for 10-15 min at RT, the sample was centrifuged at 13,200 rpm for 15 min at 4ºC. The resulting aqueous top layer was transferred to a new 1.5 mL tube and 0.5 mL of isoproponal was added. After mixing, the RNA was precipitated by leaving the sample at RT for 10 min. The RNA was then spun at 13,200 rpm for 10 min at 4°C. After carefully removing the supernatant from the RNA pellet, 1 mL of chilled 70% EtOH was added and mixed by inverting the tube. At this point the sample was either incubated at -20°C for 10 min or kept for long term storage at -80°C.

After removal from the cold, the RNA was once again spun at 13,200 rpm for 10 min at 4°C, discarding supernatant. To remove excess ethanol, samples were air dried for 10-15 min. The dried RNA pellet was then re-suspended in 20 µL of DEPC treated water by mixing gently with a pipette tip and/or heating at 55-65°C for 10-15 min. The RNA quality and quantity was then determined by running out 3µL of RNA on a denaturing gel. The RNA was also quantified using a spectrophotometer set at 260 and 280 nm. The RNA was stored at -80°C.

cDNA Synthesis

In order to create cDNA, components of an Ambion cDNA synthesis kit were utilized. To begin, 0.1-0.5 µg (or 2 µL) of template RNA was incubated with 1 µL of oligo $(dT)_{18}$ primer (0.5 µg/µL) and 11 µL of nuclease free dH_2O in a 0.5 mL microfuge tube at 70°C for 5 min. After incubation, the tube was placed on ice and 4 µL of 5x reaction buffer (250mM Tris-HCl [pH 8.3], 250 mM KCl, 20mM $MgCl_2$, 50mM DTT), 1 µL of ribonuclease inhibitor (20 µg/µL) and 2 µL of 10 mM dNTP mix were added. After mixing with a pipette tip, the mixture was incubated at 37°C for 5 min and 2 µL of M-MuLV reverse transcriptase (20µg/µL) was added. The cDNA was then initiated at 37°C for 1 hr and stopped at 70°C for 10 min. The cDNA was stored at -20°C.

Crude Protein Extraction

All of the following steps were performed on ice. For each sample, 50-100 mg of leaf tissue was homogenized in three volumes of Super Buffer to leaf (5 mM dithiolthreitol, 50 mM 4-[2-hydroxyethyl]-1-piperazineethanesulphonic acid [HEPES pH 7.2], 1mM EDTA [pH 8.0], 50 mM citric acid pH 4.2, 10 mM boric acid pH 6, 20 mM Na-metabisulphate, 4% w/v polyvinylpyrrolydone [Bio Basics Inc. DBO436; MW 40,000]) using a conical glass homogenizer. The crude extract was then placed in a 1.5 mL microfuge tube and spun at 13,200 rpm for 2 min, transferring the resulting supernatant to a new tube. The above step was repeated twice.

In order to remove contaminating molecules such as purines, nucleosides and bases, the crude extract was run through a homemade Sephadex G25 column. The Sephadex G25 beads (medium grade, Amersham) were prepared by soaking in 50 mM HEPES buffer pH 7.2 overnight (O/N). Once the beads had absorbed the buffer, 1.2 mL of the

swollen beads were added to a 1.5 mL centrifuge tube. A small hole was then made on the bottom of the tube with a 20 gauge needle. The filled and punctured tubes were each placed in 13x100 test tubes, and spun at 2000 g for 15 sec on table top centrifuge (IEC HN-S, Damon) to remove excess buffer. Once the buffer was removed, the column was transferred to a new test tube and 100-150 μL of crude extraction was applied. The tube was once again spun at 2000g, with the resulting elutant being removed and placed in a 1.5 mL microfuge tube on ice or kept at 4°C O/N.

Protein Quantification and Storage

Quantification of crude protein extract was performed with the Bradford assay (Bradford, 1976) using BioRad (BioRAd, #500-0006) solution diluted to 1:4 with ddH_2O and bovine serum albumin (BSA) as a standard. Samples were tested in duplicate, using 2 μL of the crude extract and a range of volumes (2-10 μL) for the standard, and read at OD_{595}. The concentration of protein was then determined using the slope of the standard values. The crude extracts were stable at 4°C for O/N, however for more long term storage the protein needed to contain 10% (v/v) glycerol before being flash frozen in liquid nitrogen and stored at -80°C. For the ADK activity assay the crude extracts were diluted in Super buffer to 0.1 mg/mL.

ADK Activity Assay

In order to examine the enzymatic activity of ADK in a sample of tissue, the rate at which tritiated adenosine is incorporated into AMP was assayed (Moffatt et al., 2002). Prior to the assay, a stock of the reaction mixture was made up of the following 50 mM HEPES [pH 7.2], 4 mM adenosine triphosphate [ATP], 1 mM magnesium chloride [$MgCl_2$], 30

mM sodium fluoride [NaF], 2.5 μM DCF, 1 mg/mL BSA, 4.09 Ci/mmol ^{3}H adenosine, 2μM adenosine. 40 μL of the stock mixture was added to individual test tubes, and because triplicate volumes of protein were to be added to the reaction (2, 4, 6 μL), appropriate volumes of water was added to top up the final volume to 50 μL. For the assay, an Eppendorf brand p10 was used to add triplicate volumes of 0.1 mg/mL crude extract to the corresponding triplicates of reaction mixture at 30ºC in a Lauda water bath (reaction mixture was incubated for 5 min at 30ºC for 5 min prior to adding the protein). After incubating the protein with the reaction mixture for 5 min, the reaction was stopped by adding 1 mL of ice cold stop reagent (50 mM sodium acetate, 2 mM dipotassium phosphate buffer [K_2HPO_4, pH 5.0]) and placing the test tube on ice. To precipitate the tritiated AMP for detection, each of the samples were incubated at 4ºC for 1 hr to O/N with 0.2 mL of 0.5 M lanthium chloride. In addition to using triplicate volumes of the protein, duplicates or triplicates of the sample were also performed to ensure precision. Three reaction mixtures, excluding protein, were also assayed for background and 2 volumes of reaction mix were set aside to determine total counts per minute.

After the appropriate incubation time with lanthium chloride, the precipitated AMP was collected through vacuum filtration on glass fibre filters (1.2 μm pore size, Enzo Diagnostics) and placed in 5 mL scintillation vials containing 4 mL of CyoScint scintillation liquid (ICN). The radioactivity was then detected using a LS 1701 scintillation counter (Beckman Instruments) and ADK activity was calculated using one-way ANOVA comparisons of means.

Morphological Analysis of ADK Deficient Lines

To help establish the impact of ADK deficiency on plant development, morphological analysis was performed on WT, sADK4-2, sADK9-1, SALK 000565 (*adk2-1*) and GARLIC D09_507 (*adk1-1*) lines. To ensure reliability, 64 plants of each mutant line were grown along side 32 WT plants and grown under carefully maintained conditions (16hrs light, 20°C, 150 m^{-2} s^{-1} PAR). Plants were observed for up to 6 weeks, after which they were left to dry and their seeds collected. Characteristics and stages of development observed includes: seed morphology, germination time, length of primary roots, rate of leaf and silique formation, rosette size, number of primary and secondary branching, internode length and mature height.

In addition to making phenotypic observations, samples from WT and sADK were taken for microscopic analysis and chlorophyll was quantified to assess senescence in the leaves. To measure chlorophyll, 100 mg of leaf was obtained from 6 individuals at 3, 8 and 12 weeks of age, and homogenized in a 1.5 mL centrifuge tube containing1 mL of 90% acetone. The homogenate was then centrifuged at 13, 200 rpm for 2 min and the supernatant along with a 90% acetone blank, was measured at 543, 643 and 661 nm using a spectrophotometer. The following calculations were then used to measure chlorophyll a/b and anthocyanin (Gamon et al., 2001):

$$\text{Anthocyanin} = 0.0821*A_{534} - .00687*A_{643} - 0.002423*A_{661}$$

$$\text{Chlorophyll b} = 0.02255*A_{643} - 0.00439*A_{534} - 0.004488*A_{661}$$

$$\text{Chlorophyll a} = 0.01261*A_{661} - 0.001023*A_{534} - .00022*A_{643}$$

SEM Analysis

Siliques stages 15-18 were collected from 5 week old WT, sADK4-2 and sADK9-1 and placed in fixative solution (4% [w/v] paraformaldehyde [pH 7], 2% [w/v] glutaraldehyde, 1x potassium bisulphite [PBS]) for 1 hr under vacuum at RT. Upon refreshing the fixative solution, the samples were left to incubate for 5 hrs at RT or O/N at 4°C. The tissue was then dehydrated by 10% ethanol gradient at 30 min intervals under vacuum. Upon reaching 95% EtOH concentration, samples were left O/N at 4°C. Once the tissue was fully dehydrated, the samples were moved to HPLC grade acetone for 24 hrs at 4°C. The samples were then dried using mass critical point freezing, mounted on 2″ studs and splattered with gold particles. The tissue was visualized using a SEM.

Light Microscopy

Leaf and meristem samples of 3-week-old WT, sADK4-2 and sADK9-1 were immediately fixed in solution (0.05 M sodium cacodylate, 2% paraformaldehyde [w/v, pH 7], 0.1% [w/v] glutaraldehyde) for 1 hr under vacuum at RT. The samples were then applied with fresh fixative and incubated for another 5 hrs at RT or O/N at 4°C. After the appropriate amount of fixation, the samples were dehydrated in a series of ethanol under vacuum at RT, going from 10 to 70% EtOH in 15% intervals for 1 hr each. The samples were left in 70% EtOH and 0.2% eosin O/N at 4°C. Once fully dehydrated, the tissue was slowly infiltrated with LR White plastic resin (hard grade, Canemco-Marivac), in a series of EtOH: resin volumes (see Table 3). Once the samples were fully embedded in resin, the tissue was moved to a 0.5 mL BEEM capsule, covered with fresh LR White and placed in a 60-65°C oven for 2-24 hrs. Once the resin had hardened, tissue was sectioned

at 4 μm thickness using a Reichert Ultracut E microtome and stained with Toluidine Blue O for visualization.

Table 3. Ratio of resin to ethanol used in infiltration of tissue

Resin : Ethanol	Ratio	Duration (min)
LR white : Ethanol (100%)	1 : 3	60
LR white : Ethanol (100%)	2 : 2	120
LR white : Ethanol (100%)	3 : 1	120
LR white only		60
LR white		O/N

Results

Identifying Adenosine Salvage Mutants

A putative ADA encoding locus (At4g04880) was identified based on the similarity of its predicated amino acid sequence with those of known bacterial ADA genes (Moffatt, unpublished). Only two expressed sequence tags of this locus from green siliques were present in Genbank records at the time so reverse transcription polymerase chain reaction (RT-PCR) was used to determine whether this gene was transcribed in other organs; databases of high-throughput transcript profiling experiments were also scanned (see Figure 6). The RT-PCR showed that ADA is evenly distributed in all tissues examined with the exception of flowers and roots, where the transcript is nearly undetectable (S. Fry, unpublished data). Data obtained from the MPSS database reflect a similar pattern of expression while the microarray data show an equal level of ADA throughout the plant including flowers and roots (see Figure 6).

In addition to establishing transcript levels in WT plant tissues, RT-PCR was also used to detect the presence of ADA transcripts in the previously identified ADA-tagged line, *ada-1-1* (SALK 010573; see Figure 6) and on various ADK-tagged lines (see Figure 7). In all cases, the tagged lines lacked the expected transcript the organs tested. Only one mutant line for each isoform used for the following experiments: GARLIC 597_D09 (*adk1-1*) and SALK 000565 (*adk2-1*).

The Effects of Reducing Adenosine Salvage

In order to establish the effects of reduced ADK in silencing and tagged lines, the development of 64 plants for each sADK4-2, sADK9-1, *adk1-1, adk2-1,* and WT was monitored from germination to 5 weeks. As well as observing the rate of organ development, samples were taken from select plants for metabolic measurements and microscopic analysis. Sampling of the sADK mutant lines was limited as they exhibit a range in silencing, with individual plants exhibiting different phenotypes; in fact in each generation a portion of the plants exhibit a phenotype indistinguishable from WT (see Figure 5) (Moffatt et al., 2002). This occurrence is not the result of heterozygous populations, as both sADK4-2 and sADK9-1 are homozygous for the ADK transgene construct. At 4.5 weeks, sADK4-2 is the more severely affected of the two with the more extreme mutants retaining 6.4% (± 0.31) ADK activity in their leaves whereas the most extreme sADK9-1 have 15.2% ± 0.26. Overall out of the 64 plants examined, 26% of the sADK4-2 appeared WT and 32% exhibited the more severe phenotype; in the sADK9-1 population 30% appeared WT and 36% were severe. As expected the ADK-tagged lines did not show variation nor were there any apparent morphological abnormalities when compared to the WT. Despite this lack of phenotype, they did have decreased ADK

Figure 6. Establishing putative ADA expression in Arabidopsis using RT-PCR and high-throughput analysis.

Expression levels of putative ADA were measured in mature Arabidopsis organs using RT-PCR (A), microarray (B) and MPSS (C). The RT-PCR performed with ADA primers showed an equal level of expression throughout the plant with the exception of the flowers and roots. T-DNA insertion mutant, *ada1-1*, was checked with ADA primers and no product was detected. PCR performed using actin primers confirmed that there were equal amounts of cDNA used in each reaction (experiment performed by S. Fry).

Analysis of data obtained from microarray databases (B) show the putative ADA to be present at a steady level in all of the Arabidopsis organs, and at considerably lower levels than both ADK1 and ADK2. MPSS data (C) also shows the ADK isoforms to be present at much higher levels, but does not detect putative ADA in the root or inflorescence (bud and flower). Thus the MPSS data supports the ADA distribution suggested by RT-PCR.

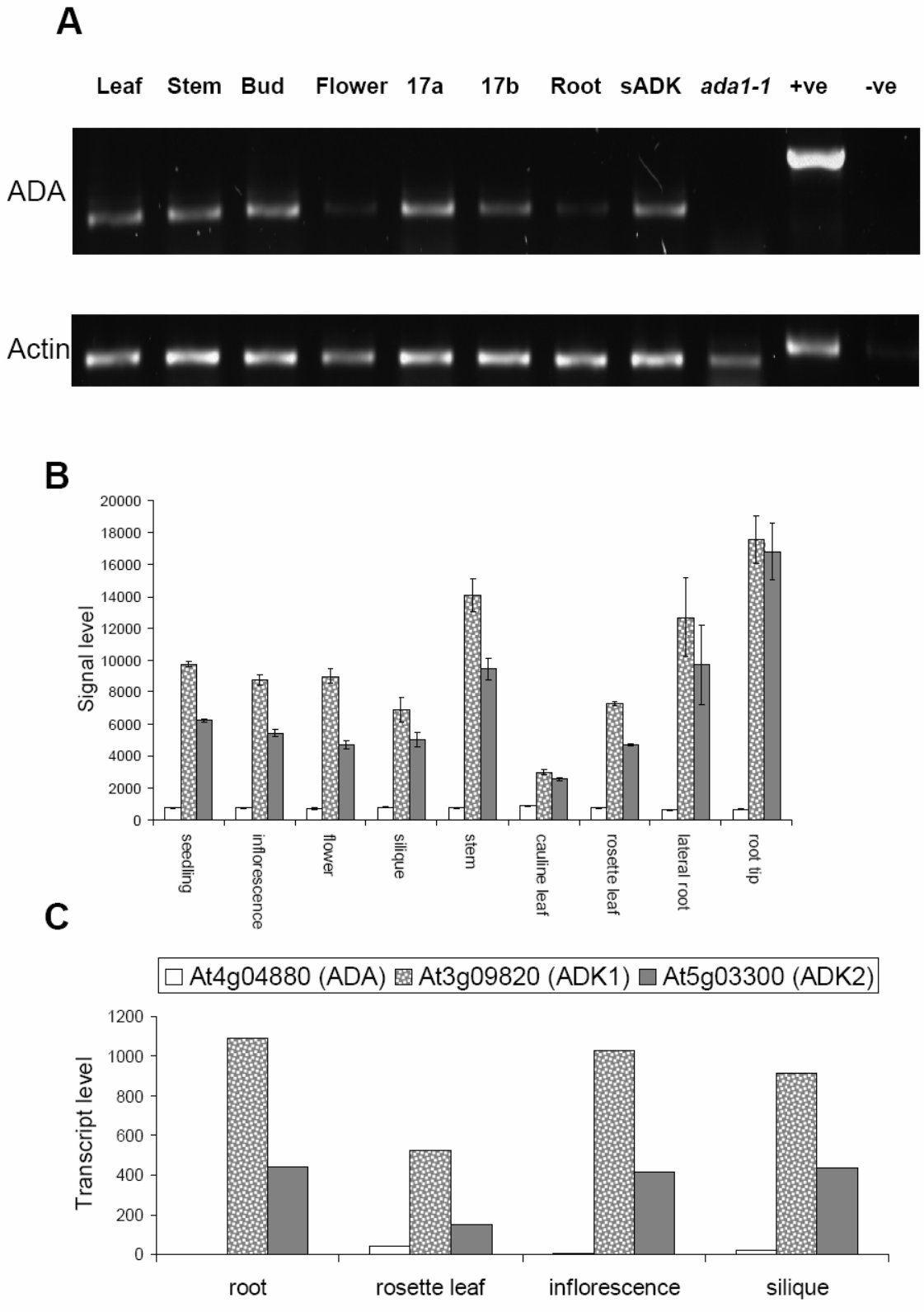
A
Leaf
Stem
Bud
Flower
17a
17b
Root
sADK
ada1-1
+ve
-ve
ADA
Actin
B
Signal level
20000
18000
16000
14000
12000
10000
8000
6000
4000
2000
0
seedling
inflorescence
flower
silique
stem
cauline leaf
rosette leaf
lateral root
root tip
C
At4g04880 (ADA)
At3g09820 (ADK1)
At5g03300 (ADK2)
Transcript level
1200
1000
800
600
400
200
0
root
rosette leaf
inflorescence
silique

Figure 7. RT-PCR analysis of ADK expression in homozygous T-DNA insertion mutant lines.

To confirm the presence of the T-DNA insert in the ADK1 (GARLIC 157_F06-7, SALK 105238-4, GARLIC 597_D09-7) or ADK2 (SALK 028066-9, GARLIC 625_D04-3, SALK 000565-3) gene, the sequence bordering the insert and the native gene was amplified using the left border primer (LB) and a flanking primer specific to the isoform. To ensure the expression of the gene is eliminated, cDNA of the mutant was amplified using isoform specific primers. No transcript was detected in the three homozygous tagged lines for ADK1 or ADK2.

ADK1

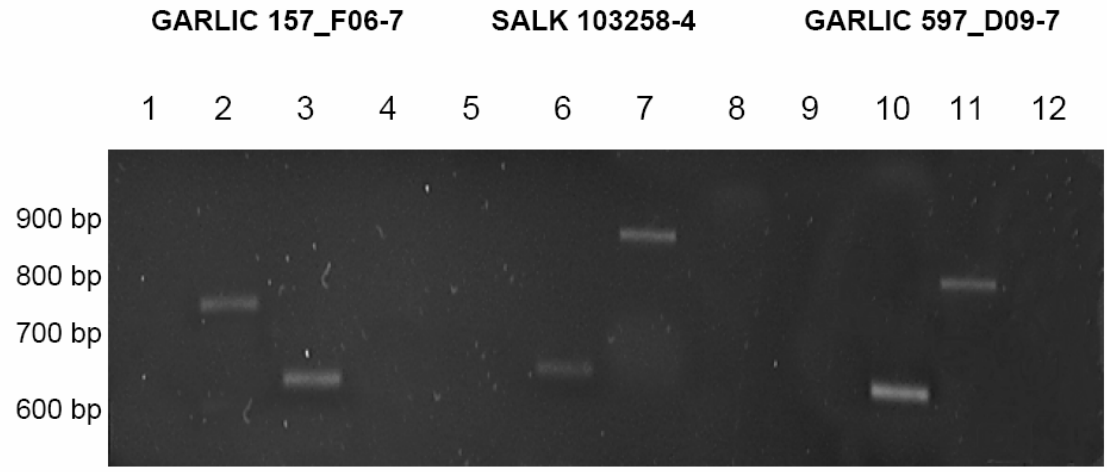
GARLIC 157_F06-7
SALK 103258-4
GARLIC 597_D09-7
1 2 3 4 5 6 7 8 9 10 11 12
900 bp
800 bp
700 bp
600 bp

ADK2

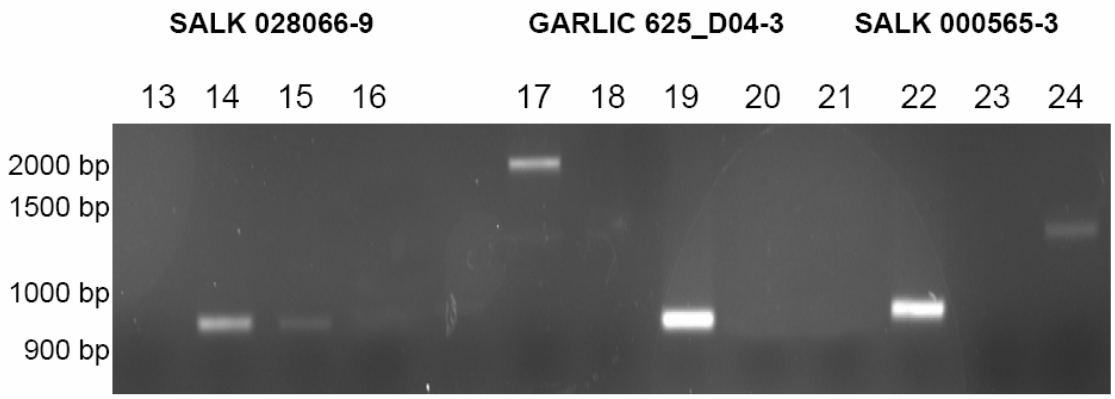
SALK 028066-9
GARLIC 625_D04-3
SALK 000565-3
13 14 15 16 17 18 19 20 21 22 23 24
2000 bp
1500 bp
1000 bp
900 bp

activity with *adk1-1* retaining 48.7% (± 1.03) and *adk2-1* 54.6% (± 1.27). To reduce the variability in the data the sADK plants that showed no sign of abnormal phenotype (wrinkled leaves, clustered inflorescences or affected primary shoot development) were removed from final data analysis presented here. The data from these removed plants are presented in the Appendix.

Analysis of ADK deficient mutants

Analysis of seed from each line revealed distinct differences between that of the WT and sADK4-2. Although no significant alterations were evident in seed of the other mutant lines examined, 35.8% of the sADK4-2 seed was wrinkled and of reduced mass as compared to the WT (see Figure 9). Approximately half of the 4-2 seed was also delayed in germination.

Examination of leaf initiation suggested that all of the sADK plants form leaves at a similar rate, with sADK4-2 developing 3 days ± 0.42 behind WT (see Table 4). The leaf size was significantly different; comparison of the rosette radii revealed WT to be 2.2-fold larger than sADK4-2 leaves and sADK9-1 to be slightly smaller in size. The characteristic wrinkling evident in mature sADK leaves was first noted in the 9th leaf (at approximately 18 days) and was present in all subsequent leaves. After 3.5 weeks this wrinkling also became apparent in leaves 1 through 8 of both severe sADK4-2 and sADK9-1 plants.

Primary shoot development was also delayed in the sADK lines with the formation of a 10 cm stem taking almost twice as many days to develop in sADK 4-2 as compared to the WT (see Figure 10). Even with the removal of WT phenotypes, variability was still evident at this stage in these plants, with 57% and 32% of sADK4-2 and sADK9-1,

Figure 8. Range of phenotypes observed in homozygous sADK lines at 5-weeks.

Top (A) and side (B) profiles of sADK lines show a range of phenotype. The more severe sADK lines lack a primary shoot and clearly exhibit clustered inflorescences and wrinkled leaves. The ADK activity relative to WT (A) is correlated to the severity of the phenotype; the more affected the plant the lower the ADK activity.

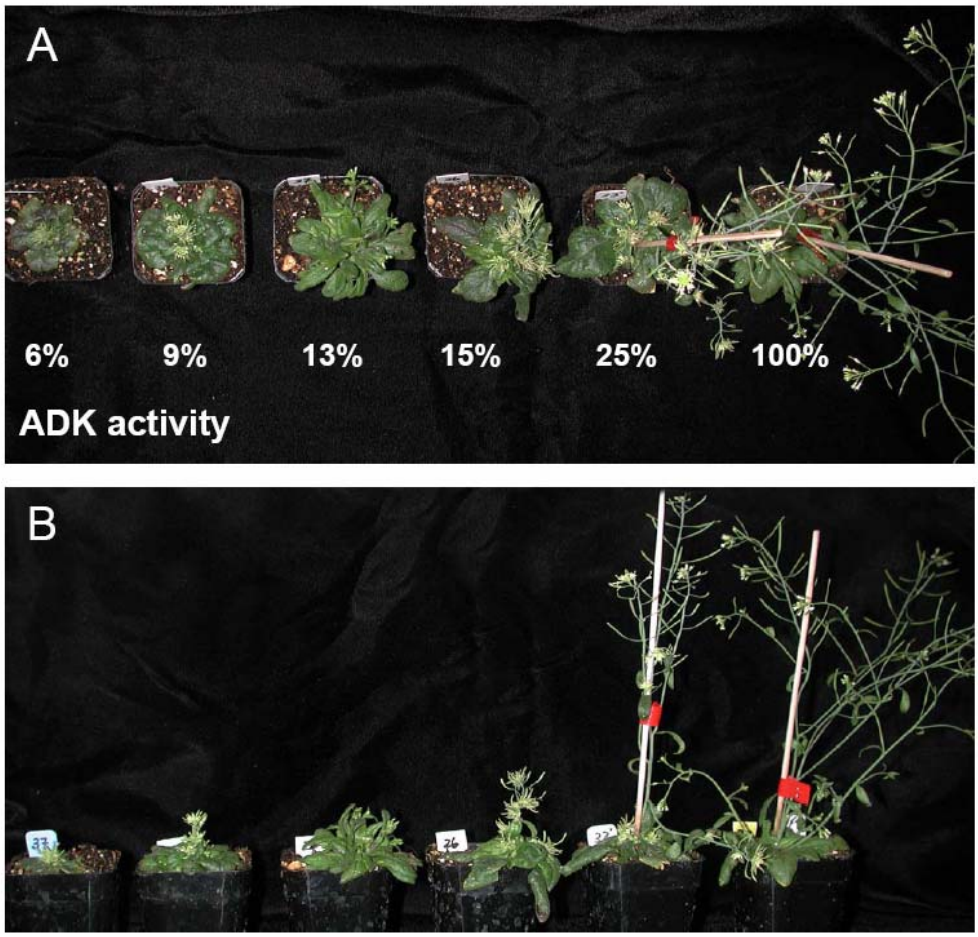
A
6%
9%
13%
15%
25%
100%
ADK activity
B

Figure 9. Examination of seed morphology in ADK deficient lines.

Five-hundred seeds for each WT and ADK-deficient line were examined for size and morphology. While there wasn't a significant difference in the size, a large majority of the sADK4-2 seeds exhibited a wrinkled phenotype. The less severe sADK9-1 and the ADK tagged lines did not show any significant differences from that of WT, see Appendix 2. Bar = 1 mm.

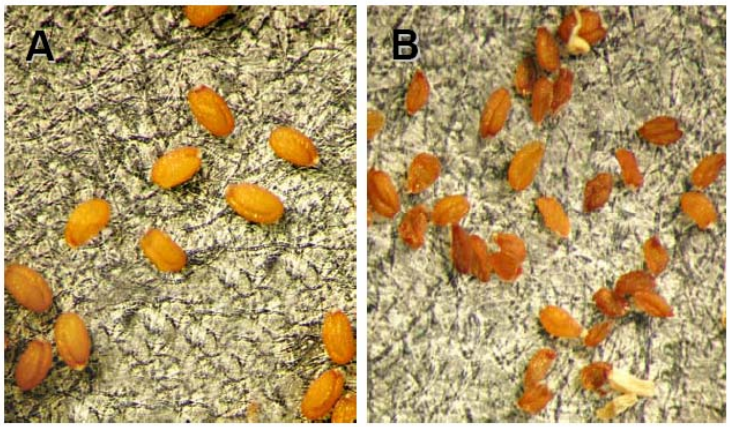

C

	WT		*adk1-1*		*adk2-1*		sADK 4-2		sADK 9-1	
	Avg	± SD	Avg	± SD	Avg	± SD	Avg	± SD	Avg	± SD
Seed Size (mm)	0.67	0.057	0.65	0.053	0.63	0.059	0.55	0.089	0.6	0.063
% wrinkled	0.8		1.1		0.5		35.8		4.4	

Table 4. Timing of rosette leaf initiation in WT and ADK deficient lines.

The number of days required to develop 1 cm length leaves were monitored in the WT, *adk1-1, adk2-1* and sADK lines. Only the sADK4-2 plants showed a significant difference in development, beginning from the 5^{th} leaf on. Statistical analysis in Appendix.

	WT		*adk1-1*		*adk2-1*		sADK4-2		sADK9-1	
	Avg	± SD	Avg	± SD	Avg	± SD	Avg	± SD	Avg	± SD
1st cotyledon	3	0	3	0.1	3	0.02	3.7	0.7	3.5	0.53
1st leaf	5	0.13	5.5	0.44	5.1	0.2	6.4	0.89	6.3	0.51
2nd leaf	9.4	0.5	9	0.23	9.2	0.67	9.8	0.78	9.3	0.42
3rd leaf	10.5	0.56	10.2	0.68	10.7	0.33	11.4	0.68	11.2	0.59
4th leaf	11.6	0.58	11.3	0.78	11.3	0.45	12.9	0.75	12.8	0.58
5th leaf	12.7	0.46	12.3	0.55	12.5	0.72	14.5	0.69	14.4	0.76
6th leaf	14.1	0.42	13.7	0.45	13.9	0.34	15.6	0.74	15.8	0.71
7th leaf	15.1	0.44	14.8	0.63	15.6	0.55	17.1	0.86	16.2	0.64
8th leaf	16.1	0.37	15.7	0.54	16.3	0.49	18.2	0.59	17.1	0.54
9th leaf	17.1	0.36	16.7	0.76	17.4	0.23	18.6	0.75	18.9	0.53
10th leaf	18.1	0.34	17.7	0.45	18.1	0.56	19.2	0.87	19.3	0.76
11th leaf	19.1	0.34	18.6	0.33	19.4	0.78	20.5	0.68	20.3	0.71
12th leaf	20.1	0.32	19.6	0.55	20.8	0.71	21.8	0.63	20.9	0.68
13th leaf	21.2	0.36	20.6	0.64	20.9	0.3	23.1	0.53	22.1	0.56
14th leaf	22.2	0.44	21.6	0.49	22.1	0.4	25.1	0.67	23.2	0.64

Figure 10. Growth analysis of WT, ADK and ADA-deficient lines I.

The percentage of successful germination (A), average rosette leaf size at 5 weeks (B) and average primary shoot length (C) in WT, *ada1-1, adk1-1, adk2-1* and sADK lines was determined. Statistical analysis in Appendix 2.

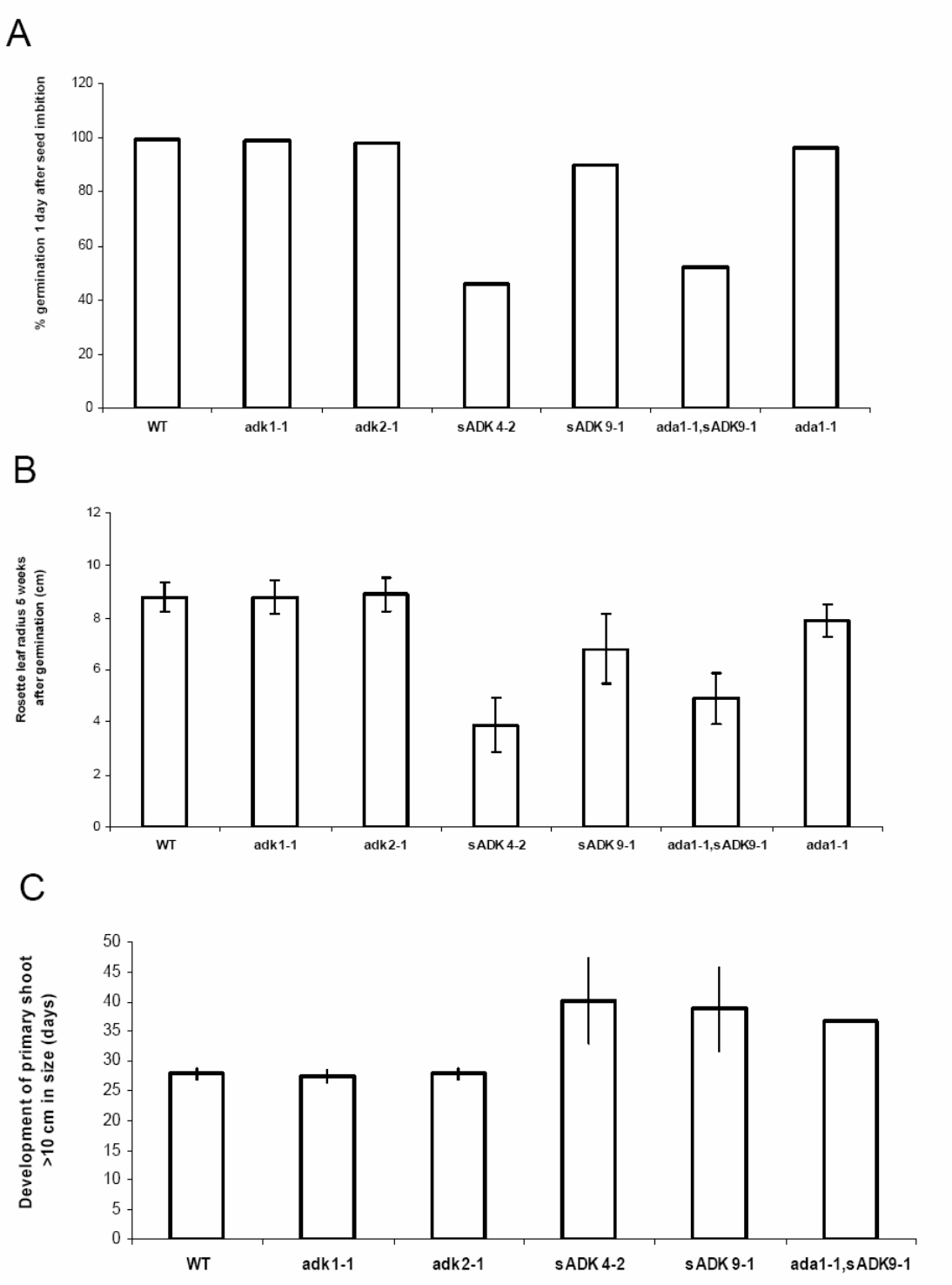
A
% germination 1 day after seed imbition
120
100
80
60
40
20
0
WT
adk1-1
adk2-1
sADK 4-2
sADK 9-1
ada1-1,sADK9-1
ada1-1
B
Rosette leaf radius 5 weeks after germination (cm)
12
10
8
6
4
2
0
WT
adk1-1
adk2-1
sADK 4-2
sADK 9-1
ada1-1,sADK9-1
ada1-1
C
Development of primary shoot >10 cm in size (days)
50
45
40
35
30
25
20
15
10
5
0
WT
adk1-1
adk2-1
sADK 4-2
sADK 9-1
ada1-1,sADK9-1

Figure 11. Growth analysis of WT, ADK deficient lines I

The number of days required to develop a stem exceeding 10 cm (A), the number of branches formed (B) and the length of mature stage 18 siliques (C) were measured on mature Arabidopsis. In addition to the sADK lines, *ada1-1*,sADK9-1 crosses were also examined. No significant values were detected between sADK9-1 and *ada1-1*,sADK9-1. Statistical analysis in Appendix 1.

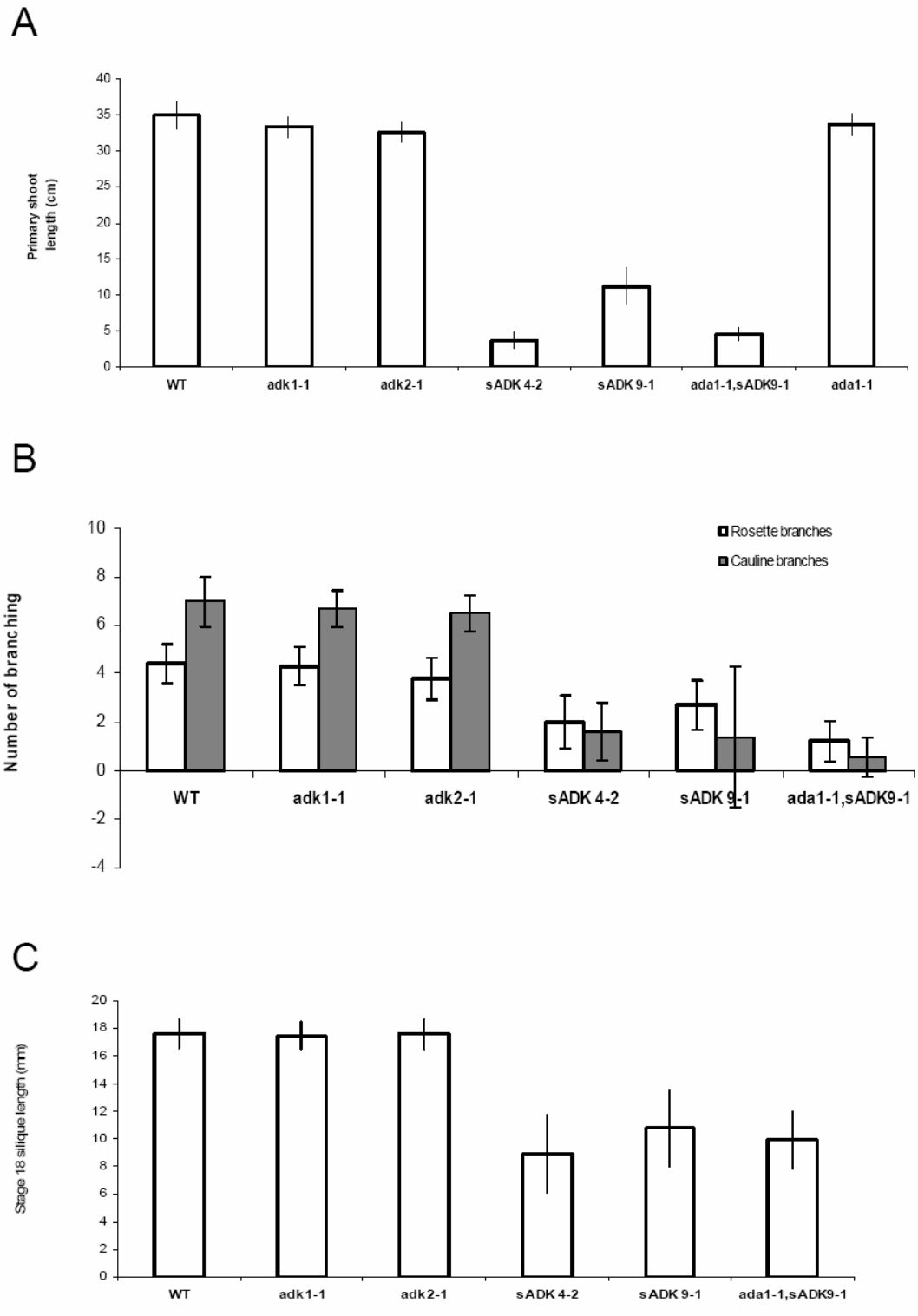
A
Primary shoot length (cm)
40
35
30
25
20
15
10
5
0
WT
adk1-1
adk2-1
sADK 4-2
sADK 9-1
ada1-1,sADK9-1
ada1-1
B
Number of branching
10
8
6
4
2
0
-2
-4
Rosette branches
Cauline branches
WT
adk1-1
adk2-1
sADK 4-2
sADK 9-1
ada1-1,sADK9-1
C
Stage 18 silique length (mm)
20
18
16
14
12
10
8
6
4
2
0
WT
adk1-1
adk2-1
sADK 4-2
sADK 9-1
ada1-1,sADK9-1

respectively, not forming stems greater than 10 cm in length. The delay or lack of primary shoot development was indicative of the final size achieved by the mature plants with sADK4-2 plants being on average 10-fold shorter than the WT (see Figure 10). Both rosette and cauline branching was also affected in the severely affected sADK mutants with some sADK4-2 plants having no branches at all, while 9-1 had 4-times fewer branches than the WT (see Figure 11).

Silique formation (see Figure 12) was of particular interest since preliminary observations of the sADK plants have siliques that do not shatter normally (Moffatt et al., 2002). As in the other stages of development, the sADK plants were delayed in bud and silique formation with the siliques in the clustered inflorescences being the most affected. The most noticeable variations observed were with respect to timing of petal senescence through stages 13-16 and the lack of silique 'shatter' at stage 18 (i.e. the siliques did not dehisce and release seeds even after 2 weeks of dehydration; see Table 5). Overall, sADK4-2 and sADK9-1 buds and siliques took longer to develop (in some stages as much as 3 days) and the fully formed siliques (stages 17a-18) were also shorter in length and contained fewer seed (see Table 5). Furthermore the pedicel length, the number of siliques per plant and overall height of the sADK4-2 plants were reduced relative to the WT. The sADK9-1 lines were also affected in these traits but to a lesser degree. In addition, sADK4-2 plants had significantly reduced primary roots and shorter lateral roots. Interestingly, 82% of the severely affected sADK plants formed rosette/cauline branches after 5 weeks that had leaves and silique development similar to that of WT (i.e.

the siliques were not arranged into clusters and no wrinkling in the cauline leaves). With respect to the traits followed in this growth analysis there were no variations in the development of the *adk1-1* and *adk2-1* tagged lines.

Affect of putative ADA deficiency

In addition to the ADK deficient lines, *ada1-1* and *ada1-1,*sADK9-1 lines were also examined at several points of development (*ada1-1* growth analysis was performed by S. Fry, unpublished data). With respect to the traits followed in this growth analysis there were no variations in the development of the *ada1-1* (see Figure 10). Introduction of the *ada1-1* allele into the sADK 9-1 background (*ada1-1,*sADK9-1; see Figure 10, 11) appeared to increase the severity of the sADK phenotype, particularly with respect to the proportion of "severe" plants detected. For example, although only 43% of the sADK9-1 had a phenotype, 68% of the *ada1-1,*sADK9-1 were distinctly abnormal. Significant differences were also evident in their rosette size, branching and leaf senescence (see Figure 13).

Chlorophyll assays were performed on fully expanded rosette leaves of WT, sADK9-1 and *ada1-1,*sADK9-1 to determine if senescence was affected. The results show the chlorophyll levels to be the same in the different lines at 3 weeks; by 8 weeks chlorophyll was reduced in WT, while sADK9-1 and *ada1-1,*sADK9-1 plants remained steady at the 3 week level. By 12 weeks sADK9-1 plants showed a loss of chlorophyll while *ada1-1,*sADK9-1 levels were still unaltered, consistent with the presence of the *ada1-1* allele (i.e. loss of ADA activity). In all cases chlorophyll a and b were present in the same amounts, and the presence of anthocyanin was inversely correlated to that of the chlorophyll a/b ratio; that is when chlorophyll levels decreased, anthocyanin increased.

Figure 12. Stages of silique development in Arabidopsis.

In order to develop into a silique (fruit), buds (stages 10-11, not shown) must self pollinate/be pollinated (stage 13), develop into a flower (stage 14), ovary is fertilized and petals begin to senesce (stage 15) and the ovary (now the silique) begins to develop, as the petals abscise (stage 16). At this point the fertilized ovary begins to distend and stage 17b the silique is fully developed and the seeds are developed. Once the silique is matured, the silique senesces and the seeds dry (stage 18); when it is completely dried the silique will dehisce and the seeds will be dispersed. Image obtained from Tordorova 2002.


1.6 cm
12
13
14
15
16
17a
17b
18

Table 5. Analysis of silique development in WT and ADK deficient lines.

Siliques for WT, *adk1-1, adk2-1,* sADK4-2 and sADK9-1 were examined from stage 16 on to stage 18 in closer detail. In addition to a delay in petal abscission and silique dehiscence, the sADK lines had smaller siliques and had half the number of siliques per plant. As observed in previous analyses, the ADK tagged lines did not exhibit a phenotype. See Appendix 2 for statistical analysis.

	WT		*adk1-1*		*adk2-1*		sADK4-2		sADK9-1	
	Avg	± SD	Avg	± SD	Avg	± SD	Avg	± SD	Avg	± SD
1st bud	16	0	16	0.95	16	0	23.1	1.56	19	2.2
1st petal dehiscence	25.6	0.89	26.3	0.53	26	0.84	40.5	0.9	27.8	2.1
1st 17a silique	27.9	1.4	28.1	1.44	27.5	1.4	31.9	2.32	29.2	2.43
1st 17b silique	31.8	2.69	31.2	2.64	31.7	2.58	34.5	1.98	32.4	2.43
1st 18 silique	38.1	0.77	35.6	1.2	37.6	0.75	38.2	2.2	36.5	1.7
1st silique shatter	41.5	0.8	41.5	1.5	41	0.82	62.1	8.9	53.7	9.1
17a silique length	11	1.49	11.5	2.1	10.8	1.2	3.5	0.56	7.3	1.4
17b silique length	12.8	3.04	12.4	2.08	12.1	2.51	4.5	1.3	8.1	1.1
18 silique length	17.6	1.04	17.5	1.03	17.6	1.08	8.9	2.81	10.8	2.76
petiole length (stg 18)	5.65	1.1	5.8	1.3	5.5	0.9	2.9	1.2	3.5	1.23
ratio of seed/silique	0.29	0.021	0.4	0.04	0.3	0.034	0.3	0.01	0.32	0.02
total siliques	299.7	58.37	286.5	46.1	274.3	35.9	143.2	34.5	170.3	44.2

Figure 13. Quantifying chlorophyll and anthocyanin levels in WT, sADK9-1 and *ada1-1,* sADK9-1.

To assess the vitality of the leaves, chlorophyll assays were performed on 9 fully extended leaves of 3, 8 and 12 week-old WT and deficient lines. sADK9-1 retained both chlorophyll a and b longer than WT, however *ada1-1*,sADK9-1 had more chlorophyll at 12 weeks than the sADK9-1 by itself. Both sADK9-1 and *ada1-1*,sADK9-1 developed less anthocyanin than that of WT. See Appendix 2 for statistical analysis.

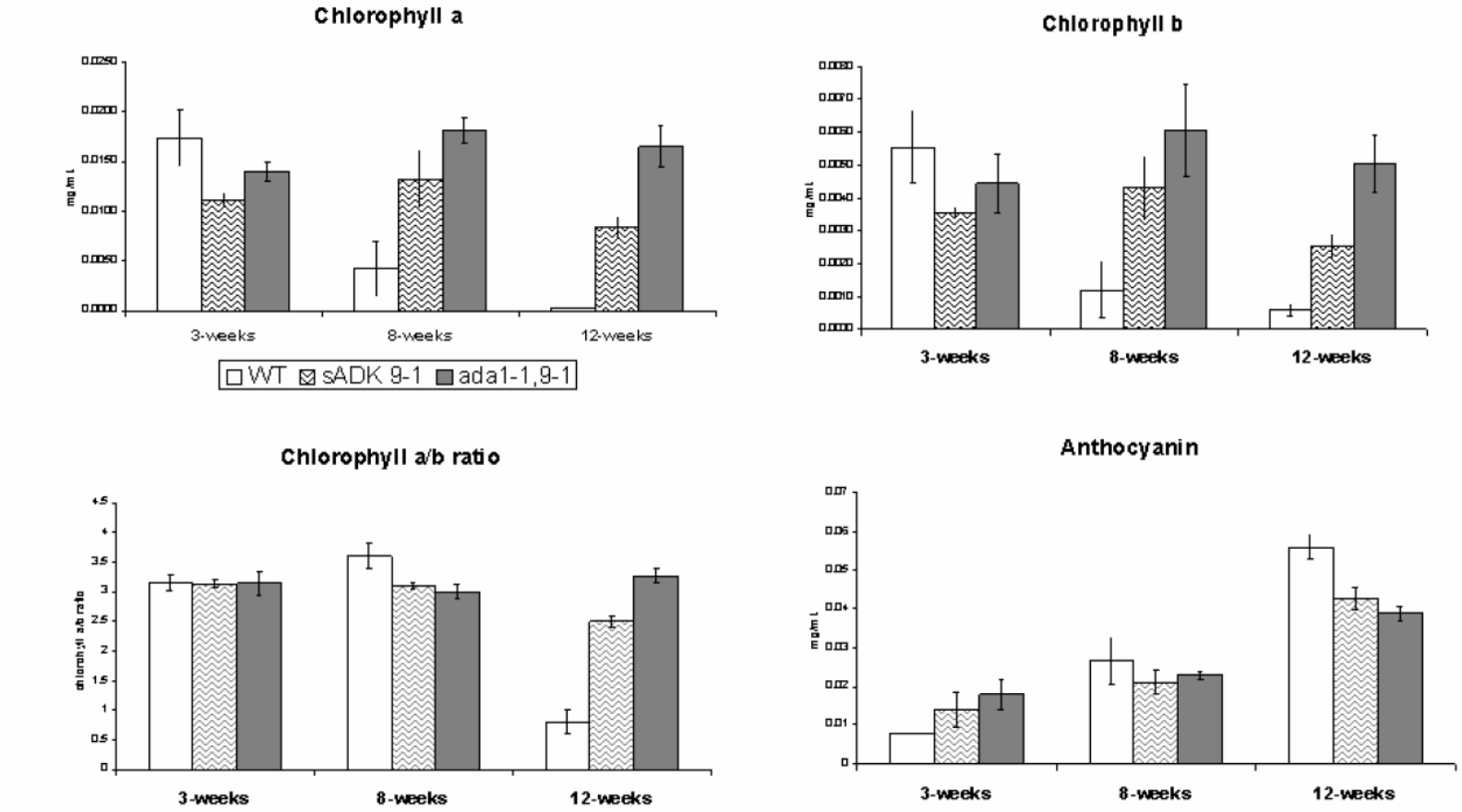
Chlorophyll a
mg/ml
0.0250
0.0200
0.0150
0.0100
0.0050
0.0000
3-weeks
8-weeks
12-weeks
WT
sADK 9-1
ada1-1,9-1
Chlorophyll b
mg/ml
0.0080
0.0070
0.0060
0.0050
0.0040
0.0030
0.0020
0.0010
0.0000
3-weeks
8-weeks
12-weeks
Chlorophyll a/b ratio
chlorophyll a/b ratio
4.5
4
3.5
3
2.5
2
1.5
1
0.5
0
3-weeks
8-weeks
12-weeks
Anthocyanin
mg/ml
0.07
0.06
0.05
0.04
0.03
0.02
0.01
0
3-weeks
8-weeks
12-weeks

Examination of sADK Lines Using Microscopy

For the following studies, only severe sADK4-2 and 9-1 individuals were examined. Due to their early senescence and subsequent inability to abscise, petals from sADK 4-2 were more closely examined using SEM. Inspection of the abscission sites of WT and sADK lines at the cellular level (see Figure 14), revealed the proliferation of new cells over the dehiscence site of the WT 17a siliques was more advanced. These results are expected as the sADK4-2 petals fall off later at stage 17b or not at all, and in the case of SEM analysis petals were manually removed at stage 16. The other major abnormality of sADK4-2 siliques, namely their inability to shatter, was also examined. At stage 17a both WT and sADK4-2 siliques were very similar in appearance, however once the siliques advanced to stage 17b the boundary between the carpels and replum of the sADK4-2 began to appear wavy while the WT boundary retained a rigid-looking linear appearance. At stage 18, the WT carpels began to dehisce from the replum in advance of shattering whereas no dehiscence was detected in the sADK4-2 siliques; instead the boundary between the two components of the silique became more distorted (see Figure 14).

Using light microscopy, the meristems of WT Arabidopsis and clustered inflorescences of sADK lines were also examined (see Figure 15). As well as emphasizing the decreased internode length of the sADK inflorescences, the sections revealed the presence of considerably enlarged bud primordia, while the meristem itself remained the same size. Both sADK4-2 and sADK9-1 meristems had this appearance (see Figure 15). Further analysis of the meristematic cells showed that the cells of the WT and sADK are of the same size.

Establishing Hypomethylation in sADK Mutants

Because decreased levels of SAH hydrolase lead to reduced DNA methylation (Tanaka et al., 1997), it was of interest to know if ADK deficiency also led to DNA hypomethylation. These studies were carried out by two other members of the Moffatt lab, Greg Perry and Katja Engel. The first experiment involved a genetic test of DNA methylation in developing embryos. FIS2 serves as a signal for embryo and endosperm development by repressing seed development until the double fertilization that occurs after pollination; a null mutation identified within the gene, *fis2,* results in withered seed coats and poor germination (Chaudhury et al., 2000). It has been previously established that this abhorrent seed development can be corrected by crossing the *fis2* line with a mutant containing decreased DNA methylation (*ddm1)* (Jeddeloh et al., 1999). The F2 seed of the sADK4-2 and sADK9-1 crosses had 36-7% of the seed revert to a WT phenotype (see Table 3) suggesting that the sADK parent lines had reduced DNA methlyltion (Perry 2004).

The second experiment measured cytosine methylation quantitatively. Analysis of 5-methylcytosine content in genomic DNA not only showed a decreased degree of methylation in the sADK lines relative to WT, but a significant decrease in the *ada1-1,* sADK9-1 line compared to that of sADK9-1 as well (see Figure 16). Overall, a direct correlation between ADK activity and CG methylation was evident; in plants with 16 % residual ADK activity, only 75-80 % of cytosines were methylated in comparison to WT. In more severely affected mutants bearing 10 % residual ADK activity, a further decrease in methylation occurs with 69 % 5-methylcytosine content in genomic DNA compared to that of *ddm1-5* at 45% (K. Engel, unpublished data).

Determining Levels of Adenosine Salvage

Leaf samples of 3.5 – 4 week-old Arabidopsis lines were sent to Dr. Neil Emery at Trent University to measure Ado, SAH and CK levels by gas chromatography tandem mass spectrometry. In addition to detecting twice the level of Ado and SAH in the sADK lines, the total level of CK ribosides increased 17-19 fold in severely affected sADK mutants (see Figure 17). No significant variation in levels was evident in the tagged lines of ADK or ADA, as compared to the WT; however, as seen in earlier measurements the sADK9-1 carrying the *ada1-1* allele resulted in higher levels of Ado and CK as compared to sADK9-1 parent.

Figure 14. SEM analysis of silique development of WT and sADK4-2.

Siliques of WT (F-J) and sADK4-2 (A-E) were examined at various stages using SEM analysis: (A,F) stage 15, (B,G) stage 16, (C,H) stage 17a, (D,I) stage 17b and (E,J) stage 18. When the petal was forcibly removed from the sADK silique at stage 15, by stage 16 the abscission zone was similar to that of WT. However, if the petal was not forcibly removed from the sADK4-2 then the petal would not abscice on its own. At stage 18, when compared to siliques of the same age, WT siliques were more senesced than the ADK deficient and dehiscence was observed. Instead of dehiscing the replum of the sADK siliques only became more wavy in appearance.

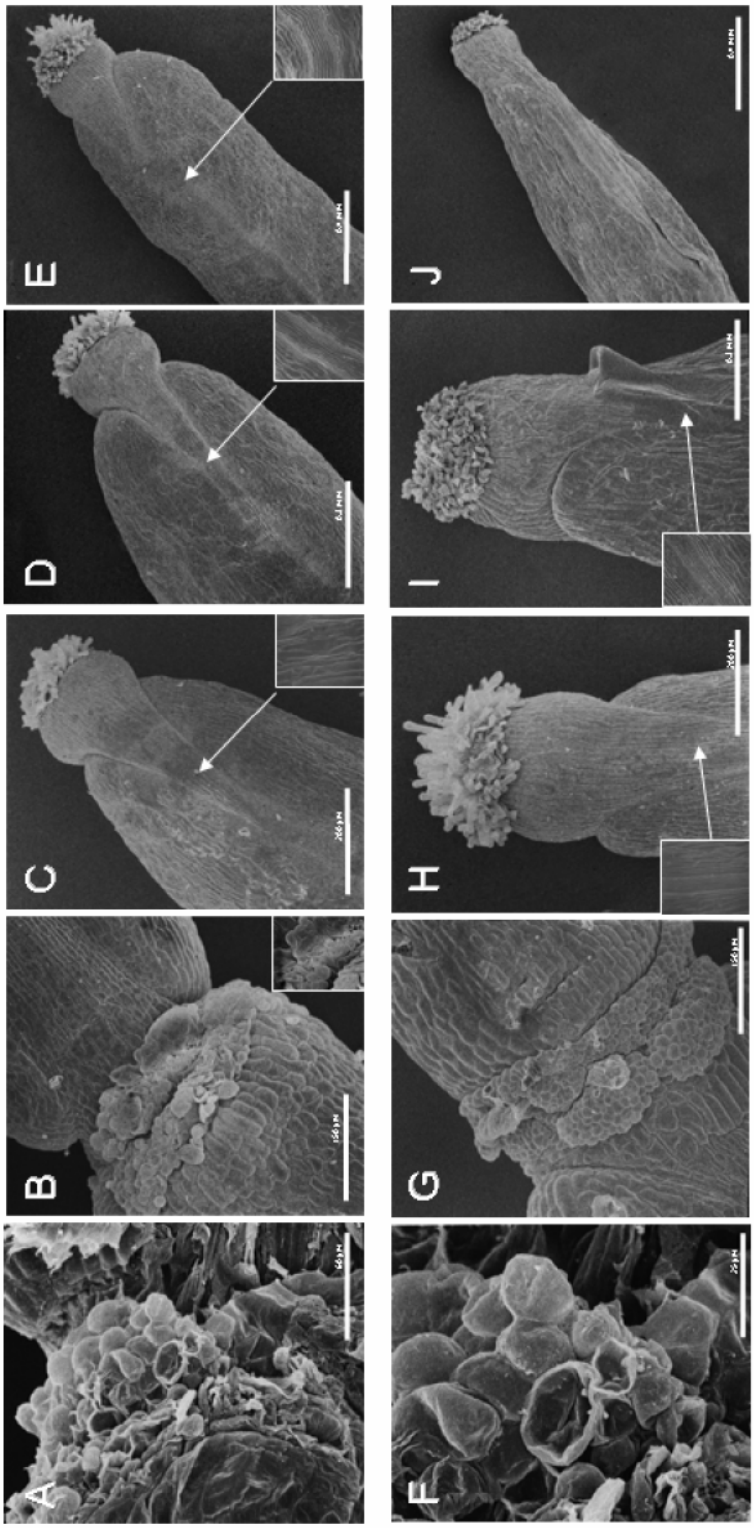
A
B
C
D
E
F
G
H
I
J

Figure 15. Microscopic analysis of 3.5 week-old WT and sADK meristems.

5 meristems of WT (A), sADK4-2 (B) and sADK9-1 (C) floral meristems were sectioned at 4 μm, stained with toluidine blue and examined at 100x magnification. The resulting meristems displayed considerably larger sADK floral primordia than that of the WT. Bar = 1 mm.

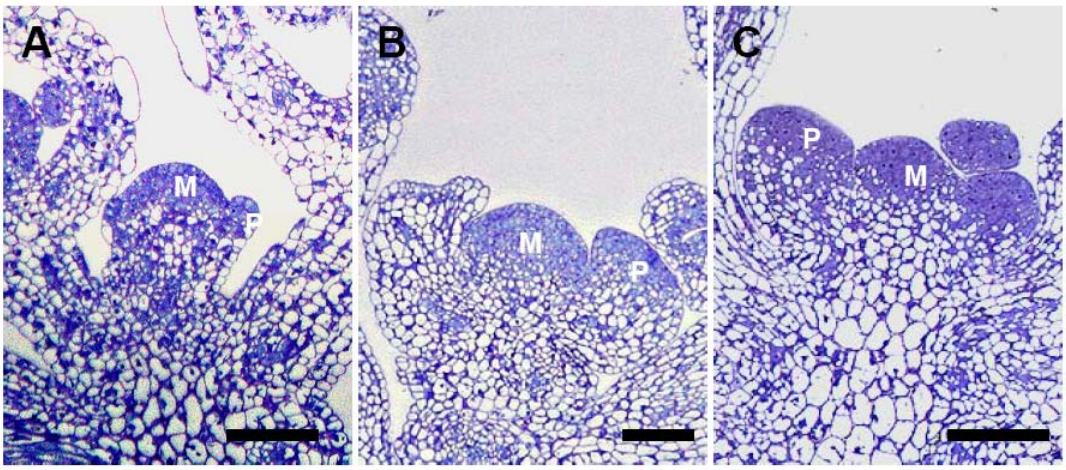
A
M
B
M
P
C
P
M

Table 6. Result of crossing sADK lines with *fis2* mutant.

To establish whether or not the genome of sADK lines have decreased methylation, sADK4-2, sADK7-1 and sADK9-1 were crossed into *fis2* mutants. Methylation facilitates the early expression of the altered *FIS2* gene and the subsequent abnormal development of seed coat and endosperm, resulting in a wrinkled phenotype and reduced successful germination. It has been shown that this phenotype can be corrected by introducing the *fis2* mutant to a hypermethylated background as found in the *ddm* mutant (Richards et al., 1999). Thus by examining the number of seeds displaying either WT or *fis2* wrinkled seed phenotypes in the F2 generation (A), it was established whether or not the sADK had reduced methylation at the embryo level. Close analysis (B,C) shows a significant number of healthy seed phenotypes in the sADK and *fis2* crosses, proving that the *fis2* phenotype caused by methylation was corrected through ADK deficiency. Data was obtained by Greg Perry, University of Waterloo.

A

Plant Line	Normal	Fis 2
WT	3	203
ddm 1	187	6
sADK4-2	42	81
sADK7-1	45	73
sADK9-1	48	73

B Chi Squared Analysis

Plant Line	Normal	Fis 2	Row Total	Row %
WT	3	203	206	36.27
sADK4-2	42	81	123	21.65
sADK7-1	45	73	118	20.77
sADK9-1	48	73	121	21.3
Column Total	138	430	568	100
Column %	24.3	75.7	100	

Chi-Square	92.749
df	3
P Value	<0.0001

C Chi Squared Analysis

Plant Line	Normal	Fis 2	Row Total	Row %
sADK4-2	42	81	123	33.98
sADK7-1	45	73	118	32.6
sADK9-1	48	73	121	33.43
Column Total	135	227	362	100
Column %	37.29	62.71	100	

Chi-Square	0.8488
df	2
P Value	0.6542

Figure 16. HPLC analysis of genomic methylation in ADK and ADA deficient lines.

The degree of cytosine methylation and their correpsonding standard deviation within the samples were determined by Katja Engel using HPLC analysis with DNA prepared from 3.5-4 week-old floral meristems of WT, *ada1-1, ada1-1,*sADK9-1, sADK4-2 and sADK9-1. The results show the percentage of methylated cytosine decreases in the sADK lines, although not to the same extent as the hypomethylation control *ddm1-5* (A). Analysis of variance supported the decrease in sADK and *ddm1-5* lines to be of significant value (B).

A

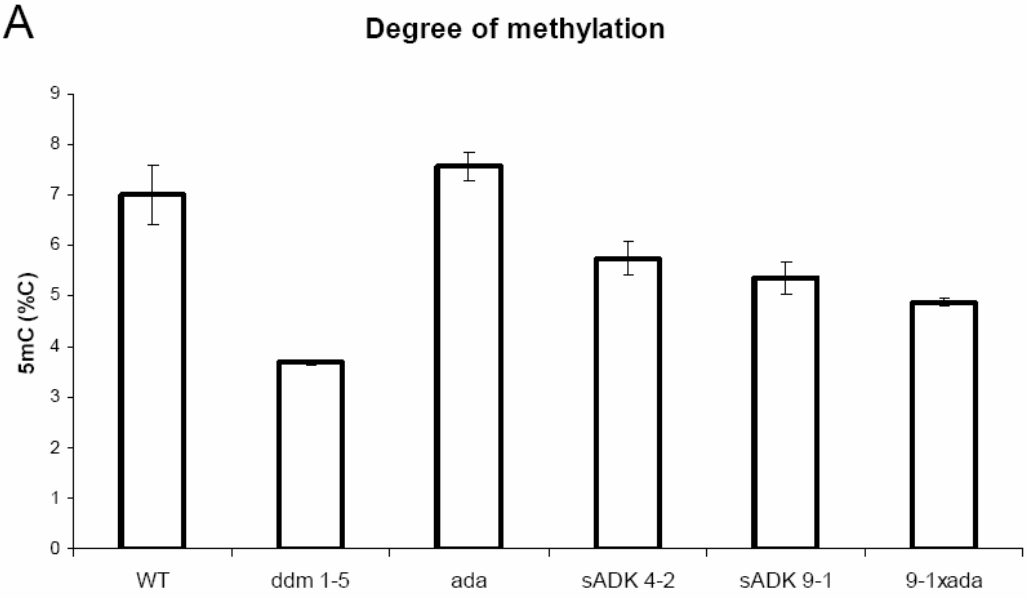

B

Comparison	*F-Ratio*	*Prob Level*	*Power (Alpha=0.05)*
1 vs 2	27.28	0.006414*	0.97
1 vs 3	58.97	0.004588*	0.997080
1 vs 4	40.82	0.001391*	0.998593
1 vs 5	34.81	0.001053*	0.997857
1 vs 6	1.97	0,232729	0,193339
1 vs 7	54.01	0.001826*	0.999421
4 vs 5	2.24	0.195096	0.230495
4 vs 6	52,46	0,005428*	0,994153
4 vs 7	5,90	0,093420	0,390267
6 vs 7	72,28	0,013555*	0,971979

* Term significant at alpha = 0.05

Figure 17. Cytokinin and Ado levels measured by GC-MS in ADK and ADA deficient lines.

Triplicates of fully extended rosette leaves from 4-week old plants were flash frozen and sent to Dr. Neil Emery at Trent University (Peterborough, ON) for GC-MS analysis of Ado, SAH and SAM abundance. The resulting averages and corresponding standard deviations, showed Ado levels to be twice the amount in the sADK lines than that of the WT, *adk1-1, adk2-1* and *ada1-1* when expressed on a dry weight basis. Even more significant was the increase in overall CKs, with the *ada1-1,* sADK 9-1 CK levels measured higher than ADK deficient lines by themselves. WT n = 9, *adk1-1* n = 3, *adk2-1* n = 3, *ada1-1* n = 3, sADK9-1 n = 6, sADK4-2 n = 6, *ada1-1,* sADK 9-1 n = 9.

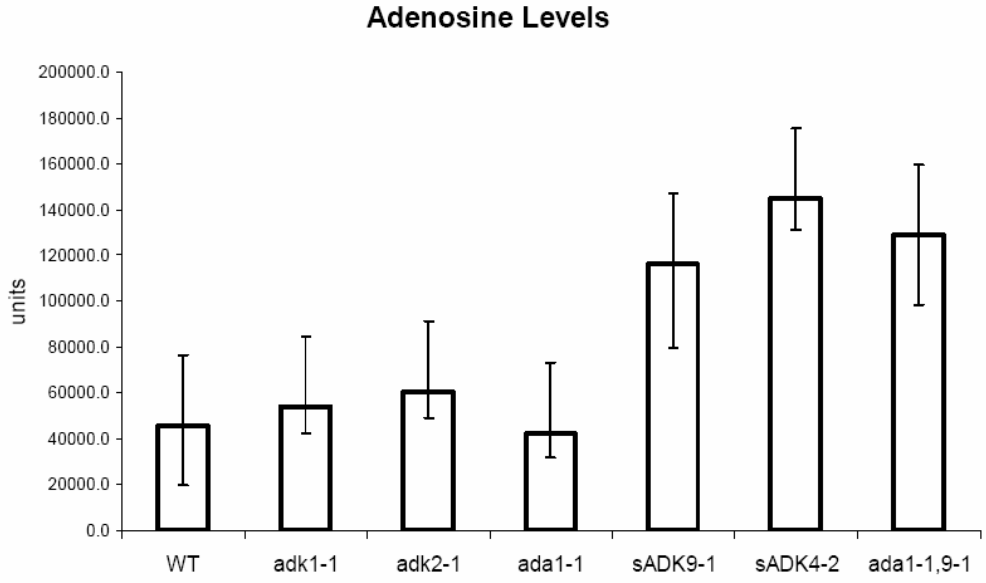
Adenosine Levels
units
200000.0
180000.0
160000.0
140000.0
120000.0
100000.0
80000.0
60000.0
40000.0
20000.0
0.0
WT
adk1-1
adk2-1
ada1-1
sADK9-1
sADK4-2
ada1-1,9-1

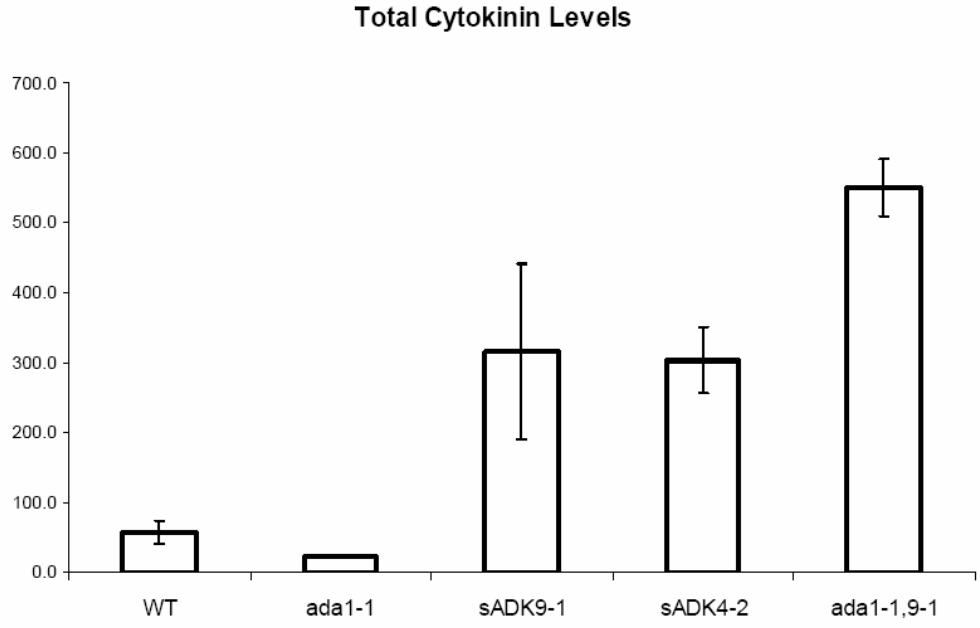
Total Cytokinin Levels
700.0
600.0
500.0
400.0
300.0
200.0
100.0
0.0
WT
ada1-1
sADK9-1
sADK4-2
ada1-1,9-1

Discussion

Using lines deficient in ADA and ADK enzyme activities, this research attempted to establish the impact of reduced Ado salvage on plant development. There was no discernable phenotype in any of the single T-DNA insertion examined for ADK1, ADK2 or ADA. Tagged lines lacking either ADK1 (*adk1-1)* or ADK2 (*adk2-1)* had approximately 50% of the ADK activity detected in WT plants but displayed no changes in morphology. Thus based on the stages of development observed in Arabidopsis, the ADK isoforms appear to be interchangeable. However, attempts to cross the two mutant lines resulted in no viable plants bearing double T-DNA insertions (Perry 2004). The inability to generate mutants entirely lacking ADK was also observed in the sADK lines. Unlike the tagged lines, sADK lines display an abnormal phenotype, analysis of which draws a correlation between decreased ADK activity and an increase in severity of phenotype which includes: wrinkled leaves and seeds, smaller lateral roots, delayed development and senescence in leaves and siliques, enlarged inflorescent meristems, lack of primary shoot and petal development, altered petal abscission and inability of siliques to dehisce.

ADA activity has not been detected in WT plants (Moffatt personal communication) so the degree of impairment could not be assessed in the tagged line for this gene; however there is only one putative ADA gene in the Arabidopsis genome so it is assumed the insertion eliminates 100% of the WT ADA activity. Interestingly crossing of sADK9-1 with *ada1-1* resulted in even lower levels of ADK activity and more severe phenotype, in particular an increased proportion of mutant phenotypes in comparision to its sADK9-1 parent and changes in both CK and chlorophyll content. Since recombinant

his-tagged Arabidopsis ADA has ADA activity based on an *in vitro* assay (R. Giercza, unpublished results), it is likely that this enzyme does utilize Ado or Ado-related substrates *in vivo* as well. If this is the case, then ADA would contribute to plant metabolism despite its modest expression level and low abundance in planta.

As adenosine salvage is involved in a wide array of functions throughout the cell, it is impossible to attribute these abnormal phenotypes to one specific defect. Previously identified tagged lines of *apt1* (Moffatt et al. 2002) in Arabidopsis have only one discernable phenotype, which is male sterility caused by defects arising after meiosis. Ultimately, this lack of pollen development has been correlated to lowered adenylate levels leading to altered lipid accumulation in the tapetal cells, changes in pollen cell wall development, and a loss of synchrony in the development of the tapetum and microspore; CK biosynthesis defects may also be contributing (Zhang et al. 2003).Therefore, although essential for pollen development, vegetative growth is not dependent on APT1.

SAH hydrolase-deficient tobacco lines generated through antisense gene silencing share a similar phenotype to that of sADK including floral organ abnormalities, stunting of growth, loss of apical dominance and delayed senescence (Masuta et al. 1995; Tanaka et al. 1997). Metabolite analysis shows that SAH levels are 10-times higher in the SAH hydrolase mutant than they are in WT, suggesting a decrease in Ado levels. Not only does this lower rate of SAH degradation lead to hypomethylation of repetitive DNA and decrease in resistance to plant viruses requiring a methylated cap for their replication, but an up to 3-fold increase of CK levels (Masuta et al. 1995; Tanaka et al. 1997). Data obtained in this study indicate there are changes in both methylation and CK levels ADK-deficient plants, both of which likely contribute to their phenotype.

ADK Deficiency Results in Hypomethylation

The inhibition of the SAM methylation cycle in the sADK lines is supported by the 40-fold increase in SAH (Moffatt et al., 2002) and 88% higher levels of Ado. Such a decrease in methylation can affect numerous cellular functions, one of which is the synthesis of secondary metabolites. Previous studies have directly linked reduced methylation to ADK deficiency in the seed coat and leaf pectin of severely affected sADKs plants (Moffatt et al., 2006). Such a decrease in methylation could impact cell wall components. For pectin in particular, removal or lack of methyl groups on the side chains of the pectin promote interconnecting Ca^{+2} or 'salt' bridges to form between the chains, resulting in a tighter confirmation. In fact it has been suggested that it is this higher level of 'sticky' de-esterfied pectin that causes the 'wrinkling' observed in the sADK lines (Pereira et al., 2006).

Another cell wall component that requires methylation is lignin (Ferrandiz, 2002). In addition to possibly affecting cell wall morphology, the improper synthesis of lignin may also be impacting the ability of the sADK siliques to dehisce. Dehiscence is the separation of valve from the replum, allowing the seeds from within to be dispersed, and one theory of this process relies heavily on lignification (Ferrandiz, 2002). As siliques develop the non-lignified dehiscence zone develops between the lignified cells of the valve and replum; upon maturity the replum becomes heavily lignified, while the valves begin to desiccate. Pod shattering then occurs due to cell wall loosening along the middle lamellae of the dehiscence zone separation layer and the tension formed as a result of differential mechanical properties formed by lignification (Ferrandiz 2002). Histochemical staining of lignin in sADK4-2 siliques and stems indicated they have a

reduced content of methylated lignin as compared to WT tissue (L. Pereira, unpublished results). However, despite the reproducibility of this observation, the stain is not considered quantitative and further study is required to document lignin differences and their association with the change in dehiscence of the sADK lines.

Gene expression and chromatin reorganization are strongly affected by DNA and histone methylation (Jacobsen et al. 2006); such influence is characterized as epigenetic alterations; meaning they are heritable but do not involve changes to the DNA sequence. HPLC analysis of the sADK lines, shows a direct correlation between ADK activity and CG methylation; the lowest level of ADK activity being associated with a 30% decrease in methylation. Mutants documented to have affected CG DNA methylation include *ddm1*, whose interrupted gene encodes a SNF2-like chromatin remodelling ATPase in Arabidopsis (Richards et al., 1999). The loss of DDM1 function can lead up to a 70% loss of genomic methylation and is associated with abnormal leaf development. This loss of methylation occurs over time, with self-pollinating mutants being more affected in later generations. As a result of this degradation in genome methylation heritable alterations also accumulate. By monitoring rosette size and plant height (Perry 2004), sADK plants were shown to develop a more pronounced phenotype over several generations, suggesting that hypomethylation and the resulting genomic alterations are indeed accumulating.

To test whether or not severely affected sADK plants are capable of maintaining their genomic methylation, the ADK deficient lines were crossed into a *fis2* mutant background (Perry 2004). By introducing the *fis2* mutant to a hypomethylated background, the expression of FIS2 is repressed and normal embryo development is once

again restored (Chaudhurry et al., 2000). The ability of the sADK lines to correct the *fis2* wrinkle seed phenotype further validates decreased methylation. In addition, these findings suggests that genomic methylation is affected at the embryonic level in the sADK lines and that their abnormal phenotype is hereditary.

A specific phenotypic alteration observed in sADK that may be caused by epigenetic alterations is the formation of relatively healthy secondary shoots on mutants that have little or no primary shoot and clustered inflorescences. Such a phenomenon has also been monitored in the bonsai mutant, whose phenotype depends on a loss in methylation in the bonsai locus (At1g07377) which encodes a protein involved in cell division (Saze and Kakutani, 2006). In addition to the normal secondary shoot development, bonsai mutants also exhibit variable phenotypes similar to sADK segregation. While this similarity in phenotype was an exciting observation, there is no abnormality in bonsai gene expression in sADK4-2 or sADK9-1 (J. Zhang, unpublished results). However, finding that another DNA methylation mutant has normal secondary branches is indeed intriguing and worthy of further investigation.

Abnormalities Due to Increased Cytokinin Levels

GC-MS-MS analysis of the sADK plants indicates they have an abnormal CK profile, with a particular increase in CK ribosides. Many of the phenotypic abnormalities observed in the sADK lines could be attributed to an increase in CK activity. At the hormone level, the interaction between auxin and CKs is believed to be essential in organ development. In roots, CKs are inhibitory to root growth and a higher auxin:CK ratio promotes root development (Mok 1994). Thus if sADK lines contain higher levels of

CKs, the auxin:CK ratio could be altered and result in smaller root systems. The same could be applied to the abnormal meristem development observed in the sADK mutants. CKs synthesized in the roots and transported to the meristem, stimulate the formation and activity of shoot meristems (Schmulling et al. 2001), while auxin acts as the inhibitor. As in the roots, the higher levels of CKs detected in the sADK mutants would affect the auxin to CK ratio and cause the over-proliferation of cells in the shoot meristem. Increasing meristemic activity would not only result in the larger meristems observed in the sADK lines but also the lack of or decreased internode length in primary shoots and formation of secondary branching.

Delayed senescence was also observed in the fruit and leaves of sADK, and in the case of the leaves higher CK levels have been found to cause such a phenotype by expressing isopentyltransferase (important in CK biosynthesis) under the control of a senescence-specific promoter in tobacco (Gan and Amasino, 1995). The recent development of the *sob5* mutant also highlights the impact of CK overexpression (Zhang et al. 2006). Although the actual function of SOB5 in cytokinin mediated development has yet to be established, RNAi lines for the gene exhibit increased levels of zeatin and iP derivatives (for example ZR is 5.1-fold higher and 2.5-fold for ZMP). These elevated CKs are believed to cause the resulting delay in leaf senescence as well as reduced apical dominance and root development (Zhang et al., 2006).

Mutants involved in CK signalling also display distinctive phenotypes. CK receptor mutants of the Arabidopsis histidine kinase family (AHK2, AHK3 and AHK4) exhibit faster primary shoot development, leaf senescence and germination as well as an increase in seed size and root development, in response to the inability of the plant to detect

cytokinins (Schmulling et al., 2006). That sADK mutants display the opposite of these characteristics, support the hypothesis that the phenotype of ADK-deficient lines is largely attributed to a shift in plant hormone homeostasis.

Conclusion

Through the use of ADK tagged lines it is apparent that at the stages of development examined, ADK1 and ADK2 isoforms do not exhibit specialized functions, while ADK-deficient lines highlight ADK's role in CK interconversion and methyl recycling. In addition analysis of ADA-tagged lines do not indicate an obvious role for this gene product in WT plants, although loss of ADA activity in an ADK-deficient background has an intriguingly large impact on plant morphology and CK metabolism.

CHAPTER 2: KEY METHYL-RECYCLING ENZYMES RESIDE IN MULTIPLE SUBCELLULAR LOCATIONS IN *ARABIDOPSIS THALIANA*

Introduction

Transmethylation occurs in most plant cellular compartments where it contributes to a wide variety of reactions ranging from mRNA capping, DNA and histone methylation in the nucleus to cell signalling in the cytosol and chlorophyll biosynthesis in plastids. The methyl donor molecule for these reactions is *S*-adenosylmethionine (SAM, AdoMet) (Poulton, 1981). In addition to the methylated acceptor, each SAM-dependent methyltransferase (MT) produces one molecule of *S*-adenosylhomocysteine (SAH). Because SAH is a feedback inhibitor of all SAM-dependent MT reactions characterized to date, it must be quickly metabolized to prevent inhibition of MT activities (Poulton 1981). SAH hydrolase (SAHH; EC 3.3.1.1) is the only enzyme capable of breaking down SAH in eukaryotes (de la Haba and Cantoni, 1959). However, the equilibrium of the SAH hydrolase reaction strongly favours SAH formation but can be driven in the hydrolysis direction by the metabolism of each reaction product, adenosine (Ado) and homocysteine. The latter is recycled into methionine and subsequently back to SAM, while in plants Ado is salvaged mainly by adenosine kinase (ADK; EC 2.7.1. 20) (Moffatt et al., 2002).

The need to metabolize SAH throughout the cell is complicated by the fact that based on their lack of targeting signals, both SAH hydrolase and ADK are considered to reside in the cytosol, the primary location of methyl recycling reactions (Hanson and

Roje, 2001). There are two solutions to this situation: SAH could be transported into the cytosol or SAH hydrolase and ADK could reside in multiple compartments. Only a few reports have addressed this issue. One has identified a SAM/SAH symporter in chloroplasts which exchanges plastid-produced SAH for SAM; this transport system is consistent with the first paradigm (Ravanel et al., 2004). A more recent report has also identified a similar SAM transporter (SAMC1) in Arabidopsis that functions in the mitochondria and possibly the chloroplast as well. Evidence for the localization of ADK and SAH hydrolase to compartments other than the cytosol comes from two independent proteomic studies; ADK was recovered from purified chloroplasts of *A. thaliana* grown under normal growth conditions (Kleffmann et al., 2004) and is also present in the chloroplasts of Dunaliella algae grown in saline conditions (Liska et al., 2004). SAH hydrolase was not detected in these studies but it is possible that due to its large size (493 kDa) (Schomburg et al., 2004), it has not been recovered. However, a recent proteomic study performed on Arabidopsis suspension cells (Shimaoka et al., 2004) identified SAH hydrolase in the tonoplast, suggesting that SAH hydrolase may be localizing elsewhere other than the cytosol. Thus it is possible that only ADK is localizing to the chloroplast, to perform other vital functions in adenosine salvage. The most compelling evidence for SAH hydrolase translocation to compartments other than the cytosol comes from studies of *Xenopus leavis* oocytes. Dreyer and colleagues found that SAH hydrolase localizes to the nucleus during times of increased transcription where it directly interacts with the MT involved in mRNA capping, one of the largest methyl demands in eukaryotic cells (Radomski et al., 2002). Given that SAH hydrolase is one of the most highly conserved

known proteins (Sganga et al., 1992) it is very possible that similar localization occurs in other eukaryotes.

Although neither ADK nor SAH hydrolase contain any discernable targeting signals in their sequences both enzymes are encoded by isoforms that share 92% amino acid identity in Arabidopsis ADK1 (At3g09820) and ADK2 (At5g02200); SAHH1 (At4g13940) and SAHH2 (At3g23810). Despite variances in their expression levels being documented (Moffatt et al., 2000; Pereira et al., 2006), no distinct role has been assigned to the isoforms of either enzyme. Thus, in addition to establishing whether or not ADK and SAH hydrolase are present in more than one subcellular compartment, this research was performed to differentiate any unique roles these isoforms may provide in subcellular targeting. To accomplish these goals, Arabidopsis knockout lines deficient in either ADK1 or ADK2 were identified in Arabidopsis and used together with WT leaf and meristemic tissue for immunogold localization studies. Further studies designed to specifically examine ADK and SAH hydrolase isoforms utilized translational fusions with β-glucuronidase (GUS) and green fluorescent protein (GFP). Upon establishing the subcellular localization of these enzymes, Western blotting and *in vitro* import assays were performed on isolated Arabidopsis chloroplasts obtained from plants at various stages of development to determine whether ADK and SAH hydrolase localization is dependent upon the metabolic demand of the plant. All transgenic lines were created by others, GFP lines examined by S. Lee.

Results of the immunogold and GUS fusion lines show ADK and SAH hydrolase to reside in three compartments: the cytosol, nucleus and chloroplast. Both methods found no differentiation in the localization of the isoforms, suggesting that neither has a

specialized transport function. Most importantly the detection of the GUS protein fusions in the nucleus indicated these enzymes do not rely on simple diffusion to enter the compartment, and instead require directed transport. However, further analysis of GFP translational fusion lines of SAHH1 and ADK1 and isolated Arabidopsis chloroplasts provided contradictory evidence as to whether or not the proteins are localizing to the chloroplast; leaving it unclear as to how, or if, the proteins enter the plastid.

Experimental Methods

Plant Materials and Growth Conditions

For all experiments the ecotype Col-0 of *Arabidopsis thaliana* was used. Both *adk1-1*(GARLIC D09) and *adk2-1* (SALK 000565) mutant stocks were ordered from ABRC, and homozygous T-DNA insertions were identified by PCR using flanking and LB primers (Ecker et al. 2003; described in Chapter 1). Plants were grown on a 50:50 mixture of Sunshine LC1 Mix and Sunshine LG3 Germination Mix (JVK) under fluorescent light (150 ± 20 μmol m^{-2} s^{-1}) in an 18-h light/6-h dark photoperiod, at 22ºC. The following experiments performed on the plants, unless otherwise stated, used minimum ACS grade Sigma products.

Generation of Antibodies

Rabbit anti-ADK and anti-SAHH antibodies were raised against His-tagged recombinant versions of ADK1 and SAHH1 expressed from pET30a (Novagen) in BL21 (DE3) pLysS by B. Moffatt, Yvonne Stevens and Luiz Pereira. After injecting the rabbits with the recombinant protein, sera was collected and affinity-purified using ADK or SAHH affinity columns (Gu et al., 1994). After injecting the rabbits with the recombinant

protein, sera was collected and affinity-purified using ADK or SAHH affinity columns. Chicken anti-SAHH antibody was prepared by Immunochem Diagnostic Technologies (IDT, Truro, Nova Scotia), using the same recombinant SAHH; unfortunately pre-immune chicken serum was not provided. The limits of detection for each antibody were determined through dot blots; the rabbit anti-ADK antibody detected 0.01 ng, rabbit anti-SAHH detected 0.001 ng and chicken anti-SAHH detected 0.005 ng (Pereira et al. 2006). All antibody preparations were specific to only one polypeptide.

Immunogold Labelling

Meristems and leaves of 3.5 week-old Arabidopsis were collected and fixed immediately in a solution of 2% (w/v) paraformaldehyde and 0.1% (v/v) glutaraldehyde prepared in 0.05 M cacodylate buffer (pH 7.0) for 1 hr under vacuum at RT. After an additional O/N incubation at 4˚C in fresh fixative, the tissue was thoroughly washed in dH_2O and 0.05 M cacodylate buffer pH 7.0. The samples were then dehydrated in an ethanol series, before being infiltrated and embedded in LR White resin. Once embedded in plastic, the samples were sectioned (70-90 nm) using a Reichert Ultracut E ultra microtome and placed onto nickel grids (Marivac, 300 mesh). Sections were stored for 48 hrs in preparation for immunogold labelling.

The first step of the immunogold labelling was to incubate sections in droplets of PBSMT blocking buffer (5% (w/v) fat free Carnation powder milk, 1% BSA, 0.5% (w/v) Tween 20 in 1x PBS) for 30 min at RT. The sections were then placed on fresh droplets of PBST (1% BSA, 0.5% (w/v) Tween 20 in 1x PBS) supplemented with 1:50 dilutions of either serum for 3 hrs. After washing the sections for 5 mins in fresh droplets of PBST 3x, they were incubated for 3 hrs in either goat anti-rabbit IgG antibody conjugated to 15

nm colloidal gold (Electron Microscope Services), or goat anti-chicken IgG conjugated to 6 nm colloidal gold (Electron Microscope Services) diluted to 1:40 in PBST. The washes in PBST were repeated after which the sections were post-fixed in 2% (w/v) glutaraldehyde in 1x PBS for 5 min and washed 3x for 15 mins in 1x PBS; subsequently the sections were counterstained with lead citrate and uranyl acetate. Negative controls consisted of omitting primary antibody, blocking primary antibodies with purified recombinant of ADK (1 mg/mL) or SAHH (1 mg/mL) and replacing rabbit anti-ADK with pre-immune rabbit serum.

The samples were then ready to be observed and photographed using a transmission electron microscope (Phillips CM10). The number of gold particles per surface area was determined for three different leaves at ten electron micrographs each using image processing software, ImageTool (Version 3, University of Texas Health Science Center in San Antonio).

Generation of GUS Fusion Lines

Transgenic plants expressing either SAHH1/2 or ADK1/2 fused to GUS were constructed by inserting either 1.5 kb of SAHH1/2 or 1 kb of ADK1/2 cDNA between the constitutive CaMV35S promoter and GUS marker gene of pCAMBIA 1305.1, using *Nco*I (see Table 7). To ensure that the fusions would be properly transcribed, cDNA was verified to not contain stop codons; CDS and junctions of the fusions were then sequenced. Once the constructs were inspected, they were introduced into 4-week-old *A. thaliana* (Columbia) using *Agrobacterium tumefaciens* (Clough and Bent, 1998). Homozygous lines were screened for hygromycin resistance on MS media containing 25 mg/mL Hygromycin B (Sigma).

Visualization of GUS Samples

In order to visualize GUS protein fused to ADK and SAHH isoforms, inflorescences and leaves from 3.5 week-old GUS fusion lines were histochemically stained as described in Jefferson et al. (1987) using X-Gluc purchased from Bioshop. Once the histochemical staining was complete, the samples were washed in 70% ethanol and fixed in 2.5% (w/v) glutaraldehyde and 2% (w/v) paraformaldehyde in 100 mM potassium phosphate buffer (pH 7.0) O/N at 4˚C. After washing the samples in 100 mM potassium phosphate buffer, the plant tissue was dehydrated in an ethanol series and embedded in LR White. After allowing the resin to harden at 65˚C, the samples were sectioned to 6μm thickness using a Reichert Ultracut E ultra microtome. The sections were examined using a Zeiss Axiophot fluorescent microscope.

Western Blots

Protein of whole leaf samples was obtained by homogenizing tissue of 2.5, 3.5 and 4.5 week-old plants in extraction buffer (5 mM dithiolthreitol, 50 mM 4-[2-hydroxyethyl]-1-piperazineethanesulphonic acid [HEPES pH 7.2], 1 mM Ethylene diamine tetraacetic acid [EDTA, pH 8.0], 50 mM citric acid pH 4.2, 10 mM boric acid pH 6, 20 mM Na-metabisulphate, 4% w/v polyvinylpyrrolydone [PVP, P-5288 MW 360,000]). Chloroplast samples were obtained from 2.5, 3.5 and 4.5 week-old Arabidopsis following the extraction protocol performed by Schulz et al. 2004.

Table 7. Generation of GUS fusion lines for ADK and SAH hydrolase isoforms in *A. thaliana.*

cDNA fragments of ADK1/2 and SAHH1/2 were isolated using primers specific to the isoform during PCR. As well as amplifying the isoform cDNA, the PCR ensured that the cDNA could be cut on either end using *Nco*I, as both primers contained the required cut site. The fragments were then inserted into the desired vector, by digesting both the cDNA and plasmid with *Nco*I, and incubating them together to allow ligation. Lines (A-B, D) used pCambia 1305.1, while (C) used pCambia 3301. The ADK1 GUS fusion containing the endogenous promoter (E) was constructed using a previously created line using pCambia 1305.1. The constructs were then introduced to DH5α electrocompetent cells using electroporation and successful transformants were screened for kanamycin resistance. Transformation of the plant was performed by exposing 4 week-old plant inflorescences to *Agrobacterium tumefaciens* (GV1030) cultures containing the construct. Seed was then collected from the transformed plant, and screened on the antibiotic specific to the vector.

Line	Plasmid	Source	cDNA size (bp)	Primers
A. 35Sp::SAHH1-GUS	pCambia 1305.1	Yong Li Jing Zhang	1440	SAHH1rev: CTCCATGGACCTGTAGTGAGGAGGCTT SAHH1cDNcF: TCAACCATGGCGTTGCTCGTC
B. 35Sp::SAHH2-GUS	pCambia 1305.1	Yong Li Jing Zhang	1451	SAHH2 for: CAACCATGGCTTTGCTTGTAGAGAAAACC SAHH2cDNcR: CTACTCCATGGACCTGTAGTGAACAGGCTTG
C. 35Sp::ADK1-GUS	pCambia 3301	Yong Li	1056	AK1cDNcR: GACCATGGTGAAGTCTGGTTTCT AK1cDNcF: CATCCATGGTTCCTCTGATTTC
D. 35Sp::ADK2-GUS	pCambia 1305.1	Yong Li	1033	AK2cDNcR: AGCCATGGTAAGTCGGGCTTC AK2cDNcF: CACCATGGCTTCTTCTTCTAACTACG
E. ADK1p::ADK1-GUS	pCambia 1305.1	Yong Li	1056	AK1cDNcR: GACCATGGTGAAGTCTGGTTTCT AK1cDNcF: CATCCATGGTTCCTCTGATTTC

Prior to chloroplast isolation, plants were placed in the dark for 2-3 hrs to remove starch from chloroplasts; in addition all solutions were cooled on ice for 1hr or O/N. After collecting 10g of leaf tissue, the leaves were homogenized in 125 mL of 1x grinding buffer (GB; 50 mM HEPES pH 7.5, 330 mM sorbitol, 0.125% BSA, 0.5 M EDTA, 1 mM magnesium chloride [$MgCl_2$], 1mM manganese chloride [$MnCl_2$], water) using a blender (Osterizer, 2 x 30 sec set to 'grind').

The homogenate was then quickly poured through two layers of cheesecloth and into a 250 mL centrifuge tube. Un-homogenized leaf tissue was removed from the cheese cloth, re-suspended in 100 mL 1x GB, re-homogenized and filtered over two new layers of cheesecloth into the centrifuge containing the original isolated chloroplasts. Samples were then centrifuged at 1000 x g for 5 min at 4ºC. The resulting chloroplast pellet was resuspended in 3 mL 2x GB (100 mM HEPES pH 7.5, 660 mM sorbitol, 0.25% BSA, 0.5 M EDTA, 1 mM $MgCl_2$, 1mM $MnCl_2$, water) and layered over a 40/85% Percoll pad. To prepare the Percoll pad, 6 mL of 40% Percoll was gently pipetted onto 3 mL of 85% Percoll (diluted in 2x GB) in 12 mL centrifuge tube. The samples were then centrifuged at 7700 x g for 15 min at 4ºC in a swinging bucket rotor centrifuge (Beckman SwiT1) set to brake off. The intact chloroplasts located between the 40 and 85% layers were then pipetted into 40 mL of HEPES-sorbitol buffer (HS; 50 mM HEPES pH 8.0, 330 mM sorbitol) in 100 mL centrifuge tube. The samples were then centrifuged at 1000 x g for 5 min at 4ºC. The resulting supernatant was discarded and the pellet re-suspended in 0.5 – 1 mL HS buffer (depending on size of pellet). The isolated chloroplasts were then treated with thermolysin to remove possible cytosolic contamination. To do this 90 µL of

chloroplasts were incubated with 12.5 µL of thermolysin (2 mg/mL; Sigma), 6.25 µL calcium chloride (200 mM) and 141.25 µL milliQ water for 40 min on ice. The reaction was stopped by adding 100 µL of 50 mM EDTA.

Protein concentrations of both chloroplast and leaf were quantified using the Bradford assay (Bradford 1976) with BioRad (BioRad, #500-0006) solution diluted to 1:4 with ddH_2O and 1 mg/mL BSA as a standard. Upon establishing their concentration, the chloroplasts were aliquoted into 10 µg samples and their protein was precipitated by incubating in 80% acetone (1:4 ratio of chloroplast sample: 100% acetone) for 1 hr or O/N on ice. After the proper incubation time, the chloroplast protein was centrifuged at 13 200 rpm for 20 min. The protein pellet was then re-suspended in 20 µL of 1 x running buffer, incubated at 65ºC for 15 min and aspirated with a pipette tip. To prepare the leaf extract, 5 µg of protein was also mixed with 1 x running buffer to a total volume of 20 µL. The samples were electrophoresed on 12.5% (v/v) sodium dodecyl sulphate polyacrylamide gels (SDS-PAGE) and transferred to a PVDF membrane. The membrane was probed with affinity-purified polyclonal anti-ADK and anti-SAHH antibodies diluted 1:8000 and 1:16000, respectively, or polyclonal anti-SAMS antibodies diluted 1:1500 (Schroder et al., 1994). Binding of antibodies was detected using anti-rabbit antibodies conjugated to horse radish peroxidase (Sigma) and visualized on Kodak film with enhanced chemiluminescence (ECL; Amersham) labelling for 30 sec, 5 min and 10 min exposures.

In vitro Import Assays

Components required in synthesizing ^{35}S labelled protein of ADK, SAH hydrolase and SSU were obtained from the TNT Coupled Reticulocyte Lysate system (Promega

L4610); with the exception of template DNA obtained from M. Smith from the Wilfrid Laurier University. In a 50 µL reaction, the following reagents were mixed and incubated at 30ºC for 1.5 hrs: 25 µL lysate, 2 µL buffer, 1 µL amino acids (without methionine [Met]), 2 µL ^{35}S (Met), 2 µL RNasin, 10 µg DNA template , 1 µL T7 RNA polymerase, sterilized milliQ water. After the required incubation, the synthesized protein was checked on 12.5% SDS-PAGE gel using a phosphoimager. Remaining protein was stored at -80ºC.

Chloroplasts used in the import assays were isolated in the same manner as those used in the western blotting, with the exception of their quantification and not being precipitated. The quantity of the chloroplasts was determined by mixing 10 µL of the chloroplast suspension with 990 µL 80% acetone in a cuvette and measuring its absorbance at 645 and 663 nm (80% acetone used as a blank). The chlorophyll content was then determined using the following equation (Jagendorf 1982): $[(A_{645} \times 202) + (A_{663} \times 80.2)] \times 10.5 = \mu g/mL$.

For each import reaction, 50 µg of chlorophyll (intact chloroplast) was mixed with 10 µL of 10 x master mix (MM), 1 µL 0.1M DTT, 5 µL 0.1M ATP, 1 µL 0.1M GTP, 5 µL 200 mM Met, 3 µL radiolabelled protein and HS buffer to a total volume of 100 µL. To allow for error and duplicate samples to treat with or without thermolysin, this was performed at a 2.1-fold volume (total 210 µL). The mixture, without the ^{35}S protein, was first incubated at 25ºC for 5 min; upon the addition of the protein, 30 min at 25ºC. To stop import, 630 µL of ice-cold HS buffer was added and the samples split up to 400 µL aliquots. The samples were then layered onto a 500 µL 40% Percoll pad (1.5 mL tube) and centrifuged at 5000 x g for 5 min. The broken chloroplasts in the upper layer were

discarded, and the intact pellet below the Percoll was re-suspended in 100 µL HS buffer. For the samples being treated with thermolysin, 1 µL of 1M $CaCl_2$ and 10 µL of 2 mg/mL thermolysin was added, incubated on ice for 40 min and the reaction stopped by adding 4 µL of 0.5 M EDTA. All of the samples (+/- thermolysin) were then mixed and centrifuged at 5000 x g for 5min. The supernatant was discarded and the chloroplast pellets re-suspended in 25 µL of 1 x SDS running buffer and incubated at 50ºC for 15 min. Starch was removed by centrifuging the chloroplast protein at 13 200 rpm for 15 min. The samples were then electrophoresed on a 15% SDS-PAGE gel; pure radiolabelled protein was also added to the gel by taking 1 µL of stock and adding it to 6.7 µL of water, mixing and adding 1 µL of dilution to 19 µL of 1xSDS buffer. The gel was then dried for 1 hr, exposed to a phosphor film for at least 48 hrs and visualized using a phosphoimager.

Results

TEM Analysis of ADK and SAHH Localization

The subcellular localization of ADK and SAH hydrolase was investigated using immunogold labelling. To detect ADK and SAH hydrolase, affinity-purified antibodies specific for the enzymes were previously developed in rabbit (Moffatt et al. 2000). Immunoblots probed with these antibodies showed the limit of detection to be 0.01 and 0.005 ng for ADK and SAH hydrolase, respectively. However, due to the high degree of identity of the isoforms, the antibodies are unable to distinguish between the two forms of ADK and SAH hydrolase (Pereira et al., 2006). To allow for the differentiation of ADK

isoforms, ADK tagged lines were examined along with leaves and meristems of 3.5 week-old WT Arabidopsis; T-DNA insertion mutants lacked either ADK1 (*adk1-1*, GARLIC 597_D09*)* or ADK2 (*adk2-1,* SALK 000565).

Immunogold labelling excluding anti-ADK or anti-SAHH antibodies or using pre-immune rabbit sera resulted in no protein detection in the tissue sections. Previous work by L. Pereira (2004) also tested the specificity of the antibodies by pre-incubating them with their respective purified protein; the purpose being to saturate their binding capacities for ADK or SAH hydrolase. In all sections examined, there was no labelling of SAHH and only one case of the ADK antibody binding. Taken together with the lack of antibody binding to pure resin sections, it was concluded that these antibodies specifically recognized their target epitopes (see Figure 18). Additional experiments carried out using anti-SAH hydrolase antiserum from chicken and rabbit resulted in the same localization, however labelling with the chicken antibody did result in some clustering of the gold particles (data not shown). This higher density of clustering is not necessarily a result of higher amounts of SAH hydrolase and is most likely due to antibody conjugates formed within the chicken serum prior to labelling (Invitrogen, technical resources). To maintain continuity, only data obtained with rabbit anti-SAHH antibodies was used in quantifying SAH hydrolase localization.

The results of the immunogold labelling experiments showed that both ADK and SAH hydrolase reside in multiple subcellular compartments. In WT samples SAH hydrolase and ADK were consistently found in the cytosol, the nucleus and the chloroplast of both the leaf and meristem tissue (see Figure 19). Of all the sections examined, only 4% of the mitochondria were identified as containing SAH hydrolase;

neither WT nor mutant tissue contained evidence of ADK in mitochondria. Perhaps surprisingly, the mutants had the same pattern of localization of ADK as in WT tissue; both *adk1-1* and *adk2-1* leaf and meristem tissues had ADK localized in the cytosol, the nucleus and the chloroplast (see Figure 20).

The occurrence of ADK and SAHH immunogold labelling per μm^2 of cellular compartment surface was quantified in 50 different microscopic fields (see Figure 21). Overall, ADK was evenly distributed throughout the cytoplasm, nucleus and chloroplast in WT as well as ADK1 and 2 deficient mutants, whereas SAH hydrolase was detected at half the level of the cytosol in the nucleus, and a third of the cytosol in the chloroplast. As only five mitochondria contained gold particles in all of the micrographs examined, SAH hydrolase's presence in the organelle on a μm^2 basis was negligible. Overall, of the mitochondria observed only 8% contained SAH hydrolase; in contrast 70% of the chloroplasts contained ADK and 56% had SAH hydrolase.

Figure 18. Controls for immunogold labelling in Wt *Arabidopsis* tissue.

Several controls were done to ensure the stringency of the labelling assays. Exclusion of either rabbit anti-ADK (A) or anti-SAHH antibody (B) resulted in no gold particles binding to cellular compartments including the cytosol, nucleus, chloroplast and mitochondria. In addition, replacing rabbit anti-ADK antibody with pre-immune rabbit serum also resulted in no binding of gold particles. In all of the above cases, non-specific binding only occurred in the 'sticky,' emptied vesicles of the starch grains. Examination of the bare resin (D) of the sections also gave no indication of non-specific binding, with the plastic being free of particle debris. Abbreviations: (CW) cell wall; (Chl) Chloroplast; (Cyt) Cytoplasm; (Mit) Mitochondria; (N) nucleolus; (Nuc) nucleus; (St) starch grain; (△) 15 nm gold particle. Bar = 100 μm

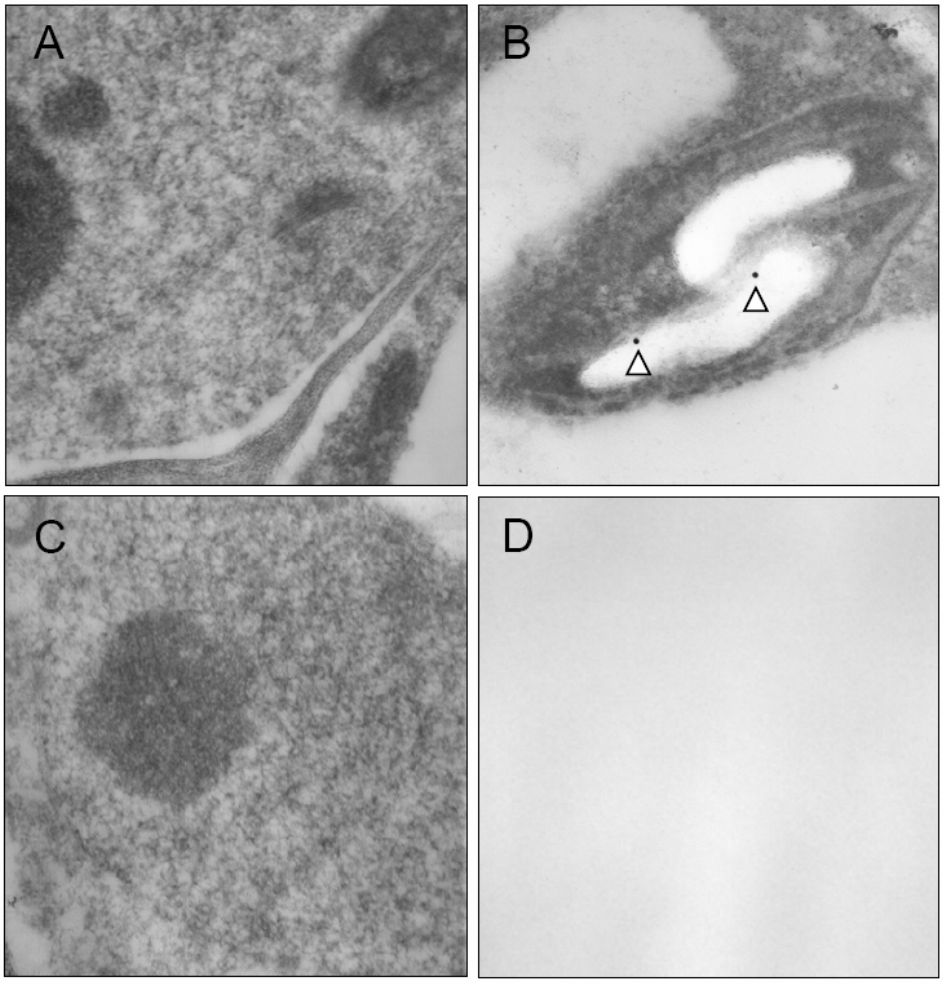
A
B
C
D

Figure 19. Immunogold labelling of ADK and SAH hydrolase in the leaf and meristemic tissue of 3.5- week-old WT Arabidopsis.

Immunogold localization of ADK (A, C, E) and SAH hydrolase (B, D, F) in the cytosol (A-B), nucleus (C-D) and chloroplast (E-F). The gold particles in the cytosol are distributed throughout the cell near chloroplasts (A), mitochondria and the cell wall (B) of the leaf. In (D) ADK and SAH hydrolase were detected near the nucleus of the meristem, apparently in the process of crossing through the nuclear envelope as well as residing in the nucleus. Staining in the leaf tissue makes some of the thylakoid stacks (grana) visible (vertical light lines distributed throughout the plastid). Closer examination of the gold particles suggest that ADK and SAH hydrolase reside outside the grana and in the darker stained stoma (E-F). Abbreviations: (CW) cell wall; (Chl) Chloroplast; (Cyt) Cytoplasm; (Mit) Mitochondria; (N) nucleolus; (Nuc) nucleus; (St) starch grain.; (△) 15 nm gold particle.

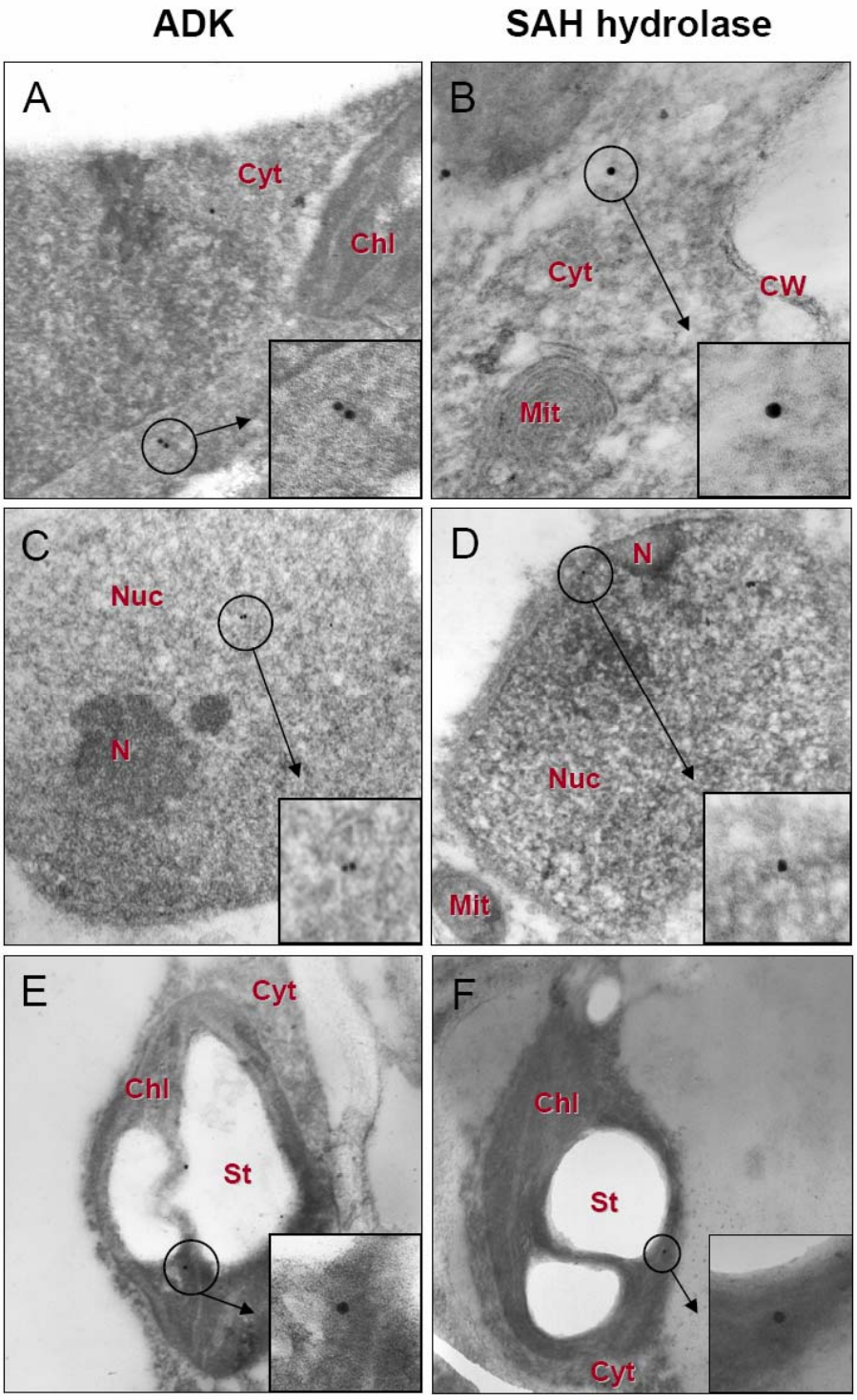
ADK
SAH hydrolase
A
Cyt
Chl
B
Cyt
CW
Mit
C
Nuc
N
D
N
Nuc
Mit
E
Cyt
Chl
St
F
Chl
St
Cyt

Figure 20. Immunogold labelling of ADK in the leaf and meristemic tissue of 3.5- week-old *adk1-1* and *adk2-1*.

Detection of ADK in tagged lines lacking either *adk1-1* (A, C, E) or *adk2-1* (B, D, F) with affinity-purified anti-ADK antibodies. Antibody binding was evident by binding of secondary anti-rabbit antibodies conjugated to 15 nm gold particles. Labelling was evident in the cytosol (A-B), nucleus (C-D) and chloroplast (E-F). Therefore both ADK1 and ADK2 localize to at least to these three subcellular compartments. Abbreviations: (CW) cell wall; (Chl) Chloroplast; (Cyt) Cytoplasm; (Mit) Mitochondria; (N) nucleolus; (Nuc) nucleus; (St) starch grain; (△) 15 nm gold particle.

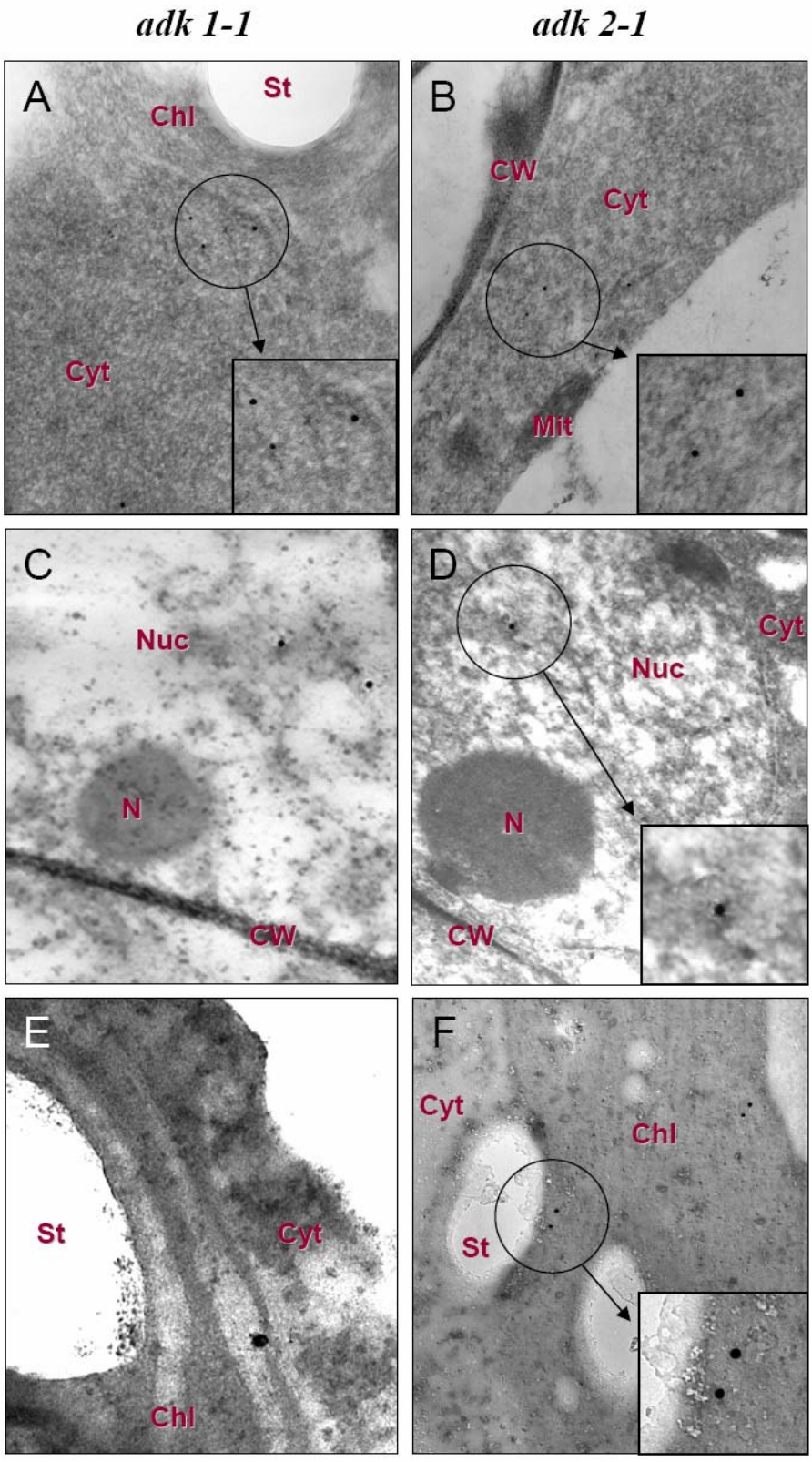
adk 1-1
adk 2-1
A
St
Chl
Cyt
B
CW
Cyt
Mit
C
Nuc
N
CW
D
Cyt
Nuc
N
CW
E
St
Cyt
Chl
F
Cyt
Chl
St

Figure 21. Density of protein labelling detected per μm^2 of cellular compartment of leaf and meristem.

To establish the distribution of gold particles throughout the cell, the surface area and the number of corresponding labelling was determined in 40 individual cells for ADK and SAH hydrolase in WT and 25 individual cells of the ADK tagged lines. Analysis of gold particles bound to ADK1 and 2 epitopes reveals ADK to be evenly distributed throughout the three compartments (cytosol, nucleus and chloroplast); SAH hydrolase appears to be most abundant in the cytosol and less so in the nucleus and almost undetectable in the mitochondria. Negative controls for ADK and SAH hydrolase both resulted in no beads binding to the tissue. Only SAH hydrolase detected using anti-rabbit antibodies were used to collect the data.

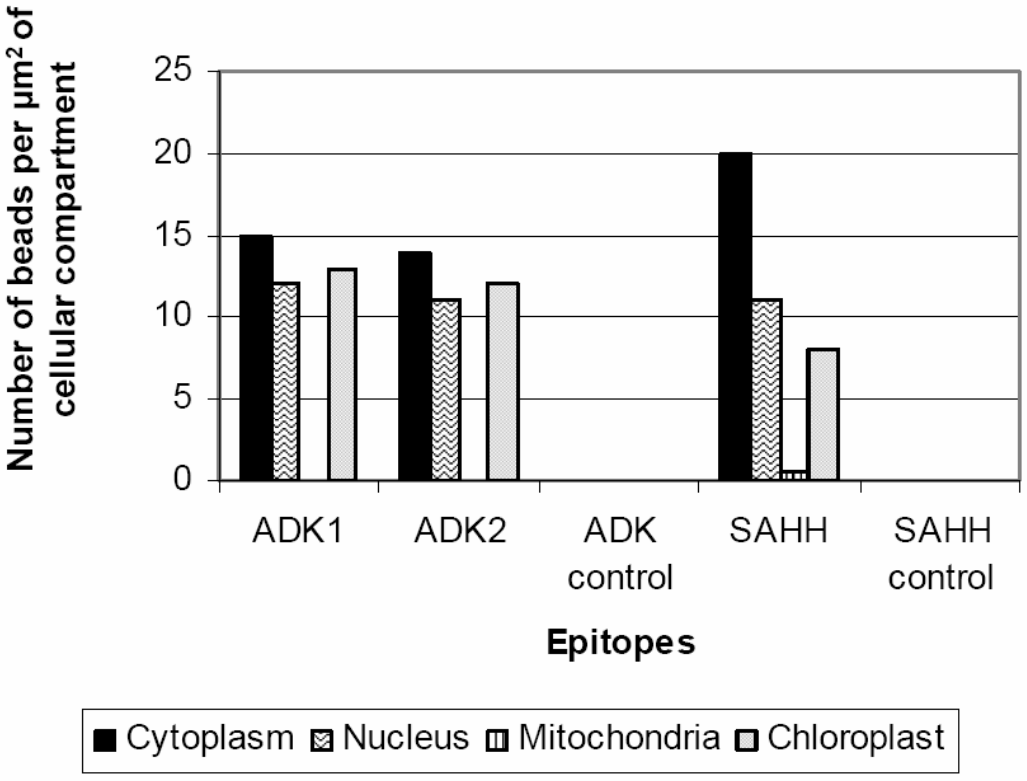
Number of beads per µm² of cellular compartment
25
20
15
10
5
0
ADK1
ADK2
ADK control
SAHH
SAHH control
Epitopes
Cytoplasm
Nucleus
Mitochondria
Chloroplast

Determining Method of Transport Using GUS Fusions

Despite establishing that ADK1, ADK2 and SAH hydrolase are capable of localizing to the chloroplast and nucleus, the immunogold studies did not provide additional information on how the proteins might be taken up by the subcellular compartments. While chloroplasts are thought to rely on active transport to take up cytosolic proteins, nuclei are known to contain pores that allow proteins up to 50-70 kDa (Merkle et al. 1996) to enter rapidly via diffusion. Since ADK is 32 kDa it should pass through these pores passively; SAH hydrolase on the hand is a tetramer of 58 kDa monomer subunits. Assuming it enters as an active enzyme, as is commonly assumed then it must interact with the importing system (Merkle et al., 1996). To rule out the possibility of diffusion of SAHH monomers translational GUS fusion lines were generated by other students in the Moffatt lab (M. Todorova and A de Neto, unpublished results).

Histochemical staining of a plant line (CS 3501) expressing GUS under the control of the constitutive 35S promoter, revealed GUS to be incapable of entering any cellular compartment other than the cytosol by simple diffusion (see Figure 22). To determine whether or not over expression might be influencing the localization of the GUS fusion proteins (i.e. overwhelming transport machinery leading to import into abnormal compartments), ADK1p::ADK1-GUS transformants were also constructed and studied. There was no difference observed in the pattern of GUS expression when the fusion protein was under control of the native versus 35S promoter. This suggests that the 35Sp::GUS fusion lines are representative of native localization ADK and SAHH.

Finally, examination of unstained and untreated tissue resulted in no detection of blue precipitate; only the starch grains of the chloroplasts were evident (see Figure 22).

Upon determining GUS is limited to the cytosol, lines were constructed which expressed GUS fused with the coding sequence of ADK1 or 2 (ADK1/2) or SAHH1 or 2 (SAHH1/2) under control of a constitutive 35S promoter. After screening, two homozygous lines of each construct were histochemically stained and fixed in triplicate. Examination of the leaves from 3.5 week-old plants confirmed the immunogold findings; SAH hydrolase and ADK were detected in the cytosol, nucleus and chloroplast (see Figure 23). It was further confirmed that the SAH hydrolase and ADK isoforms do not differentially localize, as blue precipitate was evident in all three compartments in the leaf tissue of all the lines.

To further validate these findings, immunogold labelling was performed on leaves obtained from 3.5-week-old 35S::SAHH1-GUS or 35S::SAHH2-GUS translational fusion lines using an antibody specific to GUS (see Figure 22). Detection of GUS showed the protein fusions localized in the same manner as revealed by immunogold labelling. Specifically, both isoforms were detected in the nucleus, chloroplast and cytosol; there were no evidence of localization in the mitochondrion (see Figure 23).

Impact of Development on Localization

Although immunogold labelling and GUS fusions showed ADK and SAH hydrolase residing in multiple compartments of the cell, both methods have only looked at one static point of development in the plant's life cycle and limited tissue types. To allow easier tracking of the enzymes' movements, Arabidopsis plants were stably transformed with GFP translational fusion lines of ADK1 or SAHH1 and examined *in vivo* with

confocal microscopy. These lines were developed by Sanghyun Lee. To prevent misinterpretation of localization, Arabidopsis expressing GFP protein under the control of a 35S constitutive promoter were also generated and examined. As anticipated, the GFP protein was found to be exclusively localized to the cytosol and nucleus (see Figure 24); the nuclear localization was anticipated since GFP, at 23 kDa, is below the exclusion limits of nuclear pores. Protein targeting throughout development was then examined using rosette leaves from plants of various ages from 1 to 5 weeks.

All GFP fusions consistently localized to the cytosol and nucleus throughout development, but showed no significant levels of fluorescence in the chloroplast (see Figure 24). Although several chloroplasts appeared to contain GFP, this was not consistently observed in all neighbouring cells. SAHH1 and ADK1 constructs under the control of their native promoters or the constitutive 35S promoter were also transiently introduced into tobacco leaves, with the same findings: GFP fusions were detected in the cytosol and nucleus. Thus the promoter did not affect the movement of the GFP fusions.

In an attempt to study a larger population of plastids at once, chloroplasts were isolated from 4-week-old leaves and examined under a fluorescent microscope. To ensure the removal of cytosolic GFP sticking to the outside of the chloroplast wall, intact chloroplasts were separated from the broken plastids using a 40% Percoll pad. Initial comparison of 35S::GFP to 35S::SAHH1/ADK1-GFP isolates show a significant decrease of GFP fluorescence suggesting the Percoll gradient was successful in removing cytosolic contaminants from the extract (see Figure 25). Of the thousands of chloroplasts observed from the protein fusions, only a few appeared to contain GFP while no fluorescence was detected in the chloroplasts of the 35S::GFP control line. However, at

the confocal microscope level there is not enough evidence to support SAHH1 and ADK1 GFP-fusion proteins localization to the chloroplast.

Establishing Localization to Chloroplast

In order to firmly establish whether or not SAH hydrolase and ADK reside in the chloroplast, immunoblots and *in vitro* import assays were performed. To do so, chloroplast isolations were performed on 3.5-week-old WT Arabidopsis, 35S::SAHH1-GFP and 35S::ADK1-GFP plants for the purpose of immunoblotting and for import. To remove contamination, intact chloroplasts were selected by centrifugation through a 40/85% (w/v) Percoll gradient and treated with thermolysin to remove cytosolic proteins sticking to the outer chloroplast envelope.

After numerous attempts to detect ADK and SAH hydrolase in the chloroplast with western blotting, no definitive answer has yet to be obtained; some blots showed the enzymes in the chloroplast whereas others did not. One of the more successful attempts using anti-ADK and anti-SAH hydrolase antibodies shows both the endogenous proteins and GFP fusions in the chloroplast fraction (see Figure 26). Detection with the cytosolic marker, phosphoenolpyruvate (PEP) carboxylase, suggests the chloroplast samples are not contaminated with cytosol and that the protein detected is in fact of plastid origin. Between ADK and SAH hydrolase, the latter was seen in higher levels in the plastid extract despite being at equal levels of detection in the leaf. However, the SAH hydrolase antibody is more sensitive than anti-ADK (0.005 ng compared to 0.01 ng), thus the apparent higher levels of SAH hydrolase in the chloroplast may be due to the level of detection of the antibody and not protein levels. Because the GFP fusions were expressed using a 35S constitutive promoter the levels of these fusions were much higher than that

of the endogenous proteins (see Figure 26). In addition, no changes were observed in the size of the proteins found in the plastid, suggesting a lack of post-import processing of the transit peptide. However as stated earlier these results have not been replicated.

In vitro import assays also provided in definitive results. Import proved to be difficult, even using the small subunit (SSU) of Rubisco positive control. In experiments that showed successful import of this control, a clear answer as to whether ADK and SAH hydrolase were entering the chloroplast was not obtained. Results showed ADK and SAH hydrolase to be present in post-import thermolysin-treated Arabidopsis chloroplasts, but not those of pea. As seen in the immunoblots (see Figure 26), the proteins also did not change in size upon import due to the removal of a signal peptide. Pre- and post-thermolysin treated chloroplasts showed the same level of import for the ADK, while showing reduced levels for SAH hydrolase (see Figure 27); it is possible that the thermolysin treatment is not effective against ADK as it is against the SAH hydrolase. Thus protein detected in the chloroplasts may be due to non-specific binding and incomplete digestion by thermolysin.

Figure 22. Control sections of 3.5 week-old Arabidopsis leaf tissue.

To ensure ADK and SAH hydrolase was not misinterpreted in the translational GUS fusions, 8 sections of 4 μm thickness from unstained WT (A-B) and 35S::GUS (C-D) leaves were examined at 400x magnification under a light microscope. In unstained tissue, only the cell wall and chloroplasts were visible (A-B). In the histochemically stained 35S::GUS sections, blue precipitate is evident in the cytosol and in one case the nucleus as well (C). However aside from the nucleus shown in (C) the GUS did not enter the nucleus and was instead seen surrounding the nuclear envelope (D). GUS was only seen surrounding the chloroplast, not within it. Abbreviations: (CW) cell wall; (Chl) Chloroplast; (Cyt) Cytoplasm; (Nuc) nucleus. Bar = 40 μm.

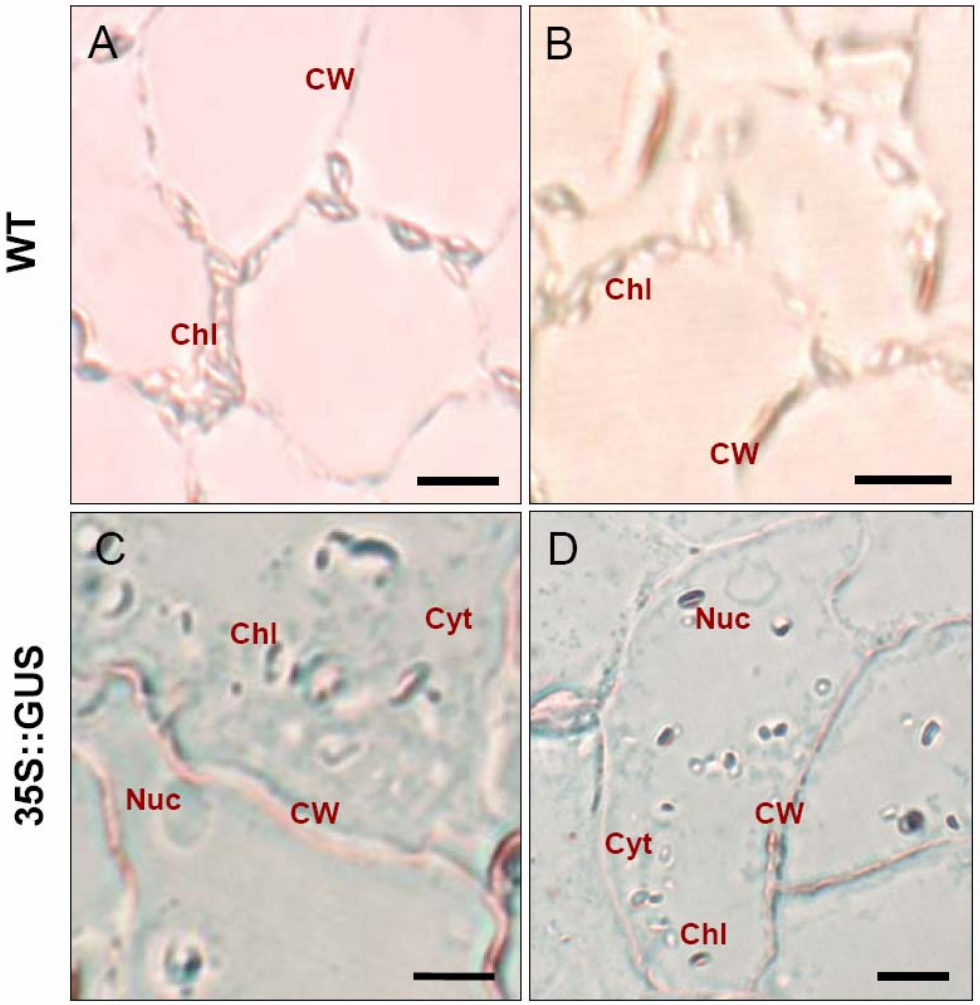
WT
35S::GUS
A
CW
Chl
B
Chl
CW
C
Chl
Cyt
Nuc
CW
D
Nuc
CW
Cyt
Chl

Figure 23. Analysis of GUS translational fusion lines in leaf tissue of 3.5 week-old Arabidopsis.

Mature rosette leaves of 35S::ADK1/2-GUS and 35S::SAHH1/2-GUS were histochemically stained and sectioned at 4 μm thickness. Both SAHH1 (A) and SAHH2 (B) displayed blue precipitate in the chloroplast, nucleus and cytosol of the cell. The same pattern of localization was also evident for ADK1 (C) and ADK2 (D) fusion proteins. To verify these findings immunogold labelling was also performed on the SAH hydrolase translational GUS fusions using rabbit anti-GUS antibody (E-F). The resulting localization of the 15 nm gold particle proved to be the same as the GUS staining. More specifically gold particles representing SAHH1 (E) and SAHH2 (F) were clearly evident in the chloroplast. Immunolabelling performed with no primary antibody and examination of bare resin, resulted in no non-specific binding of the GUS antibody (data not shown). Abbreviations: (Chl) Chloroplast; (Cyt) Cytoplasm; (Nuc) nucleus. Bar = 40 μm.

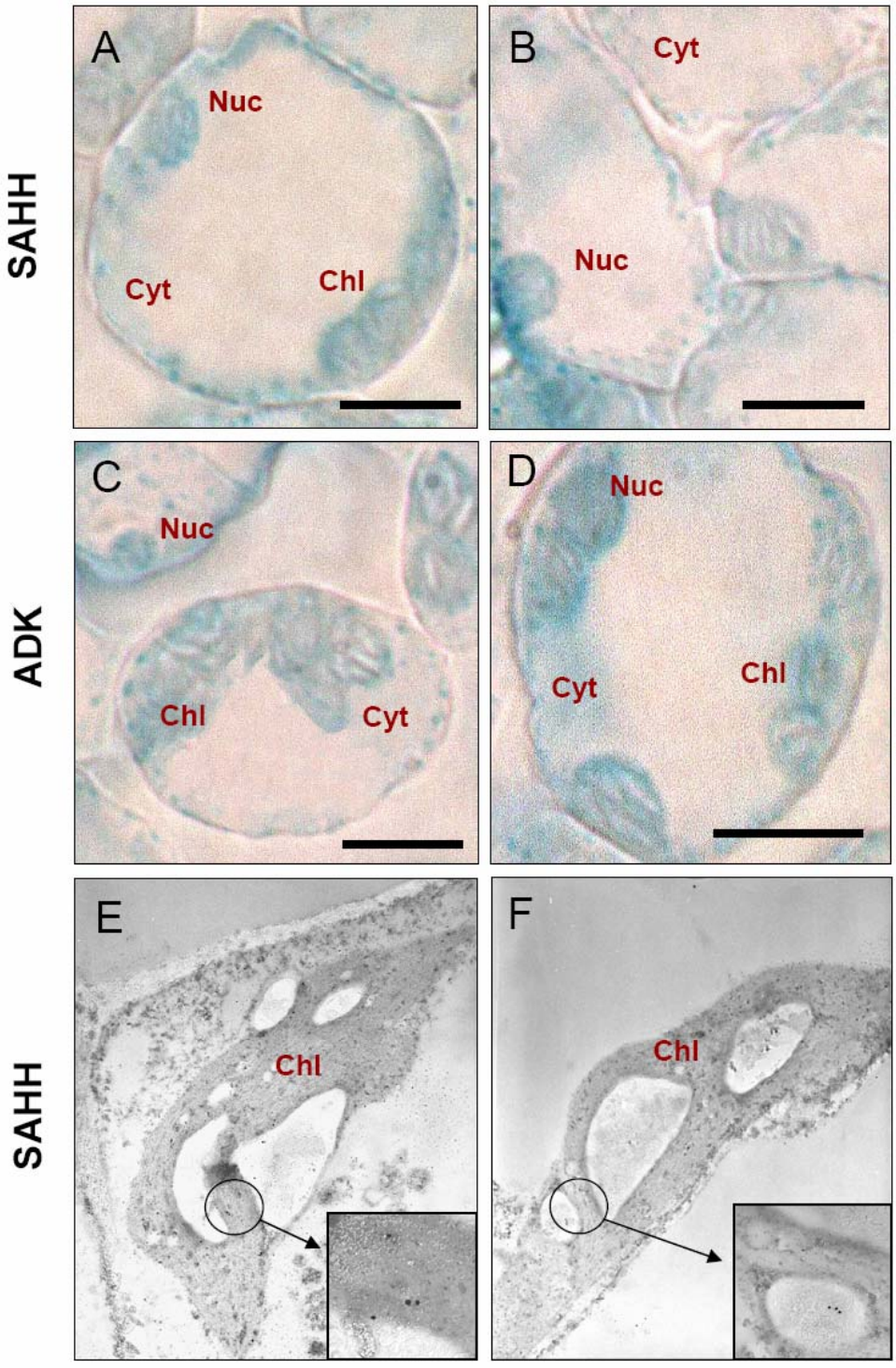
SAHH
ADK
SAHH
A
Nuc
Cyt
Chl
B
Cyt
Nuc
C
Nuc
Chl
Cyt
D
Nuc
Cyt
Chl
E
Chl
F
Chl

Figure 24. Analysis of GFP translational fusion lines of ADK1 and SAHH1 in leaves of 3-week-old Arabidopsis.

Examination of 35S::ADK1-GFP (A-C) 35S::SAHH1-GFP (D-F) and 35S::GFP (G-I) using a confocal microscope showed all three lines to have the same pattern of localization; cytosol and nucleus. (A, D) GFP representing ADK1 and SAHH1 respectively were not detected in the chloroplast. (B, E, H) Chloroplasts were represented by red autofluorescence made visible at 650 nm emission. Abbreviations: (Chl) Chloroplast; (Nuc) nucleus. (Sanghyun Lee, unpublished data).

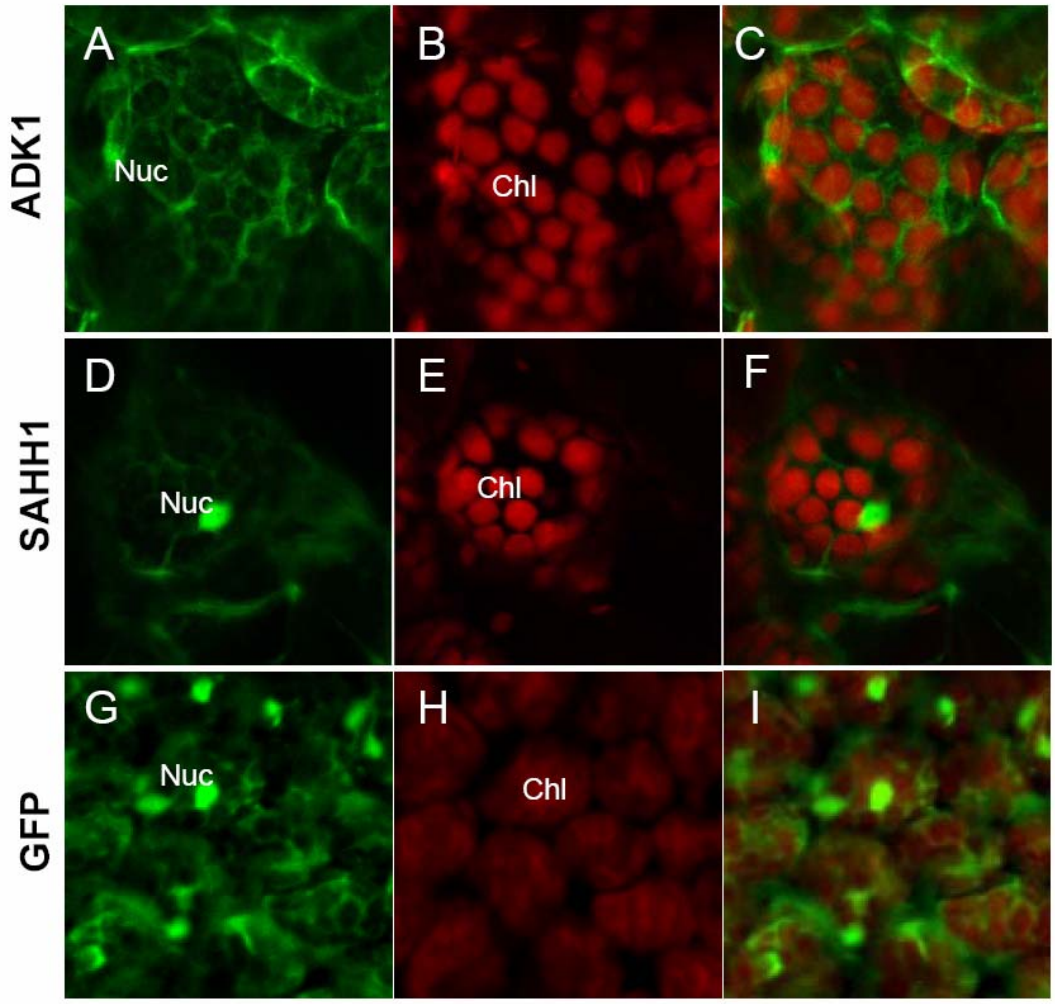
ADK1
SAHH1
GFP
A
B
C
D
E
F
G
H
I
Nuc
Chl
Nuc
Chl
Nuc
Chl

Figure 25. Examination of chloroplasts isolated from 4 week-old GFP translational fusion lines.

35S::ADK1-GFP (A, C-E), 35S::GFP (B) and 35S::SAHH1-GFP (F-H) chloroplast extracts were examined under the confocal microscope. Compared to the protein fusions (A), 35S::GFP had much of the cytosolic GFP removed and only the autofluorescence of the chlorophyll could be seen (B). Approximately 1/1000 intact chloroplasts had ADK1-GFP (C) and SAHH1-GFP (F) detected resulting in an overlapping yellow colour (E, H).

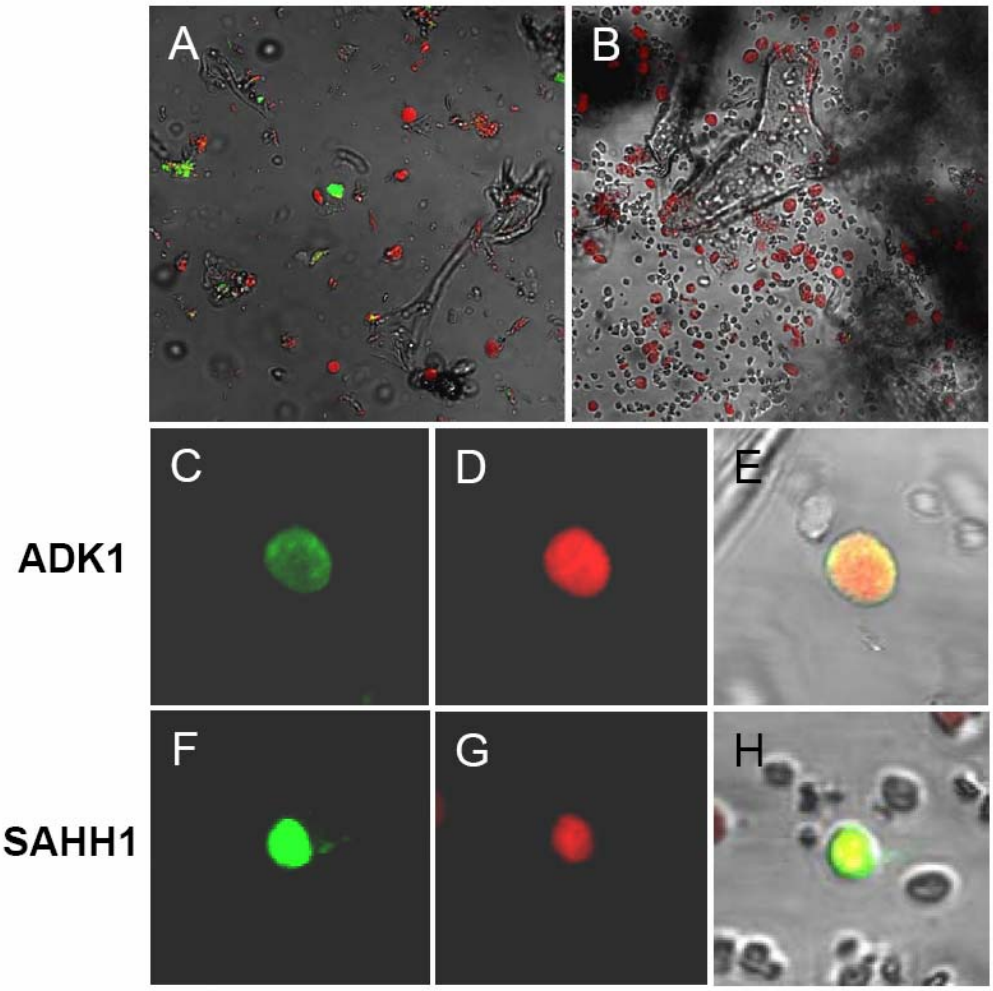
A
B
C
D
E
ADK1
F
G
H
SAHH1

Figure 26. Immunoblot analysis of chloroplasts isolated from WT and GFP translational fusion lines.

Chloroplast protein (10 μg) isolated from 3.5 week-old WT, 35S::ADK1-GFP and 35S::SAHH1-GFP and 5 μg of corresponding leaf protein were electrophoresed through a 12.5 % SDS-PAGE gel. Detection of the samples was performed using rabbit anti-ADK, anti-SAHH and anti-PEP carboxylase (to test for contamination of the cytosolic protein in chloroplast isolates) antibodies and anti-rabbit antibody conjugated to horse radish peroxidase as a secondary. Representative samples are shown: (1) WT chloroplast, (2) 35S::ADK1-GFP chloroplast, (3) 35S::SAHH1-GFP chloroplast, (4) WT leaf extract, (5) 35S::ADK1-GFP chloroplast and (6) 35S::SAHH1-GFP chloroplast.

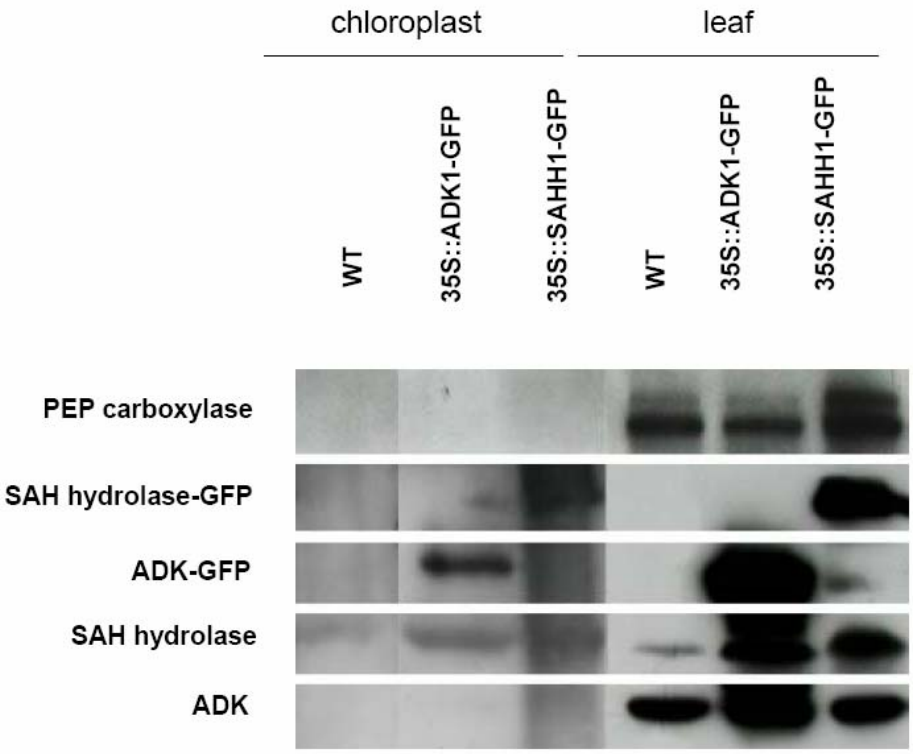
chloroplast
leaf
WT
35S::ADK1-GFP
35S::SAHH1-GFP
WT
35S::ADK1-GFP
35S::SAHH1-GFP
PEP carboxylase
SAH hydrolase-GFP
ADK-GFP
SAH hydrolase
ADK

Figure 27. *In vitro* import assays using chloroplasts isolated from 3.5 week-old Arabidopsis and 2-week-old Pea

Radiolabelled ADK, SAH hydrolase and pSSU (positive control) were incubated with isolated with intact chloroplasts (from Arabidopsis and pea) in standard *in vitro* import assays. The chloroplasts were then treated with (+ Th) or without thermolysin to remove cytosolic contamination and 25 µL was analysed by electrophoresis through a 15% SDS-PAGE gel; the proteins were detected by autoradiography. The order of the samples are: (1) 1/10 of the radiolabelled ADK protein used in the import assay, (2) import of ADK into pea chloroplasts, (3) import of ADK into pea chloroplast (+Th), (4) import of ADK into Arabidopsis chloroplast, (5) import of ADK into Arabidopsis chloroplast (+Th), (6) 1/10 of the radiolabelled SAH hydrolase protein used in the import assay, (7) import of SAH hydrolase into pea chloroplasts, (8) import of SAH hydrolase into pea chloroplasts with thermolysin treatment (+Th), (9) import of SAH hydrolase into Arabidopsis chloroplast, (10) import of SAH hydrolase into Arabidopsis chloroplast with thermolysin treatment (+Th), (11) 1/10 of the radiolabelled pSSU used in the import assay, (12) import of SSU in pea chloroplasts, (13) import of SSU in pea chloroplast after thermolysin treatment (+Th), (14) import of SSU in Arabidopsis chloroplasts and (15) import of SSU in Arabidopsis chloroplasts (+Th).

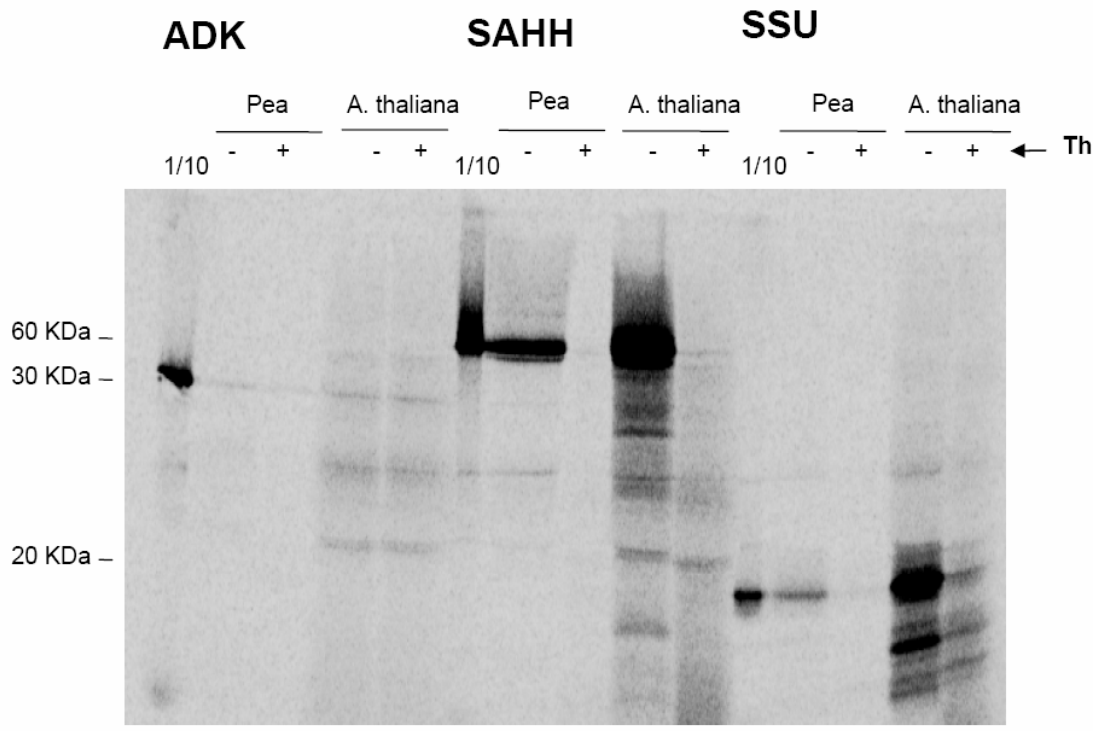
ADK
SAHH
SSU
Pea
A. thaliana
Pea
A. thaliana
Pea
A. thaliana
1/10
- + - +
1/10
- + - +
1/10
- + - +
Th
60 KDa
30 KDa
20 KDa

Discussion

Localization to Multiple Subcellular Compartments

Determining the subcellular localization of ADK and SAH hydrolase is vital to understanding how methylation is maintained throughout plant cells. With this in mind, various techniques have been used to establish the localization of both enzymes. These constructs were designed to test whether both enzymes are present in several cellular compartments, or whether they only reside in the cytosol where they hydrolase SAH which is imported from other organelles. Results from this study indicate the answer may be both. For as well as being found in the cytosol, ADK and SAH hydrolase were also detected in the nucleus and chloroplast. However, their presence in the chloroplast is still questionable. While both immunogold and fusion protein systems support ADK and SAH hydrolase residing in the nucleus, the same was not true for localization to the chloroplast. The results of GFP fluorescence and immunoblot analysis of isolated chloroplasts from ADK- and SAHH-GFP expressing plants have not consistently demonstrated the presence of these enzymes in plastids, although immunogold and GUS fusions clearly showed this localization.

One possible cause of this disparity may be that the 23 KDa GFP protein is interfering with the folding of the ADK or SAHH fusion protein in ways the 89 KDa GUS does not. Folding is a natural mechanism of the polypeptide and contributes to the regulation of localization of dual targeted proteins, by making a targeting signal inaccessible or accessible to protein/chaperone binding (Karniely and Pines, 2005). Thus it is possible that the GFP folding blocks a target peptide sequence for chloroplast

transport or allows a protein to bind and inactivate the signal, leaving the fusion only open to nuclear transport. To address this theory, constructs were later made with the GFP on the C terminus and middle of each protein; no differences were observed in the localization of the corresponding fusions suggesting that this hypothesis is not correct (S. Lee, unpublished results).

Of the immunoblots performed, both the endogenous and fusion proteins of ADK and SAH hydrolase were present in within plastids at levels approximately one quarter that found in total leaf extracts; in comparison to the fluorescence observed in the cytosol and the even brighter nucleus, these levels may be less apparent. As further research is performed protein targeting it is becoming more common find proteins that are disproportionably allocated to one compartment over the other. In a well documented case, the acotinase enzyme in *Saccharomyces cerevisiae* (ACO1), once believed to be exclusive to the mitochondria, was found in the cytosol as well (Regev-Rudzki et al., 2005). As a result of the small cytosolic amounts, the localization of ACO1 to this compartment was overlooked due to 'eclipsed distribution' (Regev-Rudzki et al, 2005). This phenomenon may be contributing to the low success rate of ADK and SAH hydrolase import in *in vitro* import assays. The optimal uptake of radiolabelled Rubisco small subunit introduced to the isolated chloroplasts during these assays was 20% in my hands; in comparison to this targeted enzyme, ADK and SAH hydrolase import would likely be much lower appear to be negligible. The stability of the GUS protein (Jefferson et al., 1987) and sensitivity of the antibodies in the immunogold and immunoblots may enhance the sensitivity of these methods as compared to GFP fluorescence.

Using the immunogold labelling results as a guide, there are half the number of gold particles in the chloroplast than the nucleus for SAH hydrolase, the difference in the two compartments is insignificant for ADK. There was some disparity in gold particle density between tissues; however this was most likely due to the varying organelle content of leaf and meristem. In leaves from 3.5 week-old plants, there was a higher proportion of chloroplast to nucleus localization, so there was a higher density of particles detected in the chloroplast than that of the nucleus; the opposite was true for the meristem, where actively dividing cells are largely comprised of the nucleus with very few chloroplasts. Overall, immunogold labelling would suggest that there is little difference between ADK and SAH hydrolase density labelling in the nucleus and chloroplast.

In the same vein, SAH hydrolase and ADK may not be consistently present in chloroplasts due to developmental differences. *In vitro* import studies performed in collaboration with Dr. Matt Smith at Wilfrid Laurier University using chloroplast extracts of 2.5 week-old seedlings import neither enzyme. Similar analysis of import studies using plastids from 2.5, 3.5 and 4.5 week-old plants revealed ADK to be imported only into chloroplasts isolated 3.5 week-old leaves; SAH hydrolase was not tested.

It has also been shown that some enzymes are targeted differentially in response to cellular or environmental stimuli (Sakamoto and Briggs, 2002; Kim and Apel, 2004; Kim et al., 2005). In the studies performed by Kim et al. isoforms of PORA and PORB only localize to the nuclei of photosynthetic leaves; in a second case phytochrome proteins have been shown to target to the nucleus only upon the appropriate exposure of light (Nagatani, 2004). The only other report of SAH hydrolase localizing to subcellular

compartments is in *Xenopus* oocytes is stage dependent; SAH hydrolase was only detected in the nucleus during times of increased mRNA synthesis (Radomski et al., 1999; Radomski et al., 2002). Thus SAH hydrolase and ADK may only be localizing to the chloroplast during certain stages of metabolism present at 3.5-4 week-old plants. However, GFP fusions were observed in Arabidopsis leaves from 1- 5 week-old plants and no significant amounts of fluorescence were detected at any age.

The final option could be that ADK and SAH hydrolase do not localize to the chloroplast. Closer examination of immunogold labelling shows that although non-specific binding is evident, a low rate of gold particles binding to cellular compartments is observed. While binding is occurring throughout the chloroplast section, the low number of particles makes it hard to interpret whether or not the antibody is simply binding to the outer envelope of the chloroplast. The evidence for chloroplast localization from sectioning of the histochemical GUS staining is stronger because the blue precipitate is evident throughout the entire cell, including the chloroplasts. Since these sections are made at 4 μm thickness, it makes it highly unlikely the GUS is merely residing on the outside of the chloroplast. However, experiments conducted subsequent to those described in this thesis showed that none of a range of N or C terminal deletions of ADK affected the ability of the corresponding GUS fusion to localize to the plastid, putting the GUS results into question (i.e. how can none of the protein be required for targeting?).

Of the other compartments that did not contain these methyl recycling enzymes (such as the mitochondria and tonoplast), it is possible that SAH produced in these organelles is removed to the cytosol. However, in the case of the mitochondria it is most

likely that the SAH is removed into the cytosol. This is supported by the recent discovery of a SAM/SAH exchange transporter (SAMC1) in Arabidopsis mitochondria by Palmieri et al. (2006) and the very low percentage (4% of total mitochondria examined) of SAH hydrolase detected in the mitochondria using immunogold studies and the lack of ADK.

Transport Relies on Alternate Pathways

Although it is now evident that ADK and SAH hydrolase localize to multiple compartments, it is not yet clear how the enzymes are targeted to their respective organelles. Protein targeting is thought to rely on the recognition of signal sequences in each polypeptide by organellar transport machinery. For example, the majority of proteins destined for mitochondria or chloroplasts contain N-terminal signal peptides that are recognized by specific protein complexes within the target organelle (Rusch and Kendall, 1995). Transport into nuclei is slightly different since they contain pores that allow proteins of up to 50-70 kDa to enter or exit by diffusion (Merkle et al., 1996); larger polypeptides contain nuclear localization signals distributed throughout their coding sequences in order to be targeted by active transport systems (Nair et al., 2003).

Given the restrictions imposed on the proteins by the organelle the 212 kDa SAH hydrolase would require directed transport into the chloroplast. Import of SAH hydrolase into the nucleus would require directed transport as well. While the small ADK monomer could potentially rely on diffusion to enter the nucleus, the fact that the ADK was still able to enter the nucleus when attached the 89 kDa GUS protein suggests that this is not occurring by simple diffusion. It seems unlikely that the nucleus would actively import ADK when it could enter by diffusion, however it is possible that facilitated transport ensures the metabolic demand for this enzyme activity is met. Another possibility is that

SAH hydrolase bears a targeting signal and ADK enters by association with SAH hydrolase. Early findings using YFP interaction studies with ADK and SAH hydrolase support the conclusion that the two enzymes interact, however, more study is required (S. Lee unpublished results).

The presence of targeting signals can be assessed using computer algorithms based on amino acid signatures associated with proteins known to be localized in specific cellular compartments. The most commonly used programs are Mitoprot (Claros and Vincencs 1996), ChloroP (Emanuelsson et al., 1999), PSORT (Nakai and Horton, 1999), TargetP (Emanuelsson et al., 2000) and Predator version 1.03 (Small et al., 2004). Analysis of Arabidopsis ADK and SAH hydrolase amino acid sequences using these programs indicate both reside in the cytosol. However, as these programs are based only on known signal motifs, proteins with unconventional targeting signals are not recognized and thus predicted to remain in the cytosol. For example, TargetP predictions are claimed to be 85% accurate (Emanuelsson et al., 2000); however, an analysis of proteomically identified chloroplast proteins using TargetP revealed that only 37% of the 370 proteins found in the chloroplast were identified by TargetP (van Wijk, 2004). Thus, the prediction that ADK and SAH hydrolase are exclusively localized to the cytosol does not mean these enzymes are incapable of being imported into other cellular compartments.

These less than perfect prediction programs only highlight how little is understood about protein targeting throughout the cell; this is particularly evident in chloroplast import. It has long been the common held belief that all nuclear encoded proteins destined for the chloroplast interior (inner envelope membrane, stroma and thylakoids)

rely exclusively on the plastid's Tic/Toc import machinery recognizing cleavable transit peptides of the protein (Jarvis and Robinson, 2004). However, recent research has raised questions about this long held view. In addition to showing that only 376 of the 604 identified chloroplast nuclear encoded proteins were accurately predicted by TargetP to be there, the study of the chloroplast proteome by Kleffmann et al. (2004) also showed that 49 of those proteins have signal tags for the ER and 142 have no cleavable targeting signal. It has been suggested that these proteins are able to enter the chloroplast through an alternate route via stromules and the endomembrane system (Jarvis and Robinson, 2004). While more study is required, it does provide promise in understanding how ADK and SAH hydrolase are able to enter different organelles despite their lack of known sequence tags.

Isoforms Do Not Exhibit Specialized Localization

While it may have once been considered unusual for a protein to be present in more than one cellular compartment, the ever growing data obtained from high-throughput proteomic analyses show that this is not uncommon. Documented cases of a protein being dual targeted to the chloroplast and nucleus are still not that common, but examination of proteomic data obtained from the SUBcellular location database for Arabidopsis proteins (SUBA) show that there are perhaps 39 proteins with this localization pattern (Heazlewood et al., 2005). The majority of these proteins have only been localized using mass spectrophotometry, a technique with a high rate of false positives (Heazlewood et al. 2005), although some have been confirmed using alternate methods, including acetyl-CoA C-acyltransferase (Kleffmann et al., 2004; Pendle et al., 2005) and glyceraldehyde-3-phosphate dehydrogenase (Bae et al., 2003). Arginine decarboxylase has been

documented to reside in both the chloroplast and nucleus of tobacco plants (Bae et al., 2003).

Multiple strategies for targeting a protein/enzyme to more than one compartment have been established including: transcriptional regulation of a single gene via multiple transcripts (Watanabe et al., 2001), translational control using alternative translation initiation (Chabregas et al., 2001) and post-translational control which includes ambiguous target sequences (Peeters and Small, 2001), post-translation modifications (Sakamoto and Briggs 2002) and competitive targeting. Despite these alternate methods, however, the vast majority of proteins/enzymes bearing a similar function in more than one organelle are encoded by distinct genes (Silva-Filho, 2003). Therefore it seems possible that SAH hydrolase and ADK isoforms carry specific targeting information, thereby localizing in distinct patterns. Initial analysis using prediction programs does not support this hypothesis as the algorithms seem unable to differentiate between the sets of isoforms. Ultimately the current data do not support SAH hydrolase and ADK isoforms displaying unique localization patterns. Assuming this limited study is representative of the whole, any specialization of function found between ADK and SAHH isoforms are not involved in subcellular localization. With that being said, more organs of *A. thaliana* and different physiological conditions need to be examined to determine whether or not this occurs throughout the entire plant system.

Conclusion

Based on these data, SAH hydrolase and ADK are localizing to at least the nucleus and cytosol and possibly to the chloroplast. No variance between isoform localization was detected, with both sets of isoforms found in all three compartments. Further study is

required to establish how the enzymes are entering their respective subcellular compartments using deletion GUS and GFP fusion lines. Further work is also required to establish SAH hydrolase and ADK localization to the chloroplast by obtaining more reliable data with chloroplast extracts analyzed with western blotting and import assays.

APPENDIX

Table 8. sADK individuals removed from statistical analysis

Due to to their WT phenotype, sADK4-2 and sADK9-1 plants were not used in the final analysis of ADK deficient plants. In addition to sharing a similar morphology to WT, the mutant individuals also developed at the same rate.

	WT		n=22 sADK4-2		n=30 sADK9-1	
	Avg	± SD	Avg	± SD	Avg	± SD
1st cotyledon	3	0	3	0.3	3	0.2
1st leaf	5	0.13	5.2	0.2	4.9	0.45
2nd leaf	9.4	0.5	9	0.6	9.6	0.3
3rd leaf	10.5	0.56	10.2	0.54	10.8	0.43
4th leaf	11.6	0.58	11.1	0.5	11.7	0.47
5th leaf	12.7	0.62	12	0.61	12.5	0.53
6th leaf	14.1	0.42	13.5	0.43	14.3	0.6
7th leaf	15.1	0.44	14.7	0.46	15.6	0.33
8th leaf	16.1	0.37	15.7	0.5	16.3	0.32
9th leaf	17.1	0.36	17.3	0.32	17.7	0.3
10th leaf	18.1	0.34	18.5	0.46	18.6	0.29
11th leaf	19.1	0.34	19.3	0.51	19.8	0.3
12th leaf	20.1	0.32	20.4	0.42	21	0.28
13th leaf	21.2	0.36	21	0.41	21.9	0.26
14th leaf	22.2	0.36	22	0.53	22.8	0.31
days for stem > 10 cm	27.7	1.21	26.6	1.3	28.6	1.6
rosette radius 3 weeks	4.7	1.25	4.9	1.01	4.5	1.34
rosette radius 4 weeks	7.5	1.56	7	1.8	7.3	1.87
rosette radius 5 weeks	8.3	1.35	8.5	1.65	8.2	1.52
rosette radius 6 weeks	8.8	1.37	8.9	1.56	8.5	1.43
1st bud	16	0	16.3	0.23	16.1	0.23
1st petal dehiscence	25.6	0.89	25.8	0.46	26.1	0.8
1st 17a silique	27.9	1.4	28.5	1.21	28.4	1.89
1st 17b silique	31.8	2.69	32.3	1.9	32.1	2.13
1st 18 silique	38.1	0.77	38.4	0.67	38.6	0.56
1st silique shatter	41.5	0.8	42	0.4	41.7	0.93
17a silique length	11	1.49	11.6	1.32	11.9	1.85
17b silique length	12.8	3.04	12.3	2.89	12.3	2.54
18 silique length	17.78	1.17	17.1	0.87	16.9	0.89
petiole length (stg 18)	5.65	1.1	5.4	0.67	5.5	0.9
ratio of seed/silique	0.29	0.021	0.32	0.032	0.27	0.032
total siliques	299.7	58.37	276.4	33.6	310.6	60.02
plant height (cm)	34.7	3.19	33.8	3.54	35.3	4.56
# rosette branching	4.2	0.7	4.5	0.45	4.4	0.78
# cauline branching	6.9	1.3	7.4	1.5	7.8	0.9

Table 9. Statistical analysis of WT versus ADK deficient lines in rate of cotyledon development

Significance of the variance observed in the mutant lines (A) was monitored using one-way ANOVA (B), with Bonferroni (C) and Tukey B (D) post-hoc analysis.Values showing a significant variation being highlighted in C.

A

Line	Mean	N	Std. Deviation
WT	12.7	32	0.46
adk1-1	12.3	32	0.55
adk2-1	12.5	32	0.72
sADK9-1	14.4	26	0.76
sADK4-2	14.5	38	0.69

B

	Sum of Squares	df	Mean Square	F	Sig.
Between Groups	150.49	4.00	37.62	91.82	0.00
Within Groups	63.51	155.00	0.41		
Total	213.99	159.00			

C

		Mean Difference			95% Confidence Interval	
(I) Line	(J) Line	(I-J)	Std. Error	Sig.	Upper Bound	Lower Bound
WT	*adk1-1*	0.375	0.160	0.204	-0.081	0.831
	adk2-1	0.219	0.160	1.000	-0.237	0.674
	sADK9-1	-1.704	0.169	0.000	-2.186	-1.223
	sADK4-2	-1.808	0.154	0.000	-2.245	-1.370
adk1-1	WT	-0.375	0.160	0.204	-0.831	0.081
	adk2-1	-0.156	0.160	1.000	-0.612	0.299
	sADK9-1	-2.079	0.169	0.000	-2.561	-1.598
	sADK4-2	-2.183	0.154	0.000	-2.620	-1.745
adk2-1	WT	-0.219	0.160	1.000	-0.674	0.237
	adk1-1	0.156	0.160	1.000	-0.299	0.612
	sADK9-1	-1.923	0.169	0.000	-2.404	-1.442
	sADK4-2	-2.026	0.154	0.000	-2.464	-1.589
sADK9-1	WT	1.704	0.169	0.000	1.223	2.186
	adk1-1	2.079	0.169	0.000	1.598	2.561
	adk2-1	1.923	0.169	0.000	1.442	2.404
	sADK4-2	-0.103	0.163	1.000	-0.567	0.361
sADK4-2	WT	1.808	0.154	0.000	1.370	2.245
	adk1-1	2.183	0.154	0.000	1.745	2.620
	adk2-1	2.026	0.154	0.000	1.589	2.464
	sADK9-1	0.103	0.163	1.000	-0.361	0.567

D

	Subset for alpha = .05	
Line	2	1
adk1-1	12.344	
adk2-1	12.500	
WT	12.719	
sADK9-1		14.423
sADK4-2		14.526

Table 10. Statistical analysis of WT versus ADK deficient lines in rate of 5th leaf extension

Significance of the variance observed in the mutant lines (A) was monitored using one-way ANOVA (B), with Bonferroni (C) and Tukey B (D) post-hoc analysis.Values showing a significant variation being highlighted in C.

A

Line	N	Mean	S.D.
WT	32	3.0	0.00
adk1-1	32	3.1	0.30
adk2-1	32	3.0	0.18
sADK9-1	26	3.5	0.71
sADK4-2	38	3.7	0.75

B

	Sum of Squares	df	Mean Square	F	Sig.
Between Groups	12.23	4	3.06	12.90	0.000
Within Groups	36.74	155	0.24		
Total	48.98	159			

C

		Mean Difference			95% Confidence Interval	
(I) Line	(J) Line	(I-J)	Std. Error	Sig.	Upper Bound	Lower Bound
WT	*adk1-1*	-0.094	0.122	1.000	-0.440	0.253
	adk2-1	-0.031	0.122	1.000	-0.378	0.315
	sADK9-1	-0.500	0.129	0.001	-0.866	-0.134
	sADK4-2	-0.658	0.117	0.000	-0.991	-0.325
adk1-1	WT	0.094	0.122	1.000	-0.253	0.440
	adk2-1	0.063	0.122	1.000	-0.284	0.409
	sADK9-1	-0.406	0.129	0.019	-0.772	-0.040
	sADK4-2	-0.564	0.117	0.000	-0.897	-0.231
adk2-1	WT	0.031	0.122	1.000	-0.315	0.378
	adk1-1	-0.063	0.122	1.000	-0.409	0.284
	sADK9-1	-0.469	0.129	0.004	-0.835	-0.103
	sADK4-2	-0.627	0.117	0.000	-0.959	-0.294
sADK9-1	WT	0.500	0.129	0.001	0.134	0.866
	adk1-1	0.406	0.129	0.019	0.040	0.772
	adk2-1	0.469	0.129	0.004	0.103	0.835
	sADK4-2	-0.158	0.124	1.000	-0.511	0.195
sADK4-2	WT	0.658	0.117	0.000	0.325	0.991
	adk1-1	0.564	0.117	0.000	0.231	0.897
	adk2-1	0.627	0.117	0.000	0.294	0.959
	sADK9-1	0.158	0.124	1.000	-0.195	0.511

D

	Subset for alpha = .05	
Line	2	1
WT	3.000	
adk2-1	3.031	
adk1-1	3.094	
sADK9-1		3.500
sADK4-2		3.658

Table 11. Statistical analysis of WT versus ADK deficient lines in rate of 14th leaf extension

Significance of the variance observed in the mutant lines (A) was monitored using one-way ANOVA (B), with Bonferroni (C) and Tukey B (D) post-hoc analysis.Values showing a significant variation being highlighted in C. Significant variation was observed in the sADK mutants to that of WT and even *adk1-1* and *adk2-1*.

A

Line	Mean	N	Std. Deviation
WT	22.2	32	0.45
adk1-1	21.6	32	0.49
adk2-1	22.0	32	0.40
sADK9-1	23.2	26	0.63
sADK4-2	25.1	38	0.67

B

	Sum of Squares	df	Mean Square	F	Sig.
Between Groups	276.49	4.00	69.12	235.53	0.00
Within Groups	45.49	155.00	0.29		
Total	321.98	159.00			

C

					95% Confidence Interval	
(I) Line	(J) Line	Mean Difference (I-J)	Std. Error	Sig.	Upper Bound	Lower Bound
WT	*adk1-1*	0.531	0.135	0.001	0.146	0.917
	adk2-1	0.125	0.135	1.000	-0.261	0.511
	sADK9-1	-1.036	0.143	0.000	-1.443	-0.629
	sADK4-2	-2.923	0.130	0.000	-3.293	-2.553
adk1-1	WT	-0.531	0.135	0.001	-0.917	-0.146
	adk2-1	-0.406	0.135	0.032	-0.792	-0.021
	sADK9-1	-1.567	0.143	0.000	-1.975	-1.160
	sADK4-2	-3.454	0.130	0.000	-3.824	-3.084
adk2-1	WT	-0.125	0.135	1.000	-0.511	0.261
	adk1-1	0.406	0.135	0.032	0.021	0.792
	sADK9-1	-1.161	0.143	0.000	-1.568	-0.754
	sADK4-2	-3.048	0.130	0.000	-3.418	-2.678
sADK9-1	WT	1.036	0.143	0.000	0.629	1.443
	adk1-1	1.567	0.143	0.000	1.160	1.975
	adk2-1	1.161	0.143	0.000	0.754	1.568
	sADK4-2	-1.887	0.138	0.000	-2.279	-1.494
sADK4-2	WT	2.923	0.130	0.000	2.553	3.293
	adk1-1	3.454	0.130	0.000	3.084	3.824
	adk2-1	3.048	0.130	0.000	2.678	3.418
	sADK9-1	1.887	0.138	0.000	1.494	2.279

D

	Subset for alpha = .05			
Line	2	3	4	1
adk1-1	21.625			
adk2-1		22.031		
WT		22.156		
sADK9-1			23.192	
sADK4-2				25.079

Table 12. Statistical analysis of WT versus ADK deficient lines in formation of shoot > 10 cm

Significance of the variance observed in the mutant lines (A) was monitored using one-way ANOVA (B), with Bonferroni (C) and Tukey B (D) post-hoc analysis.Values showing a significant variation being highlighted in C. Significant variation was observed in the sADK mutants and to that of WT and even *adk1-1* and *adk2-1*.

A

Line	Mean	N	Std. Deviation
WT	27.8	32.00	1.03
adk1-1	27.3	32.00	1.07
adk2-1	27.8	32.00	0.90
sADK9-1	37.8	26.00	7.82
sADK4-2	39.7	38.00	7.98
ada1-1 **, sADK9-1**	36.8	30.00	5.96

B

	Sum of Squares	df	Mean Square	F	Sig.
Between Groups	5,956.10	5.00	1,191.22	57.77	0.00
Within Groups	3,793.79	184.00	20.62		
Total	9,749.89	189.00			

C

(I) Line	(J) Line	Mean Difference (I-J)	Std. Error	Sig.	95% Confidence Interval Upper Bound	95% Confidence Interval Lower Bound
WT	*adk1-1*	0.469	1.135	1.000	-2.907	3.845
	adk2-1	0.000	1.135	1.000	-3.376	3.376
	sADK9-1	-10.918	1.199	0.000	-14.484	-7.353
	sADK4-2	-12.319	1.089	0.000	-15.559	-9.079
	ada1-1 , sADK9-1	-8.954	1.154	0.000	-12.386	-5.522
adk1-1	WT	-0.469	1.135	1.000	-3.845	2.907
	adk2-1	-0.469	1.135	1.000	-3.845	2.907
	sADK9-1	-11.387	1.199	0.000	-14.953	-7.821
	sADK4-2	-12.788	1.089	0.000	-16.028	-9.548
	ada1-1 , sADK9-1	-9.423	1.154	0.000	-12.855	-5.991
adk2-1	WT	0.000	1.135	1.000	-3.376	3.376
	adk1-1	0.469	1.135	1.000	-2.907	3.845
	sADK9-1	-10.918	1.199	0.000	-14.484	-7.353
	sADK4-2	-12.319	1.089	0.000	-15.559	-9.079
	ada1-1 , sADK9-1	-8.954	1.154	0.000	-12.386	-5.522
sADK9-1	WT	10.918	1.199	0.000	7.353	14.484
	adk1-1	11.387	1.199	0.000	7.821	14.953
	adk2-1	10.918	1.199	0.000	7.353	14.484
	sADK4-2	-1.401	1.156	1.000	-4.838	2.036
	ada1-1 , sADK9-1	1.964	1.217	1.000	-1.654	5.583
sADK4-2	WT	12.319	1.089	0.000	9.079	15.559
	adk1-1	12.788	1.089	0.000	9.548	16.028
	adk2-1	12.319	1.089	0.000	9.079	15.559
	sADK9-1	1.401	1.156	1.000	-2.036	4.838
	ada1-1, sADK9-1	3.365	1.109	0.041	0.067	6.663
ada1-1 , sADK9-1	WT	8.954	1.154	0.000	5.522	12.386
	adk1-1	9.423	1.154	0.000	5.991	12.855
	adk2-1	8.954	1.154	0.000	5.522	12.386
	sADK9-1	-1.964	1.217	1.000	-5.583	1.654
	sADK4-2	-3.365	1.109	0.041	-6.663	-0.067

D

	Subset for alpha = .05		
Line	**2**	**3**	**1**
adk1-1	27.344		
WT	27.813		
adk2-1	27.813		
ada1-1 , sADK9-1		36.767	
sADK9-1		38.731	38.731
sADK4-2			40.132

Table 13. Statistical analysis of WT versus ADK and ADA deficient lines in comparison to mature height

Significance of the variance observed in the mutant lines (A) was monitored using one-way ANOVA (B), with Bonferroni (C) and Tukey B (D) post-hoc analysis.Values showing a significant variation being highlighted in C. Significant variation was observed in the sADK mutants and to that of WT and even *adk1-1* and *adk2-1*.No significant difference was observed between WT and *ada1-1,* however crossing the mutant into sADK9-1 did.

A

Line	Mean	N	Std. Deviation
WT	8.8	32	0.54
adk1-1	8.9	32	0.63
adk2-1	8.9	32	0.63
sADK9-1	6.8	26	1.35
sADK4-2	4.0	38	1.05
ada1-1	8.0	32	0.63
ada1-1, sADK9-1	4.6	30	0.97

B

	Sum of Squares	df	Mean Square	F	Sig.
Between Groups	868.20	6.00	144.70	195.22	0.00
Within Groups	159.36	215.00	0.74		
Total	1,027.56	221.00			

C

(I) Line	(J) Line	Mean Difference (I-J)	Std. Error	Sig.	95% Confidence Interval Upper Bound	95% Confidence Interval Lower Bound
WT	*adk1-1*	-0.011	0.215	1.000	-0.673	0.651
	adk2-1	-0.061	0.215	1.000	-0.723	0.601
	sADK9-1	2.062	0.227	0.000	1.363	2.761
	sADK4-2	4.792	0.207	0.000	4.157	5.427
	ada1-1	0.883	0.215	0.001	0.221	1.545
	ada1-1 , sADK9-1	4.252	0.219	0.000	3.580	4.925
adk1-1	WT	0.011	0.215	1.000	-0.651	0.673
	adk2-1	-0.050	0.215	1.000	-0.712	0.612
	sADK9-1	2.073	0.227	0.000	1.374	2.772
	sADK4-2	4.803	0.207	0.000	4.168	5.438
	ada1-1	0.894	0.215	0.001	0.232	1.556
	ada1-1 , sADK9-1	4.263	0.219	0.000	3.591	4.936
adk2-1	WT	0.061	0.215	1.000	-0.601	0.723
	adk1-1	0.050	0.215	1.000	-0.612	0.712
	sADK9-1	2.123	0.227	0.000	1.424	2.822
	sADK4-2	4.853	0.207	0.000	4.218	5.488
	ada1-1	0.944	0.215	0.000	0.282	1.606
	ada1-1 , sADK9-1	4.313	0.219	0.000	3.641	4.986
sADK9-1	WT	-2.062	0.227	0.000	-2.761	-1.363
	adk1-1	-2.073	0.227	0.000	-2.772	-1.374
	adk2-1	-2.123	0.227	0.000	-2.822	-1.424
	sADK4-2	2.730	0.219	0.000	2.056	3.403
	ada1-1	-1.179	0.227	0.000	-1.878	-0.480
	ada1-1 , sADK9-1	2.190	0.231	0.000	1.481	2.900
sADK4-2	WT	-4.792	0.207	0.000	-5.427	-4.157
	adk1-1	-4.803	0.207	0.000	-5.438	-4.168
	adk2-1	-4.853	0.207	0.000	-5.488	-4.218
	sADK9-1	-2.730	0.219	0.000	-3.403	-2.056
	ada1-1	-3.909	0.207	0.000	-4.544	-3.274
	ada1-1, sADK9-1	-0.539	0.210	0.231	-1.186	0.107
ada1-1	WT	-0.883	0.215	0.001	-1.545	-0.221
	adk1-1	-0.894	0.215	0.001	-1.556	-0.232
	adk2-1	-0.944	0.215	0.000	-1.606	-0.282
	sADK9-1	1.179	0.227	0.000	0.480	1.878
	sADK4-2	3.909	0.207	0.000	3.274	4.544
	ada1-1 , sADK9-1	3.370	0.219	0.000	2.697	4.042
ada1-1 , sADK9-1	WT	-4.252	0.219	0.000	-4.925	-3.580
	adk1-1	-4.263	0.219	0.000	-4.936	-3.591
	adk2-1	-4.313	0.219	0.000	-4.986	-3.641
	sADK9-1	-2.190	0.231	0.000	-2.900	-1.481
	sADK4-2	0.539	0.210	0.231	-0.107	1.186
	ada1-1	-3.370	0.219	0.000	-4.042	-2.697

D

Line	Subset for alpha = .05 2	3	4	5	1
sADK4-2	4.047				
ada1-1 , sADK9-1		4.587			
sADK9-1			6.777		
ada1-1				7.956	
WT					8.839
adk1-1					8.850
adk2-1					8.900

SUMMARY

The purpose of this research was to further our understanding of the enzymes involved in Ado salvage and to establish the localization of ADK and along with SAH hydrolase. In order to study the Ado recycling enzymes ADK and ADA, mutants were identified and studied. Tagged lines lacking in either ADK1 (*adk1-1*) or ADK2 (*adk2-1*) had no discernable phenotype. Thus, at the development stages examined, ADK isoforms have no specialized function and appear to be interchangeable. Reducing overall ADK levels to 6-20% with genes silencing transgenes does result in a phenotype: wrinkled leaves, reduced internode length, clustered inflorescences, delayed senescence and lack of petal abscission/silique dehiscence. ADK tagged lines most likely did not display such a phenotype due to the retention of approximately half of WT ADK activity. Therefore ADK activity is necessary for viable Arabidopsis. Evidence supports both a decrease in methylation and increased CK levels as causes for the phenotype observed in the sADK lines; severe sADK mutants exhibit up to a 30% reduction in cytosine methylation and a >10-fold increase of total cytokinins. Both of these deviations appear to be due to the decrease in Ado salvage: higher levels of Ado result in higher levels of inhibitory SAH and it would appear that ADK does play a role in CK interconversion.

T-DNA insertion lines of putative ADA (*ada1-1*) were also examined, and like the ADK tagged lines resulted in no phenotypic abnormality. However when the ADA was crossed with sADK9-1 (*ada1-1*,sADK9-1) the sADK phenotype became more severe, particularly in the occurrence of the sADK phenotypes observed and delayed leaf senescence. Analysis using HPLC and GC-MS also supports the decrease in adenosine salvage as both genomic methylation and CK levels were also affected. Thus the loss of

the putative ADA does not appear to affect Arabidopsis metabolism unless ADK levels are lowered. This would suggest that the putative ADA does perform some function in adenosine salvage, although its role is less significant than that of ADK. Further study is required to determine whether or not the putative ADA has ADA activity and the generation of more stable miRNA lines to assess ADK loss.

Localization of ADK and SAH hydrolase was examined using various methods. TEM analysis of immunogold labelling for the two enzymes indicated they reside in the nucleus, cytosol and chloroplast. Use of GUS translational fusion lines of ADK and SAH hydrolase isoforms supports this pattern of localization. Aside from supporting the immunogold findings, the GUS fusions also support the possibility of active transport into the nucleus as the large GUS protein attached to the proteins would make it impossible for them to simply diffuse into the nucleus. However, examining GFP translational fusion lines casts doubt as to whether the enzymes are capable of localizing to chloroplasts as no GFP fluorescence was detected in the plastid. Further analysis using chloroplast extracts for immunoblotting and *in vitro* import assays also provide questionable results. Possible explanations for this contradicting information are that the enzymes are only present in small amounts undetectable by GFP fluorescence, improper folding of the GFP translational fusion lines and ADK and SAH hydrolase needing to be tightly bound to outer envelope to allow transport (which subsequent thermolysin treatment removes from the chloroplast extracts). Future research will be dedicated to establishing whether or not ADK and SAH hydrolase are capable or localizing to the chloroplast and how they are targeted to the nucleus using GFP deletion lines.

REFERENCES

Ashihara,H. and Crozier,A. (1999). Biosynthesis and catabolism of caffeine in low-caffeine-containing species of Coffea. J. Agric. Food Chem. *47*, 3425-3431.

Ashihara,H. and Crozier,A. (2001). Caffeine: a well known but little mentioned compound in plant science. Trends Plant Sci. *6*, 407-413.

Astot,C., Dolezal,K., Nordstrom,A., Wang,Q., Kunkel,T., Moritz,T., Chua,N.H., and Sandberg,G. (2000). An alternative cytokinin biosynthesis pathway. Proc. Natl. Acad. Sci. U. S. A *97*, 14778-14783.

Avni,A., Bailey,B.A., Mattoo,A.K., and Anderson,J.D. (1994). Induction of ethylene biosynthesis in Nicotiana tabacum by a Trichoderma viride xylanase is correlated to the accumulation of 1-aminocyclopropane-1-carboxylic acid (ACC) synthase and ACC oxidase transcripts. Plant Physiol *106*, 1049-1055.

Bae,M.S., Cho,E.J., Choi,E.Y., and Park,O.K. (2003). Analysis of the Arabidopsis nuclear proteome and its response to cold stress. Plant J. *36*, 652-663.

Bethin,K.E., Petrovic,N., and Ettinger,M.J. (1995). Identification of a major hepatic copper binding protein as S-adenosylhomocysteine hydrolase. J. Biol. Chem. *270*, 20698-20702.

Bowman,J. (1994). Arabidopsis: An Atlas of Morphology and Development. (New York: Springer-Verlag).

Bradford,M.M. (1976). A rapid and sensitive method for the quantitation of microgram quantities of protein utilizing the principle of protein-dye binding. Anal. Biochem. *72*, 248-254.

Brady,T.G. and Hegarty,V.J. (1966). An investigation of plant seeds for adenosine deaminase. Nature *209*, 1027-1028.

Brenner,S., Johnson,M., Bridgham,J., Golda,G., Lloyd,D.H., Johnson,D., Luo,S., McCurdy,S., Foy,M., Ewan,M., Roth,R., George,D., Eletr,S., Albrecht,G., Vermaas,E., Williams,S.R., Moon,K., Burcham,T., Pallas,M., DuBridge,R.B., Kirchner,J., Fearon,K., Mao,J., and Corcoran,K. (2000). Gene expression analysis by massively parallel signature sequencing (MPSS) on microbead arrays. Nat. Biotechnol. *18*, 630-634.

Brigneti,G., Voinnet,O., Li,W.X., Ji,L.H., Ding,S.W., and Baulcombe,D.C. (1998). Viral pathogenicity determinants are suppressors of transgene silencing in Nicotiana benthamiana. EMBO J. *17*, 6739-6746.

Brough,C.L., Gardiner,W.E., Inamdar,N.M., Zhang,X.Y., Ehrlich,M., and Bisaro,D.M. (1992). DNA methylation inhibits propagation of tomato golden mosaic virus DNA in transfected protoplasts. Plant Mol. Biol. *18*, 703-712.

Cao,Y., Song,F., Goodman,R.M., and Zheng,Z. (2006). Molecular characterization of four rice genes encoding ethylene-responsive transcriptional factors and their expressions in response to biotic and abiotic stress. J. Plant Physiol *163*, 1167-1178.

Carimi,F., Zottini,M., Formentin,E., Terzi,M., and Lo,S.F. (2003). Cytokinins: new apoptotic inducers in plants. Planta *216*, 413-421.

Caspi,R., Foerster,H., Fulcher,C.A., Hopkinson,R., Ingraham,J., Kaipa,P., Krummenacker,M., Paley,S., Pick,J., Rhee,S.Y., Tissier,C., Zhang,P., and Karp,P.D. (2006). MetaCyc: a multiorganism database of metabolic pathways and enzymes. Nucleic Acids Res. *34*, D511-D516.

Chabregas,S.M., Luche,D.D., Farias,L.P., Ribeiro,A.F., van Sluys,M.A., Menck,C.F., and Silva-Filho,M.C. (2001). Dual targeting properties of the N-terminal signal sequence of Arabidopsis thaliana THI1 protein to mitochondria and chloroplasts. Plant Mol. Biol. *46*, 639-650.

Chen,C.M. and Eckert,R.L. (1977). Phosphorylation of Cytokinin by Adenosine Kinase from Wheat Germ. Plant Physiol *59*, 443-447.

Clark,D.G., Richards,C., Hilioti,Z., Lind-Iversen,S., and Brown,K. (1997). Effect of pollination on accumulation of ACC synthase and ACC oxidase transcripts, ethylene production and flower petal abscission in geranium (Pelargonium x hortorum L.H. Bailey). Plant Mol. Biol. *34*, 855-865.

Claros,M.G. and Vincens,P. (1996). Computational method to predict mitochondrially imported proteins and their targeting sequences. Eur. J. Biochem. *241*, 779-786.

Clough,S.J. and Bent,A.F. (1998). Floral dip: a simplified method for Agrobacterium-mediated transformation of Arabidopsis thaliana. Plant J. *16*, 735-743.

Cristalli,G., Costanzi,S., Lambertucci,C., Lupidi,G., Vittori,S., Volpini,R., and Camaioni,E. (2001). Adenosine deaminase: functional implications and different classes of inhibitors. Med. Res. Rev. *21*, 105-128.

Dancer,J.E., Hughes,R.G., and Lindell,S.D. (1997). Adenosine-5'-phosphate deaminase. A novel herbicide target. Plant Physiol *114*, 119-129.

de la Haba,G. and Cantoni,G.L. (1959). The enzymatic synthesis of S-adenosyl-L-homocysteine from adenosine and homocysteine. J Biol Chem *234*, 603-608.

Dennis,C. and Surridge,C. (2000). Arabidopsis thaliana genome. Introduction. Nature *408*, 791.

Eckermann,C., Eichel,J., and Schroder,J. (2000). Plant methionine synthase: new insights into properties and expression. Biol. Chem *381*, 695-703.

Edwards,R. and Dixon,R.A. (1991). Purification and characterization of S-adenosyl-L-methionine: caffeic acid 3-O-methyltransferase from suspension cultures of alfalfa (Medicago sativa L.). Arch. Biochem. Biophys. *287*, 372-379.

Emanuelsson,O., Nielsen,H., Brunak,S., and von,H.G. (2000). Predicting subcellular localization of proteins based on their N-terminal amino acid sequence. J. Mol. Biol. *300*, 1005-1016.

Emanuelsson,O., Nielsen,H., and von,H.G. (1999). ChloroP, a neural network-based method for predicting chloroplast transit peptides and their cleavage sites. Protein Sci. *8*, 978-984.

Faye, F. and Le Floch, F. (1997). Adenosine kinase of peach tree flower buds: purification and properties. Plant Physiol Biochem *35*, 15-22.

Gomi,T., Date,T., Ogawa,H., Fujioka,M., Aksamit,R.R., Backlund,P.S., Jr., and Cantoni,G.L. (1989). Expression of rat liver S-adenosylhomocysteinase cDNA in Escherichia coli and mutagenesis at the putative NAD binding site. J. Biol. Chem. *264*, 16138-16142.

Guranowski,A. (1979). Plant adenosine kinase: purification and some properties of the enzyme from Lupinus luteus seeds. Arch. Biochem. Biophys. *196*, 220-226.

Guranowski,A. and Pawelkiewicz,J. (1977). Adenosylhomocysteinase from yellow lupin seeds. Purification and properties. Eur. J. Biochem. *80*, 517-523.

Guranowski,A. and Wasternack,C. (1982). Adenine and adenosine metabolizing enzymes in cell-free extracts from Euglena gracilis. Comp Biochem. Physiol B *71*, 483-488.

Hanson,A.D., Rivoal,J., Paquet,L., and Gage,D.A. (1994). Biosynthesis of 3-dimethylsulfoniopropionate in Wollastonia biflora (L.) DC. Evidence that S-methylmethionine is an intermediate. Plant Physiol *105*, 103-110.

Hanson,A.D. and Roje,S. (2001). One-carbon metabolism in higher plants. Annu. Rev. Plant Physiol Plant Mol. Biol. *52*, 119-137.

Heazlewood,J.L., Tonti-Filippini,J., Verboom,R.E., and Millar,A.H. (2005). Combining experimental and predicted datasets for determination of the subcellular location of proteins in Arabidopsis. Plant Physiol *139*, 598-609.

Hoth,S., Ikeda,Y., Morgante,M., Wang,X., Zuo,J., Hanafey,M.K., Gaasterland,T., Tingey,S.V., and Chua,N.H. (2003). Monitoring genome-wide changes in gene expression in response to endogenous cytokinin reveals targets in Arabidopsis thaliana. FEBS Lett. *554*, 373-380.

Huang,S., Cerny,R.E., Qi,Y., Bhat,D., Aydt,C.M., Hanson,D.D., Malloy,K.P., and Ness,L.A. (2003). Transgenic studies on the involvement of cytokinin and gibberellin in male development. Plant Physiol *131*, 1270-1282.

Ishaque,A. and Al-Rubeai,M. (2002). Role of vitamins in determining apoptosis and extent of suppression by bcl-2 during hybridoma cell culture. Apoptosis. *7*, 231-239.

Ishiki,Y., Oda,A., Yaegashi,Y., Orihara,Y., Arai,T., Hirabayashi,T., Nakagawa,H., and Sato,T. (2000). Cloning of an auxin-responsive 1-aminocyclopropane-1-carboxylate synthase gene (CMe-ACS2) from melon and the expression of ACS genes in etiolated melon seedlings and melon fruits. Plant Sci *159*, 173-181.

Jakubowicz,M. (2002). Structure, catalytic activity and evolutionary relationships of 1-aminocyclopropane-1-carboxylate synthase, the key enzyme of ethylene synthesis in higher plants. Acta Biochim. Pol. *49*, 757-774.

Jarvis,P. and Robinson,C. (2004). Mechanisms of protein import and routing in chloroplasts. Curr. Biol. *14*, R1064-R1077.

Jeddeloh,J.A., Stokes,T.L., and Richards,E.J. (1999). Maintenance of genomic methylation requires a SWI2/SNF2-like protein. Nat. Genet *22*, 94-97.

Kakimoto,T. (2003). Biosynthesis of cytokinins. J. Plant Res. *116*, 233-239.

Kamachi,S., Sekimoto,H., Kondo,N., and Sakai,S. (1997). Cloning of a cDNA for a 1-aminocyclopropane-1-carboxylate synthase that is expressed during development of female flowers at the apices of Cucumis sativus L. Plant Cell Physiol *38*, 1197-1206.

Karniely,S. and Pines,O. (2005). Single translation--dual destination: mechanisms of dual protein targeting in eukaryotes. EMBO Rep. *6*, 420-425.

Kato,M., Hayakawa,Y., Hyodo,H., Ikoma,Y., and Yano,M. (2000). Wound-induced ethylene synthesis and expression and formation of 1-aminocyclopropane-1-carboxylate (ACC) synthase, ACC oxidase, phenylalanine ammonia-lyase, and peroxidase in wounded mesocarp tissue of Cucurbita maxima. Plant Cell Physiol *41*, 440-447.

Kawalleck,P., Plesch,G., Hahlbrock,K., and Somssich,I.E. (1992). Induction by fungal elicitor of S-adenosyl-L-methionine synthetase and S-adenosyl-L-homocysteine hydrolase mRNAs in cultured cells and leaves of Petroselinum crispum. Proc. Natl. Acad. Sci. U. S. A *89*, 4713-4717.

Kim,C. and Apel,K. (2004). Substrate-dependent and organ-specific chloroplast protein import in planta. Plant Cell *16*, 88-98.

Kim,C., Ham,H., and Apel,K. (2005). Multiplicity of different cell- and organ-specific import routes for the NADPH-protochlorophyllide oxidoreductases A and B in plastids of Arabidopsis seedlings. Plant J. *42*, 329-340.

Kleffmann,T., Russenberger,D., von,Z.A., Christopher,W., Sjolander,K., Gruissem,W., and Baginsky,S. (2004). The Arabidopsis thaliana chloroplast proteome reveals pathway abundance and novel protein functions. Curr. Biol. *14*, 354-362.

Kocsis,M.G., Ranocha,P., Gage,D.A., Simon,E.S., Rhodes,D., Peel,G.J., Mellema,S., Saito,K., Awazuhara,M., Li,C., Meeley,R.B., Tarczynski,M.C., Wagner,C., and Hanson,A.D. (2003). Insertional inactivation of the methionine s-methyltransferase gene eliminates the s-methylmethionine cycle and increases the methylation ratio. Plant Physiol *131*, 1808-1815.

Kwade,Z., Swiatek,A., Azmi,A., Goossens,A., Inze,D., Van,O.H., and Roef,L. (2005). Identification of four adenosine kinase isoforms in tobacco By-2 cells and their putative role in the cell cycle-regulated cytokinin metabolism. J. Biol. Chem. *280*, 17512-17519.

Lelievre,J.M., Tichit,L., Dao,P., Fillion,L., Nam,Y.W., Pech,J.C., and Latche,A. (1997). Effects of chilling on the expression of ethylene biosynthetic genes in Passe-Crassane pear (Pyrus communis L.) fruits. Plant Mol. Biol. *33*, 847-855.

Liska,A.J., Shevchenko,A., Pick,U., and Katz,A. (2004). Enhanced photosynthesis and redox energy production contribute to salinity tolerance in Dunaliella as revealed by homology-based proteomics. Plant Physiol *136*, 2806-2817.

Liu,J., Prunuske,A.J., Fager,A.M., and Ullman,K.S. (2003). The COPI complex functions in nuclear envelope breakdown and is recruited by the nucleoporin Nup153. Dev. Cell *5*, 487-498.

Llop-Tous,I., Barry,C.S., and Grierson,D. (2000). Regulation of ethylene biosynthesis in response to pollination in tomato flowers. Plant Physiol *123*, 971-978.

Maier,S.A., Galellis,J.R., and McDermid,H.E. (2005). Phylogenetic analysis reveals a novel protein family closely related to adenosine deaminase. J. Mol. Evol. *61*, 776-794.

Masuta,C., Tanaka,H., Uehara,K., Kuwata,S., Koiwai,A., and Noma,M. (1995b). Broad resistance to plant viruses in transgenic plants conferred by antisense inhibition of a host gene essential in S-adenosylmethionine-dependent transmethylation reactions. Proc. Natl. Acad. Sci. U. S. A *92*, 6117-6121.

Masuta,C., Tanaka,H., Uehara,K., Kuwata,S., Koiwai,A., and Noma,M. (1995a). Broad resistance to plant viruses in transgenic plants conferred by antisense inhibition of a host gene essential in S-adenosylmethionine-dependent transmethylation reactions. Proc. Natl. Acad. Sci. U. S. A *92*, 6117-6121.

Mathews,I.I., Erion,M.D., and Ealick,S.E. (1998). Structure of human adenosine kinase at 1.5 A resolution. Biochemistry *37*, 15607-15620.

Matzke,M.A., Matzke,A.J., Pruss,G.J., and Vance,V.B. (2001). RNA-based silencing strategies in plants. Curr. Opin. Genet. Dev. *11*, 221-227.

McMahon,R.J. (2002). Biotin in metabolism and molecular biology. Annu. Rev. Nutr. *22*, 221-239.

Merkle,T., Leclerc,D., Marshallsay,C., and Nagy,F. (1996). A plant in vitro system for the nuclear import of proteins. Plant J. *10*, 1177-1186.

Miller,M.W., Duhl,D.M., Winkes,B.M., rredondo-Vega,F., Saxon,P.J., Wolff,G.L., Epstein,C.J., Hershfield,M.S., and Barsh,G.S. (1994). The mouse lethal nonagouti a(x) mutation deletes the S-adenosylhomocysteine hydrolase (Ahcy) gene. EMBO J. *13*, 1806-1816.

Mlejnek,P. and Prochazka,S. (2002). Activation of caspase-like proteases and induction of apoptosis by isopentenyladenosine in tobacco BY-2 cells. Planta *215*, 158-166.

Moffatt,B. and Somerville,C. (1988). Positive Selection for Male-Sterile Mutants of Arabidopsis Lacking Adenine Phosphoribosyl Transferase Activity. Plant Physiol *86*, 1150-1154.

Moffatt,B.A., McWhinnie,E.A., Agarwal,S.K., and Schaff,D.A. (1994). The adenine phosphoribosyltransferase-encoding gene of Arabidopsis thaliana. Gene *143*, 211-216.

Moffatt,B.A., Stevens,Y.Y., Allen,M.S., Snider,J.D., Pereira,L.A., Todorova,M.I., Summers,P.S., Weretilnyk,E.A., Martin-McCaffrey,L., and Wagner,C. (2002). Adenosine kinase deficiency is associated with developmental abnormalities and reduced transmethylation. Plant Physiol *128*, 812-821.

Moffatt,B.A., Wang,L., Allen,M.S., Stevens,Y.Y., Qin,W., Snider,J., and von,S.K. (2000). Adenosine kinase of Arabidopsis. Kinetic properties and gene expression. Plant Physiol *124*, 1775-1785.

Mudd,S.H. and Datko,D. (1986). Methionine methyl group metabolism in *Lemna*. Plant Physiol *81*, 103-114.

Nagatani,A. (2004). Light-regulated nuclear localization of phytochromes. Curr. Opin. Plant Biol. *7*, 708-711.

Nair,R., Carter,P., and Rost,B. (2003). NLSdb: database of nuclear localization signals. Nucleic Acids Res. *31*, 397-399.

Nakai,K. and Horton,P. (1999). PSORT: a program for detecting sorting signals in proteins and predicting their subcellular localization. Trends Biochem. Sci. *24*, 34-36.

Nakatsuka,A., Murachi,S., Okunishi,H., Shiomi,S., Nakano,R., Kubo,Y., and Inaba,A. (1998). Differential expression and internal feedback regulation of 1-aminocyclopropane-1-carboxylate synthase, 1-aminocyclopropane-1-carboxylate oxidase, and ethylene receptor genes in tomato fruit during development and ripening. Plant Physiol *118*, 1295-1305.

Palmieri,L., Arrigoni,R., Blanco,E., Carrari,F., Zanor,M.I., Studart-Guimareas,C., Fernie,A.R., and Palmieri,F. (2006). Molecular identification of an Arabidopsis thaliana S-adenosylmethionine transporter: analysis of organ distribution, bacterial expression, reconstitution into liposomes and functional characterization. Plant Physiol.

Pandey,S., Ranade,S.A., Nagar,P.K., and Kumar,N. (2000). Role of polyamines and ethylene as modulators of plant senescence. J. Biosci. *25*, 291-299.

Peeters,N. and Small,I. (2001). Dual targeting to mitochondria and chloroplasts. Biochim. Biophys. Acta *1541*, 54-63.

Pendle,A.F., Clark,G.P., Boon,R., Lewandowska,D., Lam,Y.W., Andersen,J., Mann,M., Lamond,A.I., Brown,J.W., and Shaw,P.J. (2005). Proteomic analysis of the Arabidopsis nucleolus suggests novel nucleolar functions. Mol. Biol. Cell *16*, 260-269.

Pereira,L.A., Schoor,S., Goubet,F., Dupree,P., and Moffatt,B.A. (2006). Deficiency of adenosine kinase activity affects the degree of pectin methyl-esterification in cell walls of Arabidopsis thaliana. Planta.

Poulton,J.E. (1981). Transmethylation and Demethylation Reactions in the Metabolism of Secondary Plant Products. The Biochemistry of Plants *7*, 667-721.

Poulton,J.E. and Butt,V.S. (1976). Purification and properties of S-adenosyl-L-homocysteine hydrolase from leaves of spinach beet. Arch. Biochem. Biophys. *172*, 135-142.

Radomski,N., Barreto,G., Kaufmann,C., Yokoska,J., Mizumoto,K., and Dreyer,C. (2002). Interaction of S-adenosylhomocysteine hydrolase of Xenopus laevis with mRNA(guanine-7-)methyltransferase: implication on its nuclear compartmentalisation and on cap methylation of hnRNA. Biochim. Biophys. Acta *1590*, 93-102.

Radomski,N., Kaufmann,C., and Dreyer,C. (1999). Nuclear accumulation of S-adenosylhomocysteine hydrolase in transcriptionally active cells during development of Xenopus laevis. Mol. Biol Cell *10*, 4283-4298.

Ravanel,S., Block,M.A., Rippert,P., Jabrin,S., Curien,G., Rebeille,F., and Douce,R. (2004). Methionine metabolism in plants: chloroplasts are autonomous for de novo methionine synthesis and can import S-adenosylmethionine from the cytosol. J. Biol. Chem *279*, 22548-22557.

Regev-Rudzki,N., Karniely,S., Ben-Haim,N.N., and Pines,O. (2005). Yeast aconitase in two locations and two metabolic pathways: seeing small amounts is believing. Mol. Biol. Cell *16*, 4163-4171.

Rusch,S.L. and Kendall,D.A. (1995). Protein transport via amino-terminal targeting sequences: common themes in diverse systems. Mol. Membr. Biol *12*, 295-307.

Sakamoto,K. and Briggs,W.R. (2002). Cellular and subcellular localization of phototropin 1. Plant Cell *14*, 1723-1735.

Schomburg,I., Chang,A., Ebeling,C., Gremse,M., Heldt,C., Huhn,G., and Schomburg,D. (2004). BRENDA, the enzyme database: updates and major new developments. Nucleic Acids Res. *32*, D431-D433.

Schroder,G., Waitz,A., Hotze,M., and Schroder,J. (1994). cDNA for S-adenosyl-L-homocysteine hydrolase from Catharanthus roseus. Plant Physiol *104*, 1099-1100.

Sebestova L, Vortuba I, and Holy A. (1983). S-adenosylhomocysteine hydrolase from Nicotiana tabacum L: Isolation and properties. Collect Czech Chem Commun *48*, 1543-1555.

Sganga,M.W., Aksamit,R.R., Cantoni,G.L., and Bauer,C.E. (1992). Mutational and nucleotide sequence analysis of S-adenosyl-L-homocysteine hydrolase from Rhodobacter capsulatus. Proc. Natl. Acad. Sci. U. S. A *89*, 6328-6332.

Shimaoka,T., Ohnishi,M., Sazuka,T., Mitsuhashi,N., Hara-Nishimura,I., Shimazaki,K., Maeshima,M., Yokota,A., Tomizawa,K., and Mimura,T. (2004). Isolation of intact vacuoles and proteomic analysis of tonoplast from suspension-cultured cells of Arabidopsis thaliana. Plant Cell Physiol *45*, 672-683.

Shimizu,S., Shiozaki,S., Ohshiro,T., and Yamada,H. (1984). Occurrence of S-adenosylhomocysteine hydrolase in prokaryote cells. Characterization of the enzyme from Alcaligenes faecalis and role of the enzyme in the activated methyl cycle. Eur. J. Biochem. *141*, 385-392.

Silva-Filho,M.C. (2003). One ticket for multiple destinations: dual targeting of proteins to distinct subcellular locations. Curr. Opin. Plant Biol. *6*, 589-595.

Small,I., Peeters,N., Legeai,F., and Lurin,C. (2004). Predotar: A tool for rapidly screening proteomes for N-terminal targeting sequences. Proteomics. *4*, 1581-1590.

Spychala,J., Datta,N.S., Takabayashi,K., Datta,M., Fox,I.H., Gribbin,T., and Mitchell,B.S. (1996). Cloning of human adenosine kinase cDNA: sequence similarity to microbial ribokinases and fructokinases. Proc. Natl. Acad. Sci. U. S. A *93*, 1232-1237.

Stasolla,C., Katahira,R., Thorpe,T.A., and Ashihara,H. (2003). Purine and pyrimidine nucleotide metabolism in higher plants. J. Plant Physiol *160*, 1271-1295.

Suzuki,M., Yasumoto,E., Baba,S., and Ashihara,H. (2003). Effect of salt stress on the metabolism of ethanolamine and choline in leaves of the betaine-producing mangrove species Avicennia marina. Phytochemistry *64*, 941-948.

Tanaka,H., Masuta,C., Uehara,K., Kataoka,J., Koiwai,A., and Noma,M. (1997). Morphological changes and hypomethylation of DNA in transgenic tobacco expressing

antisense RNA of the S-adenosyl-L-homocysteine hydrolase gene. Plant Mol. Biol. *35*, 981-986.

van Wijk,K.J. (2004). Plastid proteomics. Plant Physiol Biochem *42*, 963-977.

Vanyushin,B.F. (2006). DNA methylation in plants. Curr. Top. Microbiol. Immunol. *301*, 67-122.

Voinnet,O., Pinto,Y.M., and Baulcombe,D.C. (1999). Suppression of gene silencing: a general strategy used by diverse DNA and RNA viruses of plants. Proc. Natl. Acad. Sci. U. S. A *96*, 14147-14152.

Von Schwartzenberg,K., Kruse,S., Reski,R., Moffatt,B., and Laloue,M. (1998). Cloning and characterization of an adenosine kinase from Physcomitrella involved in cytokinin metabolism. Plant J. *13*, 249-257.

Walters,D.R. (2003). Polyamines and plant disease. Phytochemistry *64*, 97-107.

Wang,H., Buckley,K.J., Yang,X., Buchmann,R.C., and Bisaro,D.M. (2005). Adenosine kinase inhibition and suppression of RNA silencing by geminivirus AL2 and L2 proteins. J. Virol. *79*, 7410-7418.

Watanabe,N., Che,F.S., Iwano,M., Takayama,S., Yoshida,S., and Isogai,A. (2001). Dual targeting of spinach protoporphyrinogen oxidase II to mitochondria and chloroplasts by alternative use of two in-frame initiation codons. J. Biol. Chem. *276*, 20474-20481.

Waterhouse,P.M., Wang,M.B., and Lough,T. (2001). Gene silencing as an adaptive defence against viruses. Nature *411*, 834-842.

Weretilnyk,E.A., Alexander,K.J., Drebenstedt,M., Snider,J.D., Summers,P.S., and Moffatt,B.A. (2001). Maintaining methylation activities during salt stress. The involvement of adenosine kinase. Plant Physiol *125*, 856-865.

Yu,J., Hu,S., Wang,J., Wong,G.K., Li,S., Liu,B., Deng,Y., Dai,L., Zhou,Y., Zhang,X., Cao,M., Liu,J., Sun,J., Tang,J., Chen,Y., Huang,X., Lin,W., Ye,C., Tong,W., Cong,L., Geng,J., Han,Y., Li,L., Li,W., Hu,G., Huang,X., Li,W., Li,J., Liu,Z., Li,L., Liu,J., Qi,Q., Liu,J., Li,L., Li,T., Wang,X., Lu,H., Wu,T., Zhu,M., Ni,P., Han,H., Dong,W., Ren,X., Feng,X., Cui,P., Li,X., Wang,H., Xu,X., Zhai,W., Xu,Z., Zhang,J., He,S., Zhang,J., Xu,J., Zhang,K., Zheng,X., Dong,J., Zeng,W., Tao,L., Ye,J., Tan,J., Ren,X., Chen,X., He,J., Liu,D., Tian,W., Tian,C., Xia,H., Bao,Q., Li,G., Gao,H., Cao,T., Wang,J., Zhao,W., Li,P., Chen,W., Wang,X., Zhang,Y., Hu,J., Wang,J., Liu,S., Yang,J., Zhang,G., Xiong,Y., Li,Z., Mao,L., Zhou,C., Zhu,Z., Chen,R., Hao,B., Zheng,W., Chen,S., Guo,W., Li,G., Liu,S., Tao,M., Wang,J., Zhu,L., Yuan,L., and Yang,H. (2002). A draft sequence of the rice genome (Oryza sativa L. ssp. indica). Science *296*, 79-92.

Zimmermann,P., Hirsch-Hoffmann,M., Hennig,L., and Gruissem,W. (2004). Genevestigator: Arabidopsis microarray database and analysis toolbox. Plant Physiol *136*, 2621-2632